ANTI-BACTERIAL AND CYTOTOXIC EFFECTS OF KING COBRA (*OPHIOPHAGUS HANNAH*) VENOM L-AMINO ACID OXIDASE

By

LEE MUI LI

THESIS SUBMITTED IN FULFILMENT OF THE REQUIREMENT FOR THE DEGREE OF DOCTOR OF PHILOSOPHY

Department of Molecular Medicine
Faculty of Medicine
University of Malaya
Kuala Lumpur
Malaysia
2014

UNIVERSITI MALAYA

ORIGINAL LITERARY WORK DECLARATION

Name of Candidate: LEE MUI LI (I.C/Passport No: 850713-12-5040)

Registration/Matric No: MHA 100047

Name of Degree: Doctor of Philosophy

Title of Dissertation/Thesis: ANTI-BACTERIAL AND CYTOTOXIC EFFECTS OF KING COBRA (OPHIOPHAGUS HANNAH) VENOM L-AMINO ACID OXIDASE.

Field of Study: Cytotoxic agent from snake venom

I do solemnly and sincerely declare that:

(1) I am the sole author/writer of this Work;
(2) This work is original;
(3) Any use of any work in which copyright exists was done by way of fair dealing and for permitted purposes and any excerpt or extract from, or reference to or reproduction of any copyright work has been disclosed expressly and sufficiently and the title of the work and its authorship have been acknowledged in this work;
(4) I do not have any actual knowledge nor ought I reasonably to know that the making of this work constitutes an infringement of any copyright work;
(5) I hereby assign all and every rights in the copyright to this work to the University of Malaya (UM), who henceforth shall be owner of the copyright in this work and that any reproduction or use in any form or by any means whatsoever is prohibited without the written consent of UM having been first had and obtained;
(6) I am fully aware that if in the course of making this work I have infringed any copyright whether intentionally or otherwise, I may be subject to legal action or any other action as may be determined by UM.

Candidate's signature Date

_____ _____

Subscribed and solemnly declared before,

Witness's signature Date

_____ _____

Name:
Designation:

ABSTRACT

King cobra (*Ophiophagus hannah*) venom L-amino acid oxidase (OH-LAAO), a heat stable enzyme, has been shown to exhibit bactericidal activity against several strains of clinical isolates Gram-positive and Gram-negative bacteria. Its potency was compared with some common antibiotics such as cefotaxime, kanamycin, tetracycline, vancomycin and penicillin. King cobra venom LAAO was effective in inhibiting Gram-positive bacteria tested, with minimum inhibitory concentration (MIC) of 0.78 μg/mL (0.006 μM) and 1.56 μg/mL (0.012 μM) against *S. aureus* and *S. epidermidis*, respectively. The MICs are comparable to the MICs of the antibiotics tested. However, the OH-LAAO was moderately effective against the Gram-negative bacteria tested (*P. aeruginosa*, *K. pneumonia*, and *E. coli*), with MIC ranges from 25 to 50 μg/mL (0.2 - 0.4 μM). Catalase (1 mg/mL) significantly abolished the bactericidal activity of OH-LAAO, indicating that the antibacterial effect of the enzyme involves generation of hydrogen peroxide. Binding studies indicated that OH-LAAO binds strongly to the Gram-positive *S. aureus* and *S. epidermidis*, but less strongly to the Gram-negative *E. coli* and *P. aeruginosa*, suggesting that specific binding to the bacteria is important for its potent antibacterial activity.

The enzyme was also shown to exhibit very potent anti-proliferative activity against human tumourigenic breast (MCF-7), lung (A549), promyelocytic leukaemia (HL-60) and prostate (PC-3) cells, with IC_{50} of 0.04 - 0.07 μg/mL after 72 h incubation. In comparison, its cytotoxicity was about 3 to 4 times lower when tested against the non-tumourigenic breast (184B5) and lung (NL 20) cells, suggesting selective anti-tumour activity. Furthermore, its potency in human tumourigenic cells was greater than the effects of doxorubicin, which has an IC_{50} of 0.1 - 0.63 μg/mL. The selective cytotoxic action of the OH-LAAO was confirmed by PE-annexin V/7-AAD apoptotic assay. The

ability of OH-LAAO in inducing apoptosis in tumour cells was further demonstrated using caspase-3/7 and DNA fragmentation assays. Apoptosis induction activity of the enzyme is via both intrinsic and extrinsic pathways as indicated by increase in caspase-9 and -8 activities as well as increased cytochrome *c* levels in both cytosolic and mitochondria fractions in the LAAO-treated cells. The generation of H_2O_2 plays a significant role in the cytotoxic action of the enzyme, as its cytotoxicity was significantly reduced in the presence of catalase (a H_2O_2 scavenger). It was postulated that the alterations of gene and protein expression in cells treated with OH-LAAO, as observed in microarray and proteomics studies, were largely caused by non-specific oxidative modifications of signalling molecules that eventually lead to apoptosis and cell death.

Administration of 1 μg/g (*i.p.*) of OH-LAAO to PC-3 tumour-bearing NU/NU mice markedly inhibited the tumour growth. TUNEL staining analysis on the tumour sections showed a significantly increase of apoptotic cells in the LAAO-treated animals. The enzyme also did not cause any significant pathology changes on the vital organs as well as the body weight of the treated mice. In view of its heat stability, its selective and potent cytotoxic action on cancer cells, OH-LAAO can be potentially developed for treating solid tumours.

ABSTRAK

L-asid amino oxidase dari bisa ular tedung selar (*Ophiophagus hannah*) (OH-LAAO) adalah enzim yang stabil terhadap haba. Kajian telah membuktikan bahawa ia mempunyai aktiviti anti-bakteria terhadap beberapa jenis bakteria klinkal Gram-negatif dan Gram-positif. Potensinya telah dibandingkan dengan beberapa jenis antibiotik yang lazim digunakan seperti *cefotaxime, kanamycin, tetracycline, vancomycin,* and *penicillin*. L-asid amino oxidase dari bisa ular tedung selar amat berkesan dalam mengawal pertumbuhan bakteria Gram-positif yang telah diuji, dengan kepekatan penghalang minimum sebanyak 0.78 μg/mL (0.006 μM) bagi *S. aureus* dan 1.56 μg/mL (0.012 μM) bagi *S. epidermidis*. Keberkesanan OH-LAAO adalah setanding dengan antibiotik yang diuji. Walau bagaimanapun, kesan anti-bakteria OH-LAAO terhadap bakteria Gram-negatif (*P. aeruginosa, K. Pneumoniae,* dan *E. coli*) yang diuji adalah sederhana sahaja, dengan julat kepekatan penghalang minimum antara 25 hingga 50 μg/mL (0.2 - 0.4 μM). Katalase (1 mg/mL) berupaya mengurangkan kesan anti-bakteria OH-LAAO. Ini menunjukkan bahawa kesan anti-bakteria enzim tersebut melibatkan pembebasan hidrogen peroksida. Hasil kajian juga menunjukkan bahawa darjah pengikatan OH-LAAO adalah lebih kuat terhadap *S. aureus* dan *S. epidermidis* (bakteria Gram-positif) berbanding dengan *E. coli* dan *P. aeruginosa* (baketria Gram-negative). Ini membuktikan bahawa pengikatan khusus terhadap bakteria adalah penting bagi kesan anti-bakteria enzim tersebut.

Enzim tersebut juga telah dibuktikan mempunyai aktiviti anti-proliferatif yang kuat terhadap sel karsinoma payudara (MCF-7), paru-paru (A549), leukemia (HL-60), dan prostat (PC-3) manusia dengan julat IC_{50}nya sebanyak 0.04 - 0.07 μg/mL, selepas 72 jam inkubasi. Kesan sitotoksik enzim tersebut adalah kira-kira 3 - 4 kali lebih rendah apabila diuji terhadap sel payudara (184B5), dan paru-paru (NL 20) normal manusia. Ini

mencadangkan bahawa enzim tersebut mempunyai activiti anti-tumor yang khusus. Selain itu, kesan anti-proliferatif OH-LAAO terhadap sel karsinoma manusia adalah jauh lebih berkesan berbanding dengan *doxorubicin,* iaitu agen klinikal kanser bagi rawatan kemoterapi yang sedia ada, dengan IC_{50}nya dalam julat 0.1 - 0.63 μg/mL. Tindakan khusus OH-LAAO ini juga telah dibuktikan dengan melalui *PE-annexin V/7-AAD assay*. Kesan sitotoksik OH-LAAO telah dibuktikan melibatkan proses apoptosis kerana terdapat peningkatan aktiviti *caspase-3/7* dan fragmentasi molekul DNA dalam sel-sel yang dirawat dengn OH-LAAO. Induksi aktiviti apoptosis enzim tersebut adalah melalui jalur intrinsik dan ekstrinsik seperti yang ditunjukkan dalam peningkatan aktiviti *caspase*-9 and -8 serta *cytochrome c* di bahagian sitosol dan mitokondria dalam sel-sel yang dirawat. Hidrogen peroksida memainkan peranan penting dalam tindakan sitotoksik OH-LAAO kerana panambahan katalase berjaya mengurangkan aktiviti sitotoksik enzim tersebut. Sebagaimana yang ditunjukkan melalui kajian *microarray* dan proteomik, perubahan gen dan protein dalam sel-sel yang dirawat dengan OH-LAAO besar kemungkinan disebabkan oleh pengubahsuaian oksidatif yang tidak spesifik terhadap isyarat molekul yang akhirnya membawa kepada proses apoptosis lalu menyebabkan kematian sel-sel.

Pertumbuhan tumor PC-3 dalam tikus NU/NU berjaya disekat dengan suntikan OH-LAAO sebanyak 1 μg/g secara *i.p*. Analisis TUNEL bagi tisu-tisu tumor menunjukkan peningkatan proses apoptosis untuk sel-sel di dalam tikus yang dirawat dengan OH-LAAO. Enzim tersebut tidak menyebabkan sebarang perubahan patologi terhadap organ-organ penting dan mahupun berat badan tikus. Disebabkan ciri-ciri istimewa OH-LAAO yang merangkumi kestabilan haba yang tinggi, tindakan sitotoksik yang amat berkesan and khusus, OH-LAAO mempunyai potensi yang baik dalam rawatan tumor.

ACKNOWLEDGEMENTS

I would like to express the deepest appreciation to my supervisors Professor Tan Nget Hong and Dr. Fung Shin Yee for their kind assistance, encouragement and support throughout the years of studies; this would not have been possible without their guidance and persistent help.

My sincere gratitude to Professor Sim Si Mui, Professor Jeyaseelan Kandiah, Professor Shamala Devi Sekaran, Professor Jayalakshmi Pailoor, Professor Cheah Swee Hung, Dr. Arunmozhiarasi, Dr. Ivy Chung, and Dr. Kanthimathi for their expert, sincere and valuable guidance and encouragement extended to me.

My sincere thank to Professor Onn Haji Hashim (Head of Department of Molecular Medicine), all the lecturers and staff of the Department of Molecular Medicine for their help and encouragement.

Last but not least, I would like to extend my heartfelt gratitude most especially to my lab members, family and friends for their understanding and motivation.

TABLE OF CONTENTS

LIST OF FIGURES

LIST OF TABLES

LIST OF SYMBOLS AND ABBREVIATIONS

7-AAD	7-Amino-Actinomycin D
ACN	acetonitrile
BSA	bovine serum albumin
Caspase	cysteine-aspartic protease
cDNA	complementary deoxyribonucleic acid
CFU	colony-forming unit
CHAPS	3-[(3-cholamidopropyl)dimethylammonio]-1-propanesulfonate
cm	centimetre
C_t	threshold cycle
CYP1A1	cytochrome P450, Family 1, Subfamily A, Polypeptide 1
CYP1B1	cytochrome P450, Family 1, Subfamily B, Polypeptide 1
DAB	3, 3'-diaminobenzidine
DCF	2', 7'-dichlorodihydrofluorescein
DCFH-DA	2', 7'-dichlorodihydrofluorescin diacetate
DMSO	dimethyl sulfoxide
DNA	deoxyribonucleic acid
dsDNA	double stranded deoxyribonucleic acid

DTT	dithiothreitol
ECF	extracellular fluid
EDTA	ethylenediaminetetraacetic acid
ELISA	enzyme-linked immunosorbent assay
FA	formaldehyde agarose
GSH	glutathione
h	hour
H_2O	water
HCl	hydrochloric acid
HPLC	high performance liquid chromatography
HRP	horseradish peroxidase
IC_{50}	half maximal inhibitory concentration
IVC	individually ventilated cages
IEF	isoelectric focusing
i.p.	intraperitoneal
IPG	immobilized pH gradient
LAAO	L-amino acid oxidase
L	litre

M	molar
MALDI-TOF	matrix-assisted laser desorption ionization/ Time-of-flight
mg	milligram
MIC	minimum inhibitory concentration
min	minute
mL	millilitre
mM	millimolar
MOPS	3-(N-morpholino)propanesulfonic acid
MS	mass spectrometry
MTT	3,(4,5-dimethythiazol-2-yl)-2,3-diphenyl tetrazolium bromide
m/z	mass-to-charge ratio
µ	micro
µg	microgram
µL	microlitre
µM	micromolar
µm	micrometer
nm	nanometer
NaCl	sodium chloride

NADPH	nicotinamide adenine dinucleotide phosphate
NF-κB	nuclear factor kappa B
ng	nanogram
NaOH	sodium hydroxide
NH_4HCO_3	ammonium bicarbonate
OD	optical density
OH-LAAO	*Ophiophagus hannah* L-amino acid oxidase
PCR	polymerase chain reaction
PBS	phosphate buffered saline
PE	phycoerythrin
PVDF	polyvinylidene fluoride
RNA	ribonucleic acid
ROS	reactive oxygen species
RT-PCR	real-time polymerase chain reaction
s.c.	subcutaneous
SDS	sodium dodecyl sulfate
SDS-PAGE	sodium dodecyl sulfate polyacrylamide gel electrophoresis
Sec	second

TBS-T	tris buffered saline-tween 20
TMB	3,3',5,5'-tetramethylbenzidine
TUNEL	TdT-mediated dUTP nicked-end labelling
UV	ultraviolet
V	voltage
v/v	volume/volume
w/v	weight/volume

LIST OF APPENDICES

CHAPTER 1

INTRODUCTION

AND

LITERATURE REVIEW

1.1 *Ophiophagus hannah* (king cobra)

Figure 1.1: *Ophiophagus hannah* (king cobra). Picture courtesy of N.H. Tan.

Ophiophagus hannah (the king cobra) is the longest venomous snake in the world, with an average length of about 3.9 m (12.8 ft) although some can grow up to 5.5 m (18 ft). The adult king cobra is brown or olive above with scales dark-edged especially on tail and posterior body with traces of whitish crossbars (Tweedie, 1983; Das, 2006). The throat is orange-yellow or cream coloured with irregular blackish markings. A unique feature of this species is the presence of a pair of large occipital shields behind the parietals that come in contact with each other on midline, which allow recognition on smaller specimens (Lim *et al*., 2011). The king cobra is widely distributed in South and Southeast Asia, including Pakistan, Bhutan, Nepal, India, Bangladesh, Myanmar, southern China, Vietnam, Cambodia, Laos, Thailand, Peninsular Malaysia, Singapore, Borneo, Sumatra, Java, Bali, Sulawesi, and the Philippines (Iskandar and Colijn, 2001). It inhabits a wide range of habitats, in forest and in populated areas.

Ophiophagus hannah is classified under the family *Elapidae*. It belongs to a unique genus *Ophiophagus*, while most others elapids are *Naja* (cobra) or *Bungarus* (krait).

Although all elapid snakes exhibit fixed front fangs that are situated in front of the upper jaw, however, king cobra can be distinguished from other cobras by the size and hood. King cobras are generally larger than other cobras, and the stripe on the neck is a chevron instead of a double or single eye shape that may be seen in most of the other Asian cobras. In addition, the hood of the king cobra is narrower and longer (Lim *et al*., 2011). The generic name *Ophiophagus* derived from the Greek language and literally means "snake eater", *ophio* = snake and *phagus* = eater, in reference to its dietary habits. The picture of king cobra is shown in Figure 1.1.

1.2 Biochemistry of snake venom L-amino acid oxidase (LAAO)

1.2.1 General aspects

L-amino acid oxidase (LAAO) (L-amino acid: O_2 oxidoreductase, E.C. 1.4.3.2.) is a flavoenzyme that catalyses the oxidative deamination of an L-amino acid to produce the corresponding α-ketoacid, hydrogen peroxide and ammonia (Tan and Fung, 2009). The enzyme is widely distributed in venoms from most genera of snakes (Tan and Ponnudurai, 1992) and generally constitutes about 1 - 4% of the total venom proteins by dried weight (Tan, 1998). L-amino acid oxidase is highly specific for the oxidation of L-enantiomer of amino acids. Generally, the best substrates for the enzyme are hydrophobic amino acids; L-leucine, L-methionine, L- phenylalanine, L-tyrosine and L-tryptophan (Tan and Fung, 2009). *Ophiophagus hannah* venom LAAO has been reported to oxidize L-lysine and L-ornithine in addition to the previously mentioned L-amino acids (Tan and Saifuddin, 1991). Differences of the catalytic activities are mainly due to variations in side-chain binding sites for substrate specificity of the enzyme (Wei *et al*., 2009).

Earlier, the studies of snake venom LAAO mainly focused on their enzymatic and physiochemical properties. Recently, its pharmacological activities such as anticancer,

antibacterial, leishmanicidal, anti-HIV, platelet aggregation as well as edema-inducing and haemorrhagic activities have been studied extensively. These studies indicated that king cobra venom LAAO has the potential to be developed as a therapeutic agent.

1.2.2 Purification of snake venom L-amino acid oxidase

Numerous LAAOs have been purified and characterized from various snake venoms (Izidoro *et al*., 2006; Samel *et al*., 2006; Toyama *et al*., 2006; Wei *et al*., 2003). The enzymes may exist in multiple isoforms in some snake venoms. Hayes and Wellner (1969) reported that there were at least 18 isoforms of *Crotalus adamanteus* venom LAAO, and the microheterogeneity of the enzyme is presumably due to the varying degree of glycosylation. However, high homogeneity of the oligosaccharide chain was found in many other snake venom LAAOs such as in *Calloselasma rhodostoma* (Pawelek *et al*., 2000) and *Ophiophagus hannah* (Tan and Fung, 2009). In general, snake venom LAAO can be easily purified to a high degree of molecular homogeneity using a single- or combination of two-step chromatography procedure (Ali *et al*., 2000; Ponnudurai *et al*., 1994; Souza *et al*., 1999; Stábeli *et al*., 2007; Toyama *et al*., 2006).

1.2.3 L-amino acid oxidase assay

Horseradish peroxidase coupled assay, a spectrophotometric method described by Bergmeyer (1983) is a commonly used LAAO assay method. In this assay, the oxidation rate is measured by the rate of formation of dye colour complex between the hydrogen peroxide and o-dianisidine (Bergmeyer, 1983). The colour complex was spectrophotometrically measured at 436 nm.

Catalytic activity of LAAO can be devided into two stages: the α-hydrogen atom of the amino acid is first abstracted by the FAD prosthetic group, forming α-imino acid as the

intermediate product, which then reacts with water to form the α-keto acid in the later stage (Figure 1.2) (Tan and Fung, 2009).

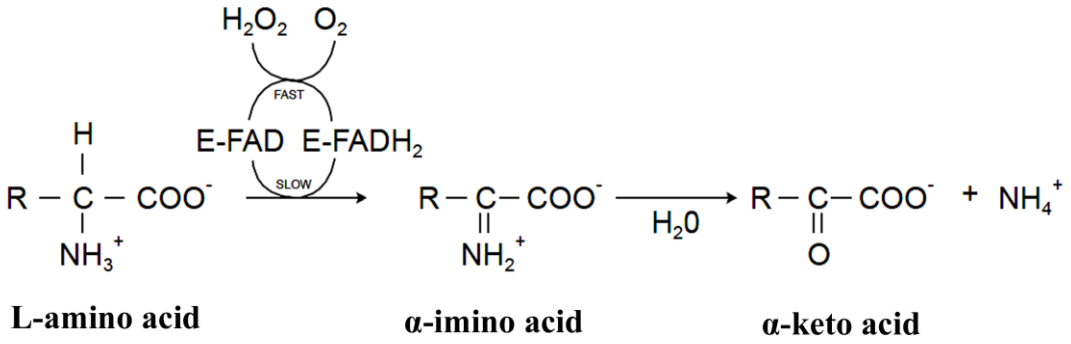

Figure 1.2: Mechanism of LAAO in catalysis oxidative deamination of L-amino acid. Figure taken from Tan and Fung 2009.

1.2.4 Physical properties of L-amino acid oxidase

Snake venom LAAO is a homodimeric flavoprotein containing two molecules of non-covalently bound FAD (flavin adenine dinucleotide) or FMN (flavin mononucleotide). The flavin group is reponsible for the yellowish colour of the enzyme. Most of the snake venom LAAOs are FAD-binding proteins.

The enzyme has a molecular weight of 112 - 140 kDa as determined by gel filtration chromatography, and a wide range of isoelectric point (pI), ranging from 4.4 to 8.12 (Tan, 1998). Generally, most of the snake venom LAAOs are thermo-labile enzymes. They are stable at room temperature and usually store at 4 °C to avoid inactivation. However, many LAAOs are inactivated by freezing and unstable under alkaline conditions. For example, LAAOs isolated from *Crotalus adamanteus* and *Vipera ammodytes* (sand viper) venoms have been reported to undergo reversible pH or temperature-dependent inactivation (Coles *et al*., 1977; Kurth and Aurich, 1976). Curti *et al.* (1968) demonstrated that *C. adamanteus* LAAO was inactivated by storage at between -60 °C and -5 °C, the maximal inactivation was observed at -20 °C. The

inactivation was believed to be due to a limited conformational change of the enzyme structure, presumably in the vicinity of the flavin prosthetic group (Curti *et al*., 1968). Unlike other snake venom LAAOs, *O. hannah* venom LAAO exhibited unusual thermal stability. At pH 7.4, the enzyme retained 100% activity after incubation at 25 °C for 30 days. The enzyme was also stable at alkaline condition and was not inactivated by freezing (Tan and Saifuddin, 1989). Because of these favourable stability properties, *O. hannah* venom LAAO has a greater potential to be developed as a therapeutic agent, when compared to other venom LAAOs. Therefore, it would be an interesting candidate for the investigation of the anti-cancer and antibacterial effects of LAAO.

1.2.5 Chemical properties of L-amino acid oxidase

Snake venom LAAO is a glycoprotein, containing 3 - 4% of carbohydrate. The sugar compositions of oligosaccharide moiety of *C. adamanteus* LAAO was first identified as fucose, mannose, galactose(N-acetyl)glucosamine and sialic acid (deKok and Rawitch, 1969). Glycosylation may improve crystallization of the enzyme as suggested by Geyer *et al*. (2001). The glycan moiety has been shown to mediate the pharmacological actions of LAAO by binding to the cell surface leading to the production of highly localize concentrations of H_2O_2 in or near to the binding interface. This in turn leads to oxidative damage to the cells (Suhr and Kim, 1996; 1999).

The N-terminal amino acid sequences of most snake venom LAAOs are highly homologous, except for *O. hannah* LAAO. The presence of a highly conserved glutamine rich motif may play an important role in substrate binding and therefore the potency of pharmacological activities of snake venom LAAOs (Tan and Fung, 2009; Guo *et al.*, 2012).

Snake venom LAAOs from *Crotalus adamanteus, Crotalus atrox, Calloselasma rhodostoma, Agkistrodon halys blomhoffii, Trimeresurus stejneggeri* and *Bothrops*

moojeni showed sequence homogeneity of approximately 80% (Rodrigues *et al.,* 2009). *Ophiophagus hannah* venom LAAO, however, has been shown to posses only 50% protein sequence homology with other known snake venom LAAOs. Phylogenetic analysis indicated that *O. hannah* venom LAAO is evolutionary distant to other snake venom LAAOs with its unique amino acid sequence (Jin *et al*., 2007).

1.2.6 Antibacterial activity of snake venom L-amino acid oxidase

The emergence of multidrug-resistant bacteria has drawn major attention among healthcare and medical practitioners ever since the introduction of penicillin in the late 1920s (Zainol *et al*., 2013). Although multidrug-resistant *Pseudomonas aeruginosa, acinetobacter sp., Staphylococcus aureus* and *E. faecium* are the best known therapeutic challenges among the gram-negative and gram-positive bacteria, resistance to the most potent antibiotics has been extended to members of the *Enterobacteriaceae* family of gram-negative bacteria, such as *Klebsiella sp., Escherichia coli*, and *enterobacter sp.* (Arias and Murray, 2009). In Malaysia, *P. aeruginosa, S. aureus, K. pneumoniae,* and *E. coli* were the most common healthcare-associated pathogens isolated from patients with nosocomial infection (Hughes *et al*., 2005; Rozaidi *et al*., 2001).

The used of currently available antimicrobial agents in the treatment of bacteria infectious diseases is becoming more challenging due to emergence of several antibiotic-resistance microbial. Therefore, it is important to search for a new potent antibacterial agent in order to supplement the currently increasingly ineffective antibiotics. Snake venom LAAO may be a promising alternative anti-microbial agent. It has been shown to exhibit potent antibacterial activity against both gram-negative and gram-positive bacteria.

Skarnes (1970) was the first to report that a LAAO isolated from *Crotalus adamanteus* venom possessed bactericidal activity. Subsequently, snake venom LAAOs isolated

from *Bothrops jararaca* (Ciscotto *et al*., 2009), *Bothrops marajoensis* (Torres *et al*., 2010), *Bothrops atrox* (Alves *et al.,* 2011), *Bothrops pirajai* (Izidoro *et al.,* 2006), *Trimeresurus jerdonii* (Lu *et al*., 2002), *Naja naja oxiana* (Samel *et al.,* 2008), *Bothrops alternatus* (Stábeli *et al.,* 2004), *Vipera lebetina* (Tõnismägi *et al*., 2006), *Crotalus durissus cascavella* (Toyama *et al*., 2006), *Trimeresurus mucrosquamatus* (Wei *et al*., 2003), *Agkistrodon blomhoffii ussurensis* (Sun *et al*., 2010), and *Bothrops pauloensis* (Rodrigues *et al.,* 2009) have been shown to exhibit antibacterial activity.

It is well established that the bactericidal activity of LAAO is due to the H_2O_2 liberated during the enzymatic reaction, as addition of catalase significantly diminished the antibacterial activity. Toyama *et al*. (2006), for example, using electron microscopic method demonstrated that the H_2O_2 generated during the enzymatic reaction induced bacterial membrane rupture, promoting the release of cytoplasmatic content and subsequently cell death. Although the H_2O_2 generated certainly plays an important role in bactericidal activity of the enzyme, the binding of the enzyme to bacterial membrane is essential for the potency of its bactericidal action. Such binding activity was observed in LAAO isolated from *Agkistrodon halys* using fluorescence labelling method (Zhang *et al*., 2004). Binding to bacteria is important for the antibacterial action of the enzyme as it enables production of highly localized concentration of H_2O_2 and this account for the high antibacterial potency of the enzyme (Ehara *et al*., 2002). Investigation of binding activity of LAAOs isolated from other organisms were also carried out by other authors, such as LAAO isolated from rockfish *Sebastes schlegelii* (Kitani *et al.,* 2008), and giant snail *Achatina fulica* (Ehara *et al*., 2002), and these enzymes were also potent anti-bacterial agent.

Compare to the pathogens, human host cells or normal flora are less sensitive to oxidative damage caused by H_2O_2 or other ROS, which implies that snake venom

LAAOs may selectively kill bacterial strains without causing significant damage to the host (Guo *et al*., 2012). Therefore, this enzyme has potential to be developed as an antibacterial agent.

1.2.7 Apoptosis-inducing activity of snake venom L-amino acid oxidase

Snake venom LAAOs have been reported to induce apoptosis in various cell lines; including mouse lymphocytic leukaemia (Suhr and Kim, 1996), human umbilical vein endothelial, human promyelocytic leukaemia (HL-60), human ovarian carcinoma (A2789), mouse endothelial (KN-3) (Torii *et al*., 1997), human lung carcinoma (A549) (Wei *et al*., 2009), Hela cervical cancer (Zhang and Wei, 2007), rat glioma (C6), human malignant glioma (RBR17T, and U251) (Sun *et al.,* 2003), human leukaemia (HL-60), Jurkat, rat pheochromocytoma (PC-12), murine melanoma (B16F10) (Alves *et al*., 2008), human gastric carcinoma (MKN-45), human colon carcinoma (RKO), human fibroblasts (LL-24), and human adenocarcinoma HUTU (Naumann *et al.*, 2011).

The apoptosis-inducing activity of the enzyme was reduced or abolished in the presence of catalase or other H_2O_2 scavengers, indicating that the H_2O_2 generated by the enzymatic reaction plays an important role in snake venom LAAO-induced apoptosis cell death. However, the morphological changes of cells induced by snake venom LAAO were different from that generated by the exogenous H_2O_2 (Guo *et al.,* 2012), suggesting that snake venom LAAO-induced apoptosis is not entirely due to the H_2O_2 liberated into the medium. Takatsuka *et al.* (2001) demonstrated that snake venom LAAOs were able to bind directly to cell surface thereby increasing the local peroxide concentration, and suggested that the binding activity played an important role in the apoptosis-inducing effect. Sun *et al.* (2003) suggested that the apoptotic effect of *Trimeresurus flavoviridis* LAAO on malignant glioma cells is mediated by the production of intracellular reactive oxygen species (ROS). Zhang and Wu (2008)

demonstrated that *Agkistrodon acutus* LAAO increased accumulation of sub-G1 phase cells, and subsequently apoptosis cell death. Zhang and Wei (2007) suggested that mitochondrial apoptosis pathway played a role in ACTX-8-induced cell apoptosis. Thus, these reports clearly demonstrated that snake venom LAAO is an apoptosis-inducing enzyme; and that its cytotoxic activities on cancer cell lines were presumably due to the production of high local concentration of H_2O_2, which depends on the molecular interaction of its glycan moiety with the cell surface.

1.3 Overview of cancers

Cancer is a class of diseases in which a group of cells display uncontrolled growth (division beyond the normal limits), invasion (intrusion on and destruction of adjacent tissues), and sometimes metastasis (spread to other locations in the body via lymph or blood) (Smart, 2010).

Cancer is the leading cause of death globally and accounted for 7.6 million deaths, which is around 13% of all deaths in 2008. The deaths are caused mainly by lung (1.37 million deaths), stomach (736 000 deaths), liver (695 000 deaths), colorectal (608 000 deaths), breast (458 000 deaths), and cervical (275 000 deaths) cancers. Deaths from cancer worldwide are projected to continue rising, with an estimated 13.1 million deaths in 2030 (WHO, 2013). In Malaysia, a total of 18,219 new cancer cases were diagnosed in 2007 and registered with National Cancer Registry (NCR). It comprises of 8,123 males and 10,096 females. The most common cancers among Malaysian during that period were breast, colorectal, lung, nasopharynx, cervical, lymphoma, leukaemia, ovary, stomach and liver (NCR, 2007).

Lung cancer was the top leading cause to overall cancer mortality of estimated 1.37 million deaths reported in 2008 worldwide (WHO, 2013). In Malaysia, it was the most common cancer among males and third most common cancer in the general population

with a total of 1,865 cases registered with NCR in 2007 (NCR, 2007). Breast cancer was the forth leading cause to overall cancer death and accounted for 458,000 deaths (WHO, 2013). In Malaysia, it was the most common cancer in females and also the most common cancer among Malaysian. A total of 3,242 cases were diagnosed in 2007 and reported to NCR. Leukaemia was the seventh most common cancer among Malaysian with a total of 741 cases registered with NCR in 2007. Prostate cancer was the fourth most common cancer in Malaysian males with a total of 502 cases diagnosed and reported to NCR in 2007 (NCR, 2007).

Chemotherapy, one of the most common modes of treatment, is also known for its potential to cause toxicity to normal cells, accompanied by a range of side effects such as vomiting, nausea and other severe complications. As such, there is always a need to search for new, potent and natural-based therapeutic agents that hopefully exhibit potent cytotoxicity against cancer cells over the normal cells, thus minimizing the undesirable side effects of chemotherapy.

1.4 Apoptosis: a cell suicide mechanism

Apoptosis, or programmed cell death, is a cell-intrinsic mechanism for suicide regulated by a variety of cellular signalling pathways (Edinger and Thompson, 2004). Apoptosis plays a crucial role in various processes during development and aging and as a homeostatic mechanism to maintain cell populations in tissues (Elmore, 2007). Dysregulation of apoptosis is implicated in various pathological states. Excessive apoptosis is associated with neurodegenerative disorders, immunodeficiency and infertility, whereas deficient apoptosis is associated with cancer, autoimmunity, and viral infections (Danial and Korsmeyer, 2004).

Apoptosis is characterized by a series morphological and biochemical changes such as shrinkage of cell, loss of plasma membrane asymmetry and attachment, plasma

membrane blebbing, chromatin condensation (pyknosis), chromosomal DNA fragmentation as well as formation of apoptotic bodies (Edinger and Thompson, 2004). Apoptotic bodies are subsequently recognized and removed by macrophages, parenchymal cells, or neoplastic cells and degraded within phagolysosomes, without causing any inflammatory response (Elmore, 2007).

Apoptosis is mediated by two inter-related signalling pathways: the intrinsic (mitochondria-mediated apoptosis) and extrinsic (death receptor-mediated apoptosis) pathways. The intrinsic pathway is associated with loss of mitochondrial membrane potential, and the release of pro-apoptotic factors into the cytosol in response to various stimuli, whereas the extrinsic pathway is mediated by the binding of ligand to cell surface death receptors and catalytically activate the caspase-8 (Bjelakovic *et al*., 2005; Beere, 2005). Regardless of which pathway is initiated, both pathways will eventually converge to a final apoptosis execution phase resulting in DNA fragmentation, degradation of cytoskeletal and nuclear proteins, and eventually the formation of apoptotic bodies (Elmore, 2007).

1.4.1 Extrinsic pathway: death receptor-mediated apoptosis

The extrinsic signalling pathway is mediated by death receptors that belong to the members of the tumour necrosis factor (TNF) receptor gene superfamily (Locksley *et al*., 2001). The well-known ligands and their corresponding death receptors are TNF-*α*/TNF-R1, FasL/FasR, Apo3L/DR-3, Apo2L/DR-4 and Apo2L/DR-5 (Elmore, 2007).

Using TNF-*α*/TNF-R1 as an example, binding of TNF ligand to TNF-R1 receptor enables the binding of multifunctional adaptor protein, TNF-R1 associated death domain (TRADD) to Fas-associated protein with death domain (FADD), with recruitment of receptor-interacting protein (RIP) (Hsu *et al*., 1995). This in turn initiates the formation of a death-inducing signalling complex (DISC), leading to caspase-8

activation and subsequently cleavage of effector caspases and leads to apoptosis (Kischkel *et al*., 1995). Table 1.1 lists the major extrinsic pathway proteins and its common abbreviations.

Table 1.1: Extrinsic pathway proteins and its abbreviations

Abbreviation	**Protein name**
Apo2L	Apo2 ligand
Apo3L	Apo3 ligand
Caspase-8	Cysteinyl aspartic acid-protease 8
DISC	Death-inducing signalling complex
DR-3	Death receptor 3
DR-4	Death receptor 4
DR-5	Death receptor 5
FADD	Fas-associated death domain
FasL	Fatty acid synthetase ligand
FasR	Fatty acid synthetase receptor
TRADD	TNF receptor-associated death domain
TNF-α	Tumour necrosis factor alpha
TNF-R1	Tumour necrosis factor receptor 1

1.4.2 Intrinsic pathway: mitochondria-mediated apoptosis

The mitochondria-mediated apoptosis pathway is activated by a variety of extracellular and intracellular death signals such as radiation, physical stress, oxidative stress, DNA damage, and protein misfolding (Crow *et al*., 2004). This pathway is associated with mitochondria dysfunction, release of apoptogenic proteins into the cytosol, and accompanied by the activation of caspase proteases which are responsible for cell disassembly (Vande *et al*., 2000).

Integrity of the mitochondrial membrane is regulated by Bcl-2 family member proteins (Borner, 2003). This protein family can be divided into three groups: the anti-apoptotic members (Bcl-2, Bcl-xL, Bcl-w, Mcl-1, and Bfl-1/A1), the BH3-only protein (Bad, Bik, Bid, Bim, Bmf, Noxa, PUMA), and the pro-apoptotic members (Bax, Bak, and Bok). The BH3-only proteins act as activators for the pro-apoptotic Bcl-2 family member proteins (Sprick and Walczak, 2004).

Activated Bax and/or Bak (Bcl-2 homologous antagonist/killer) results in an opening of the mitochondrial permeability transition (MPT) pore, and release of the cytochrome *c*, Smac/DIABLO, serine protease HtrA2/Omi, apoptosis-inducing factor (AIF), endonuclease G, and caspase-activated DNAse (CAD) from the mitochondrial intermembrane space (Elmore, 2007). Association of cytochrome *c*, dATP, Apaf-1, and procaspase-9 forming a functional apoptosome, leading to procaspase-9 activation and subsequently triggers the execution-phase of cell apoptosis through the activation of effector procaspase-3 (Arya *et al*., 2007). Smac/DIABLO and serine protease HtrA2/Omi promote apoptosis by inhibiting IAP (inhibitors of apoptosis proteins) activity (Schimmer, 2004; Loo *et al*., 2002). Apoptosis-inducing factor (AIF), endonuclease G, and CAD are involved in nuclear DNA fragmentation (Enari *et al*.,

1998; Joza *et al*., 2001; Li *et al*., 2001). Table 1.2 lists the major intrinsic pathway proteins and its common abbreviations.

Table 1.2: Intrinsic pathway proteins and its abbreviations

Abbreviation	Protein name
AIF	Apoptosis inducing factor
Apaf-1	Apoptotic protease activating factor
Bad	Bcl-2 antagonist of cell death
Bak	Bcl-2 antagonist killer 1
Bax	Bcl-2 associated X protein
Bcl-2	B-cell lymphoma protein 2
Bcl-w	Bcl-2 like 2 protein
Bcl-xL	Bcl-2 related protein, long isoform
Bfl-1/A1	Bcl-2-related protein A1 isoform 2
Bid	BH3 interacting domain death agonist
Bik	Bcl-2 interacting killer
Bim	Bcl-2 interacting protein BIM
Bmf	Bcl-2-modifying factor
Bok	Bcl-2 related ovarian killer
CAD	Caspase-activated DNAse
Caspase-9	Cysteinyl aspartic acid-protease-9
HtrA2/Omi	High temperature requirement protein A2/ Omi stress-regulated endoprotease
Mcl-1	Myeloid cell leukaemia sequence 1
Noxa	Phorbol-12-myristate-13-acetate-induced protein 1
PUMA	Bcl-2 binding component 3
Smac/DIABLO	Second mitochondrial activator of caspases/direct IAP binding protein with low PI

1.4.3 Cross-talk between extrinsic and intrinsic pathways

Cross-talk between extrinsic and intrinsic pathways occurs through truncated Bid (tBid), which is generated upon the proteolysis of BH3-interacting domain death agonist (Bid) by the activated caspase-8 (derived from the extrinsic pathway), The translocation of tBid to mitochondria promotes outer membrane permeabilization, release of apoptogenic factors, and thereby activating the intrinsic pathway (Khosravi and Esposti, 2004). Schematic relations between intrinsic, extrinsic, and the cross-talk of the two apoptosis pathways is illustrated in Figure 1.3.

Evidence has shown that both extrinsic and intrinsic apoptosis pathways can activate each other. Activation of caspase-3 by caspase-9 triggers the activation of caspase-8 in a feedback amplification loop. It is also speculated that activated caspase-3 might activate caspase-9 in a similar retrograde manner (Hotchkiss and Nicholson, 2006).

Both extrinsic and intrinsic parthways converge at the execution phase. At this point, caspase-3, caspase-6, and caspase-7 function as effector or “executioner” caspases activate cytoplasmic endonuclease that ultimately cause the morphological and biochemical changes seen in apoptotic cells (Elmore, 2007).

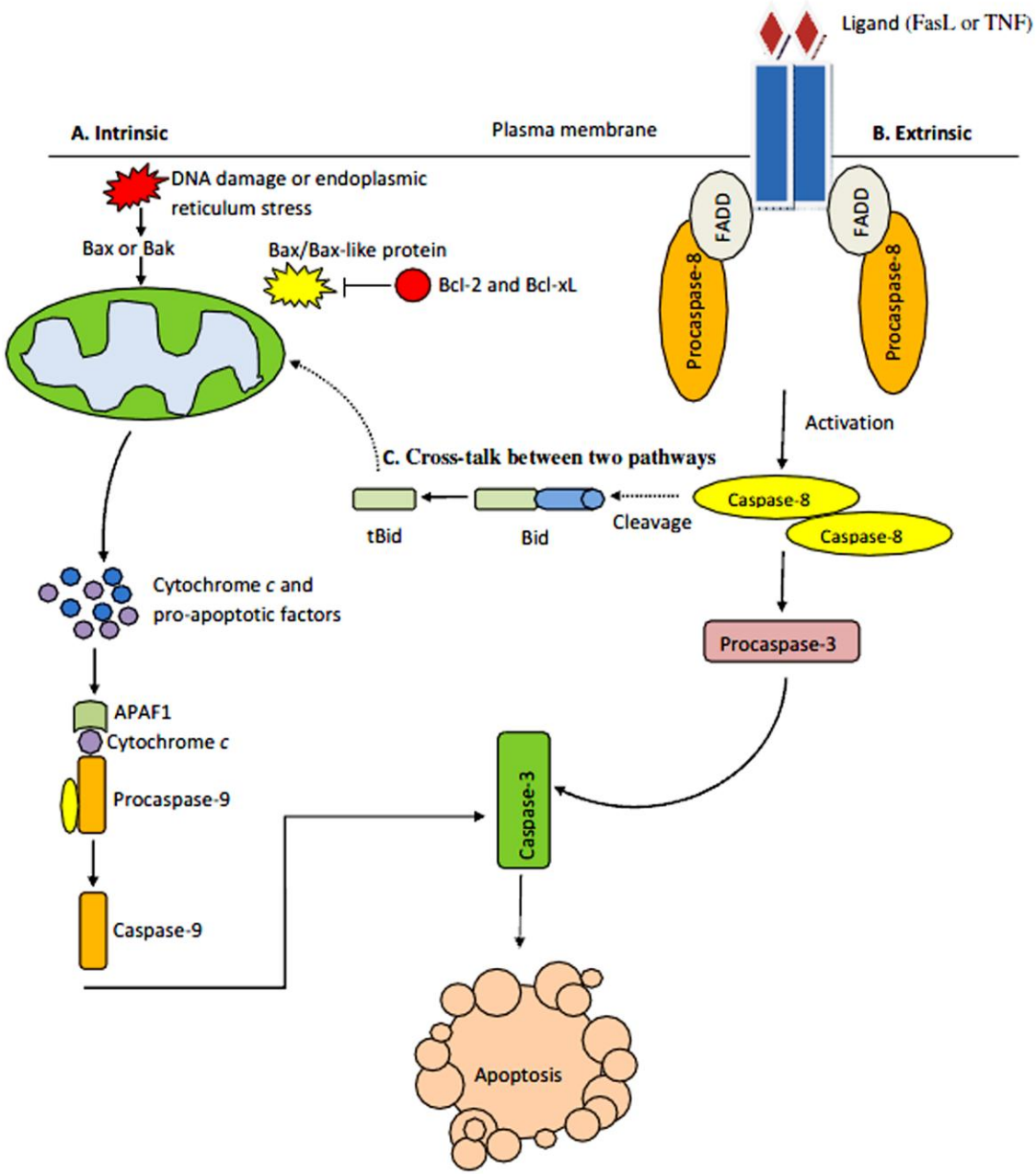

Figure 1.3: Schematic relations between intrinsic, extrinsic, and the cross-talk of the two apoptosis pathways. Apoptosis is mediated by two signalling pathways: A) intrinsic (mitochondria) and B) extrinsic (death receptor) pathways. The intrinsic pathway is associated with loss of mitochondrial membrane potential, release of cytochrome *c* into the cytosol, and accompanied by activation of caspase-9. The extrinsic pathway is mediated by the binding of ligand to cell surface death receptors and catalytically activate the caspase-8. C) The two pathways are interconnected by truncated Bid (tBid) that is formed when Bid is cleaved by active caspase-8.

1.5 Oxidative stress and apoptosis

Mitochondria is the main site of generation of oxygen radicals, such as, superoxide anions (O_2^-), hydroxyl radicals (OH·), singlet oxygen ($^1O_2$) and hydrogen peroxide (H_2O_2) within the cell (Kannan and Jain, 2000). Imbalance between the reactive oxygen species (ROS) generation and elimination could disrupt cellular redox homeostasis, leading to an overall increase of intracellular ROS levels, or oxidative stress (Trachootham *et al*., 2008). It has been suggested that the global shutdown of mitochondrial function under oxidative stress conditions could contribute to apoptosis due to dramatically decrease in cellular energy supply (Morel and Barouki, 1999).

Reactive oxygen species are known to serve as second messengers for various signalling pathways as well as a potent mediator of signal transduction via oxidative modification of signalling proteins (Trachootham *et al*., 2008; Verzola *et al*., 2004). Activation of Jun N-terminal kinase (JNK) has been shown to induce mitochondria-mediated apoptosis, in response to oxidative stress. Induction of apoptosis by activated JNK involves direct activation of BH3-only proteins (Bim, Bmf, and Bad), and inhibition of anti-apoptotic proteins (Bcl-2, Bcl-xL, and Mcl-1). This in turn promotes translocation and activation of Bax/Bak, leading to mitochondria-mediated apoptosis (Weston and Davis, 2002). Furthermore, activation of JNK was shown to promote its dissociation from p53, leading to stabilization of p53 which ultimately leads to apoptosis (Trachootham *et al*., 2008).

Recent studies also raised the possibility that Akt (v-Akt murine thymoma viral Oncogene)/PKB (protein kinase-B), a serine/threonine kinase pathway may be activated by Fas ligand under oxidative stress condition and that this signalling pathway may be involved in Fas-mediated cell death (extrinsic pathway) (Lu *et al*., 2006). Activation of

this pathway is mainly through oxidative modification of Cys-dependent phosphatases (CDPs) and protein kinases in a redox-sensitive manner (Trachootham *et al*., 2008).

1.6 Cytotoxic and apoptosis detection assays

1.6.1 The MTT assay

The MTT (3-[4,5-dimethylthiazol-2-yl]-2,5-diphenyltetrazolium bromide) assay, a method developed by Mosmann (1983) is most commonly employed for the detection of cytotoxicity or cell viability following exposure to the treatment compound *in vitro.* The principle of this assay is based on the cleavage of the tetrazolium salt MTT (3-[4,5-dimethylthiazol-2-yl]-2,5-diphenyltetrazolium bromide) into an insoluble purple formazan by the mitochondria enzyme succinate dehydrogenase (Fotakis and Timbrell, 2006). The reduction activity takes place only in living cells and the amount of the formazan product is proportional to the number of viable cells that present in the culture (Denizot and Lang, 1986).

The MTT assay has been tested for its validity and reproducibility in various cell lines (Mosmann, 1983). Subsequently, Denizot and Lang (1986) and Hansen *et al*. (1989) developed improved versions of the assay.

1.6.2 DNA fragmentation assay

Apoptosis is often accompanied by the cleavage of chromosomal DNA into internucleosomal fragments of about 180 - 200 base pairs (bp) (Collins *et al*., 1997). Caspase-activated DNase (CAD) was identified as a DNase that is responsible for the process of DNA fragmentation in 1998 (Nagata *et al*., 2003). Caspase-activated DNase is produced as a complex with inhibitor of caspase-activated DNase (ICAD). Recombinant ICAD specifically inhibits CAD-induced degradation of nuclear DNA and its DNase activity. During apoptosis, activated caspases cleave ICAD, allowing CAD to enter to the nucleus and degrade chromosomal DNA into internucleosomal fragments

by cleaving the DNA at the linker sites between nucleosomes (Enari *et al*., 1998). Fragmented DNA was often analysed using agarose gel electrophoresis to demonstrate a "ladder" pattern at ~200 bp intervals (Collins *et al*., 1997).

1.6.3 Terminal deoxynucleotidyl transferase dUTP nick end labelling (TUNEL) assay

Another method for examining apoptosis via detection of fragmented DNA is by the terminal deoxynucleotidyl transferase-dUTP nick end labelling (TUNEL) assay that was originally introduced by Gavrieli *et al*. (1992). TUNEL assay has become a widely used staining method in detection of apoptotic cells in tissue sections (Labat-Moleur *et al*., 1998).

TUNEL is based on the ability of the enzyme terminal deoxynucleotidyl transferase (TdT) to incorporate labelled dUTP into free 3′-hydroxyl termini ends of the fragmented DNA (Gavrieli *et al*., 1992). After proteolytic treatment of tissue sections, TdT incorporates X-dUTP (X = biotin, digoxigenin, or fluorescein) at sites of DNA strand breaks (Blankenberg, 2008). Terminally modified nucleotides are then allowed to bind with the antibody that is conjugated to a peroxidase reporter molecule. The bound peroxidase antibody conjugate enzymatically generates a permanent, intense, localized signal from chromogenic substrates, providing sensitive detection using light or fluorescent microscopy, flow cytometry, or via immunohistochemistry.

1.6.4 Annexin-V binding assay

Annexin-V binding assay is a rapid and reliable method for detecting early stages of apoptosis. This assay is based on the relocation of phosphatidylserine (PS) from the inner leaflets of the plasma membrane to the cell surface, soon after the apoptosis is initiated (Zhang *et al*., 1997). Viable cells maintain an asymmetric distribution of

different phospholipids between the inner and outer leaflets of the plasma membrane; phosphatidylcholine and sphingomyelin are exposed on the external leaflet of the lipid bilayer, while PS is located on the inner surface. During apoptosis, asymmetry of the cell membrane is disrupted and membrane PS is translocated from the inner to the outer leaflet of the plasma membrane while maintaining their intact plasma membrane integrity (Van Engeland *et al*., 1996). Annexin V is a 35 - 36 kDa Ca^{2+}-dependent phospholipid-binding protein with high affinity for PS, and binds to exposed apoptotic cell surface PS (Van Engeland *et al*., 1996; Vermes *et al*., 1995). Annexin V can be conjugated to fluorochromes such as phycoerythrin (PE) or fluorescein isothiocyanate (FITC) to serve as a sensitive probe for detection using flow cytometry while retaining its high affinity for PS.

Staining with Annexin V is typically used in conjunction with a vital dye such as propidium iodide (PI) or 7-amino-actinomycin (7-AAD) to allow differentiation of apoptotic cells. Viable cells with intact membranes exclude vital dye, whereas the membranes of dead and damaged cells are permeable to the viable dye. Therefore, apoptotic populations can be distinguished from dead or damage cells using double staining method (Hingorani *et al*., 2011). For example, using Annexin V/7-AAD staining, three populations of cells are distinguishable in two colour flow cytometry:

Viable cells: Annexin-V negative and 7-AAD negative;

Early apoptotic cells: Annexin-V positive and 7-AAD negative;

Necrotic cells or late apoptotic cells: Annexin-V positive and 7-AAD positive.

1.7 An overview of immunodeficient nude mouse model

A nude mouse is a genetic mutant that has a deteriorated or removed thymus gland, resulting in immunodeficient due to a greatly reduced number of T cells (Belizário,

2009). They are characterized by lack of body hair (hairless) due to abnormal keratinization of hair follicles, reduced body growth rate, decreased fertility and usually die within 3 to 14 weeks of age (Flanagan, 1966). The genetic basis of the nude mouse mutation is a disruption of the *Foxn*1 gene or the HNF-3/forkhead homolog 11 gene (Nehls *et al*., 1994).

The immune system of nude mouse is characterized by a reduced number of T cells, antibody response confined to IgM class, low T-dependent response to antigens and an increased natural killer cell response. Consequently the rudimentary thymus produces small population of mature T cells, with the result that nude mouse do not reject allografts or xenografts as they mount no rejection response (Belizário, 2009). Nude mouse are commonly employed for studies of imaging testing as well as pharmacological treatment of human tumour xenografts (Vidal and Richert, 2012).

1.8 The study of gene expression

Gene expression is a process by which the information encoded in the gene is transformed into a functional gene product. The gene products are often proteins, but some are functional RNAs. Study of gene expression will assist in the understanding of the functions of genes and the gene products, as well as the cellular regulatory networks that are involved in response to various stimuli by looking at the alteration of gene transcription profiles. Gene expression study becomes a powerful tool in various research fields after the introduction of microarray technology, which enables the study of the gene expression alteration profile of thousands of genes simultaneously.

Analysis of gene expression patterns using microarray-based technology have been adopted in cancer research (Cooper, 2001; Grant *et al*., 2004; Kumar *et al*., 2012), as well as in studying the expression pattern of inflammatory diseases (Heller *et al*., 1997;

Torri *et al*., 2010). This approach has become a crucial tool in disease therapy, drug discovery, diagnostic applications, and finally to improve the treatment outcome.

Global gene expression study using microarray technology enables simultaneous measurement of the expression of thousands of genes in a high-throughput fashion and allows characterization of gene transcription profiles which reflect the changes in the biological processes within the cells. However, much of the regulation of physiological processes occurs post-transcriptionally. Thus, measurement of mRNA levels alone is insufficient to give a complete picture of cellular activity and some other approaches such as proteomic study may be necessary in coupling with gene expression analysis.

1.8.1 Microarrays

Microarrays consist of hundreds to thousands of discrete DNA fragments or synthetic oligonucleotides that are immobilized on the glass or silicone surfaces using a variety of technologies such as photolithography, mechanical microspotting, and ink-jet printing (Schena *et al*., 1998). This technology has been applied to a wide range of studies, including gene expression analysis (Braxton and Bedilion, 1998; Schulze and Downward, 2001), genomic analysis (Meltzer, 2001; Sapolsky *et al*., 1999), and drug discovery process (Lockhart and Winzeler, 2000).

Microarrays can be divided into two major groups based on the arrayed material. Oligonucleotide microarrays which can either be produced by spotting pre-synthesised short oligonucleotides onto the glass or synthesised *in situ* on the silicone wafer surface by photolithography. DNA microarrays consist of longer DNA fragments that are typically generated using the polymerase chain reaction (PCR) or inserted from cDNA libraries. The DNA fragments are printed on the glass slides or nylon (Schulze and Downward, 2000).

Oligonucleotide-based microarrays are becoming increasingly useful for the analysis of gene expression and single nucleotide polymorphisms because of its certain advantages over cDNA microarrays. In addtion to its capacity to screen whole genomic regions for gene function discovery study (Shoemaker *et al*., 2001), oligonucleotide microarrays has unique oligomer probes designed that specifically represent the cognate gene and minimizing cross-hybridization between similar sequences (Harrington *et al*., 2000), which makes it particularly useful for the analysis of single nucleotide polymorphisms (LaForge *et al*., 2000) or mutational analysis (Drobyshev *et al*., 1997). Since biological samples or cDNA collections are not required to generate oligonucleotide array elements, the handling and tracking of oligonucleotide microarrays are generally easier compared to cDNA microarrays (Relogio *et al*., 2002).

The principle of microarray technology involves manufacturing of microarrays, target preparation and array hybridization, and image acquisition and data analysis. It is based on the fact that the complementary nucleic acid sequences (target) hybridize with the oligonucleotide probes, which are immobilized on the solid support.

1.8.1.1 Manufacturing of microarrays

Microarray fabrication involves the printing and attachment of probes on the array. The key considerations in selecting a fabrication technology include microarray density and design, biochemical composition and versatility, reproducibility, throughput, quality, cost and ease of prototyping. The most widely used printing technologies are photolithography, mechanical microspotting, and ink-jet printing (Schena *et al*., 1998).

In general, there are two types of microarray-fabricating technologies: synthesis and delivery (Schena *et al*., 1998). Synthesis approach is based on photolithographic synthesis of oligonucleotides *in situ.* In this approach, ultraviolet light is used to direct the adding of nucleotides to the growing nucleotide chains until the desired length is

achieved (Henriksen and Kotelevtsev, 2002; Schena *et al*., 1998). In contrast, delivery approach involves robotic deposition of cDNA clones amplified by PCR fragments onto known regions of the arrays (Schena *et al*., 1995).

1.8.1.2 Target labelling and hybridization

Several methods for target-producing are currently available for microarray hybridization and can be broadly classified into three categories: direct, indirect, and DNA dendrimer labelling. In direct labelling approach, the target sequence used in hybridization is prepared by reverse transcription in the presence of fluorescently labelled deoxynucleotides to produce fluorescently labelled cDNA, which will competitively hybridize to cDNA or oligonucleotides on the array (Hegde *et al*., 2000). This method however, results in lower nucleic acid target yields and significant fluor-dependent dye bias due to steric hindrance of the large fluorescent moieties that were attached to the labelled nucleotides (Ouellet *et al*., 2009).

In indirect labelling approach, modified (amino-allyl) nucleotides are introduced into the target samples during reverse transcription, and fluorescent dyes which can emit fluorescent light when excited with a laser are conjugated to these group in a subsequent reaction (Manduchi *et al*., 2002). Although indirect labelling method is able to improve dye incorporation and minimize dye bias, this method however, increased the amount of the starting material used and sample preparation time (Ouellet *et al*., 2009).

Dendrimer labelling method was developed mainly aimed to increase specific fluorescence of the labelled product and decreasing the use of the starting material (Ouellet *et al*., 2009). In this technique, the initial reverse transcriptase reaction is primed with an oligonucleotide containing specific capture sequences that can bind with cyanine dye-tagged dendrimers. The cDNAs containing the “capture” sequences are first hybridized to the microarrays, and the bound cDNAs on the microarrays are

detected by incubating the arrays with the fluorescent dye-tagged dendrimers (Manduchi *et al*., 2002).

Microarray hybridization is based on the association of a single stranded nucleic acid molecule labelled with a fluorescent tag with its complementary strand molecule that are immobilized on a solid support. Hybridization and washing steps are performed under highly stringent conditions to minimize the likelihood of cross-hybridization between similar genes and to remove the non-specific target binding (Macgregor and Squire, 2002; Tarca *et al*., 2006).

1.8.1.3 Data-mining

The complexity and vast amount of data generated by a single microarray experiment typically require a dedicated data analysis tools to process the data set prior to the analysis and interpretation of the results. Several data analysis tools have been developed to facilitate the analysis of microarray data. The methods used for data mining and data interpretation are varied, ranging from straightforward lists of increased and decreased genes expressed, based on user-defined thresholds to the integration of sophisticated clustering and visualization programs, such as hierarchical clustering, self-organizing maps and k-means clustering (Harrington *et al*., 2000). Pre-processing step is necessary in order to extract or enhance the meaningful data characteristics and to prepare the data set for the application of data analysis methods (Tarca *et al*., 2006).

Basically, there are three steps required for efficient and effective data analysis: data normalization, data filtering, and pattern identification. Data normalization is necessary to correct for any bias arises from variation in labelling and detection efficiencies for the fluorescent intensity (Hegde *et a*l., 2000). Following data normalization, data filtering can be done to exclude genes that are expressed below the defined threshold level. By using this method, quantity of the dataset can be reduced. The last step is to identify the

expression patterns and to classify the data to assign biological meanings/significance to the expression profiles (Harrington *et al*., 2000).

Integrating data analysis tool with a comprehensive database such as GenBank, Entrez, BLAST, and PubMed, provided by National Centre for Biotechnology Information (NCBI, http://www.ncbi.nlm.nih.gov/) would allow identification of common properties and biological functions of the differentially regulated genes and hence, more valuable information can be obtained from the microarray data (Harrington *et al*., 2000). Although the use of normalization approach during microarray data analysis can minimize the introduction of systematic bias when working with large numbers of the variables, nevertheless variable errors may be introduced at any points between the production of microarrays and the analysis of hybridization signals. The two critical steps that may strongly affect the microarray results are the isolation of RNA and labelling of target samples. Therefore, important results obtained from microarrays must be confirmed with other technique, such as real-time polymerase chain reaction (RT-PCR) (Lucchini *et al*., 2001).

1.8.2 Real-time polymerase chain reaction (RT-PCR)

The real-time, fluorescence-based reverse transcription followed by polymerase chain reaction (PCR) has become an extensively applied technique in molecular biology study, medicine, and diagnostics fileds. It enables analysis of expression pattern of messenger RNA (mRNA) and to compare the relative levels of mRNA within distinct biological samples. Most importantly, this technique has become a method of choice for validation of microarray results (Jozefczuk and Adjaye, 2011).

Several factors have contributed to the transformation of this technology into a mainstream research tool: (i) as a homogenous assay it avoids the need for post-PCR processing; (ii) a wide (> 10^7-fold) dynamic range allows straightforward comparison

between RNAs that differ widely in their abundance; and (iii) the assay realizes the inherent quantitative potential of the PCR, making it a quantitative as well as a qualitative assay (Ginzinger, 2002).

Real-time PCR uses fluorescent reporter molecules to monitor the amplification products during each cycle of the PCR reaction (Bustin *et al*., 2005). Because the amount of product is detected as a reaction progresses in "real time", real-time PCR has advantages in providing a wide linear quantification dynamic range, demonstrating high sensitivity, and good reproducibility (Bustin, 2000; Lockey *et al*., 1998; Orlando *et al*., 1998). However, errors will be introduced due to minor differences in the starting amount of RNA, quality of RNA or differences in efficiency of cDNA synthesis and PCR amplification. In order to minimize these errors and correct for sample-to-sample variations, an endogenous control gene is usually introduced to normalize the PCRs for the amount of RNA added to the reverse transcription reactions (Arya *et al*., 2005; Livak and Schmittgen, 2001). The most common housekeeping genes used for normalization include β-actin, glyceraldehyde 3-phosphate dehydrogenase (GAPDH), β_2-microglobulin, and ribosomal RNA (rRNA) (Livak and Schmittgen, 2001). It is essential that the housekeeping gene is minimally regulated and exhibit a constant and cell cycle-independent basal level of transcription (Selvey *et al*., 2001). However, none of the housekeeping genes are ideal for each specific experiment. The selection of the housekeeping gene is depending on the cells type and the experimental condition

1.8.2.1 Detection methods

Two common methods for quantitative detection of real-time PCR products have been established: non-specific double-stranded DNA (dsDNA)-intercalating agents (DNA-binding dyes), and sequence-specific fluorescent probes (Arya *et al*., 2005). The formar includes SYBR® Green 1 or ethidium bromide. SYBR® Green 1 binds to dsDNA and

exhibits enhancement of fluorescent signal. An increase in PCR products during reverse transcription reactions therefore leads to an increase in fluorescence intensity that was measured at the end of each PCR cycle, thus allowing amount of the PCR products to be quantified. This detection method is relatively inexpensive and can be used to monitor the amplification of any dsDNA sequence. As the presence of any dsDNA generates fluorescent, specificity and accuracy of this method is greatly decreased due to amplification of non-specific PCR products and primer-dimer (Ririe *et al.*, 1997).

The sequence-specific TaqMan® hydrolysis probes are mainly dependent on 5'-3' exonuclease activity of Taq polymerase to quantitate the target amplicons in the samples (Holland *et al*., 1991). TaqMan® probes are oligonucleotides labelled with a fluorescent reporter dye at 5' end and a quencher moeity at the other 3' end, designed to hybridize specifically to an internal region of a PCR products. In the unhybridized state, the proximity of the reporter and quencher dyes prevent fluorescent emission to occur. During PCR amplification, the probe anneals to the target and cleaved by 5'-nuclease activity of Taq polymerase, resulting in emission of fluorescent signals from the reporter dye. The increased in fluorescent intensity is directly proportional to the amount of probe cleavage (Arya *et al*., 2005; Tsai *et al*., 2012). The advantages of TaqMan® chemistry is that the fluorescent signal is generated only when there is specific hybridization of the probe to the target sequence, because the probes can be labelled with spectrally distinct reporter dyes, it allows the amplification of multiple target sequences within a single tube (multiplex real-time PCR). The primary disadvantage of TaqMan® hydrolysis probes is that the synthesis of different probes is required for different target sequence, which renders the method less cost effective.

Other detection methods using target-specific hybridization to sdDNA (single-stranded DNA) have been introduced, including molecular beacons, scorpions, an expanded

genetic information system *(*AEGIS), labelled primers, and light-up probes (Rickert *et al*., 2004).

1.8.2.2 Quantitation of results

The basic principle of real-time PCR is straightforward: the initial amount of template DNA used is inversely proportional to the threshold cycle (Ct). Threshold cycle is defined by amplification cycles that are required for the fluorescent signal to reach the threshold level of detection (Bustin *et al*., 2005). The Ct value will be employed to quantify the results obtained by real-time PCR. Generally, the levels of expressed genes can be measured by absolute or relative quantitative methods.

In absolute or standard-curve quantitation, a standard curve (log of concentration of known standards versus Ct) is first constructed. The standard curve is then used as a reference standard to determine the amount of the target in the unknown sample by comparing to the Ct value. The most common source of the standards is plasmid of the gene of interest or synthetic single-stranded oligonucleotide for the amplicon (Arya *et al*., 2005). By using standard-curve quantitation method, it is possible to calculate the number of nucleic acid targets present in the sample in relation to a specific unit, this allow data comparison between different assays and laboratories (Mackay, 2004). However, this method is time consuming to quantify and validate an independent reliable standard for each gene that is subjected to analysis (Bolha *et al*., 2012).

Relative quantitation involves the use of mathematical equation to calculate the expression levels of the target gene in relative to a reference control gene (calibrator) (Pfaffl, 2001). This approach is relatively easier to perform because a calibration curve is not necessary and is useful for most purposes for investigation of the physiological changes in gene expression levels (Bolha *et al*., 2012). Since relative quantitation is widely applied in real-time PCR analysis, several mathematical models for calculating

relative expression ratio have been established. The most commonly used model is comparative threshold ($2^{-\Delta\Delta Ct}$) method. In this method, the amount of target, which is normalized to an endogenous reference and relative to a calibrator, is given by $2^{-\Delta\Delta Ct}$, where $\Delta\Delta Ct = \Delta Ct$ (sample) – ΔCt (control), and ΔCt for both the sample and control of the target gene are normalized to an appropriate endogenous housekeeping gene. In order for $\Delta\Delta C_t$ calculation to be valid, amplification efficiencies of the target and reference must be approximately equal (Livak and Schmittgen, 2001).

1.9 Proteomics

Proteomics is a study of structure, function and expression of proteins in a complex biological sample. Study of protein expression is important in coupling with gene expression analysis due to the reasons that: protein expression and its activity levels can differ significantly from RNA levels, and the regulation of gene activity occurs at the translational level (Michaud and Snyder, 2002).

In combination with large-scale protein separation and mass spectrometry (MS) analyses, proteomics has become a popular approach for the study of proteome profiling, comparative protein expression analysis, localization and identification of protein post-translational modifications, and protein-protein interactions (Chandramouli and Qian, 2009). Protein expression analysis could provide useful information on cellular processes that occur during development, response of cells to the treatment conditions, as well as differential proteomic profiling between normal and disease state tissues (Michaud and Snyder, 2002).

1.9.1 Two-dimensional polyacrylamide gel electrophoresis

Two-dimensional polyacrylamide gel electrophoresis (2D-PAGE) is routinely applied for quantitative and qualitative expression profiling of complex protein mixtures in the

whole cell or tissue lysates (Gorg *et al*., 2004). This approach involves the separation of complex protein mixtures by molecular charge in the first dimension and followed by molecular weight in the second dimension (Chandramouli and Qian, 2009). In the first dimension, proteins are isoelectrically focused in a pH gradient, allowing for separation based on the isoelectric point (pI). In the second dimension, an electric field is applied to separate the proteins based on their mass or mobility through a polyacrylamide gel matrix (Michaud and Snyder, 2002; McDonald and Yates, 2000).

The 2D-PAGE allows separation and comparison of thousands of proteins on a single gel and information such as the protein pI, the apparent molecular weight, and the abundance of each protein can be obtained (Chandramouli and Qian, 2009). A numbers of dedicated 2D-PAGE image databases have been constructed to provide proteomic profile for different cells and tissues (Hoogland *et al*., 1999). This approach has been widely adopted in cancer research (Chen *et al*., 2002; Chuthapisith *et al*., 2007; Hathout *et al*., 2002).

1.9.2 Mass spectrometry (MS)

Mass spectrometry (MS) is a fundamental tool for protein identification in proteomics research. It can precisely measure the mass and determine the amino acid sequence of a peptide (Michaud and Snyder, 2002). A mass spectrometer consists of three components: ion source, mass analyser, and detector. Analysis of proteins by MS occurs in three major steps (a) protein ionization and generation of gas-phase ions, (b) separation of ions according to their mass-to-charge ratio (m/z), and (c) detection of ions (Mann *et al*., 2001).

For protein analysis, the two most common types of ionization sources are matrix-assisted laser desorption ionization (MALDI) and electrospray ionization (ESI) (McDonald and Yates, 2000). Matrix-assisted laser desorption ionization utilizes a laser

ion source to excite a crystalline mixture of analyte molecules and release the ions into the gas phase. This type of ionization source measures the mass of peptides derived from a digested protein and generates the "mass fingerprints" (Karas and Hillenkamp, 1988; Medzihradszky *et al*., 2000). This is a pulsed ionization technique because separate ionization event occurs when mixture is irradiated with the laser (McDonald and Yates, 2000). Using ESI, analyte is transferred from the solution into the gas phase by generating a fine spray from a high voltage needle, which results in the ionization of the analyte and generation of multiple consecutive ions (Chandramouli and Qian, 2009). A constant ionization event can be achieved but this ionization source is more sensitive to salts, buffers, and detergents contamination compare to MALDI (McDonald and Yates, 2000).

Time-of-flight (TOF) mass analyser is a single stage mass spectrometer that has the widest application in proteomics research. The TOF analyser measures the mass-to-charge ratio of an ion by the time it takes to progress through the analyser and strike to the detector (Kicman *et al*., 2007). Its high accuracy and ability to desorb a wide range of molecular mass (1 - 300 kDa), render it as a useful tool for protein mass determination in combination with MALDI ioniser (Kicman *et al*., 2007; Marvin *et al*., 2003). Protein identification by MALDI-TOF mass spectrometry is carried out by peptide mass mapping or peptide mass fingerprinting technique, in which the specific peptide masses determined by MALDI-TOF mass spectrometry is searched against the databases of known protein sequences (Marvin *et al*., 2003).

The use of tandem mass spectrometry (MS/MS) has become a popular method of choice for protein identification due to its ability to determine the amino acid sequence (Aebersold and Goodlett, 2001; Chandramouli and Qian, 2009). Tandem mass spectrometry analysis involves separation of a peptide mixture in the first stage of

analysis; individual peptides are isolated and fragmented at their peptide bonds, and the selected fragments are further separated in the second stage of analysis. This allows direct protein identification by comparing the peptide sequence obtained with those predicted in the database (Michaud and Snyder, 2002).

1.10 Objectives of the study

The objectives of this study are:

1) To investigate the antibacterial activity of king cobra venom L-amino acid oxidase and compare its potency with some commonly used antibiotics.
2) To investigate the cytotoxic effect of king cobra venom L-amino acid oxidase on human tumourigenic and non-tumourigenic cell lines, and compare its potency with doxorubicin (a common anti-cancer drug).
3) To elucidate the possible mechanism(s) of cell death induced by king cobra venom L-amino acid oxidase using oligonucleotide microarray and proteomics approaches.
4) To examine the antitumour effect of king cobra venom L-amino acid oxidase in a PC-3 tumour xenograft mouse model implanted in immunodeficient NU/NU mice, and evaluate its toxicity on vital organs.

CHAPTER 2

MATERIALS AND GENERAL METHODS

MATERIALS

2.1 King cobra (*Ophiophagus hannah*) venom

King cobra (*Ophiophagus hannah*) venom was milked from several adult Malaysian king cobras from Snake Valley (Seremban, Malaysia).

2.2 Bacteria strains

The bacteria *Escherichia coli* ATCC 25922 was purchased from American Type Cell Culture (ATCC), USA. Clinical isolates of *Staphylococcus aureus*, *Staphylococcus epidermidis*, *Pseudomonas aeruginosa*, *Klebsiella pneumonia* and *Escherichia coli* were obtained from Department of Medical Microbiology, University of Malaya, Kuala Lumpur, Malaysia.

2.3 Animals

2.3.1 *ICR* mice

Male *ICR* mice (20-30 g) were obtained from Animal Experimental Unit (AEU), University of Malaya, Malaysia. Mice were maintained in individually ventilated cage (IVC) system (4 mice per cage). Mice were fed with standard pellets and water *ad libitum.*

2.3.2 Nude (NU/NU) mice

Four-weeks-old, male NU/NU mice (18-25 g) were purchased from BioLASCO, Taiwan (certificate no: VP302S10023105). Mice were housed under specific pathogen free (SPF) conditions (3 mice per cage). Mice were fed with sterilized pellets and water *ad libitum.*

2.3.3 Animal handling

Mice were housed for a week prior experiment to facilitate adaption to the new environment. All animal handling and procedures were performed according to the Council for International Organization of Medical Sciences (CIOMS) guidelines (Howard-Jones, 1985). The use of animals in this study was approved by the Institutional Animal Care and Use Committee (IACUC) of the University of Malaya (Ethical clearance letter No. 2013-06-07/MOL/R/FSY). Animal ethical clearance is attached in Appendix I.

2.3.4 Anaesthesia

Mice were anaesthetized with an intraperitoneal (*i.p.*) injection of a combination of ketamine and xylazine at the dosage of 100 mg/kg and 10 mg/kg body weight, respectively. The degree of anaesthesia was monitored until the required depth was attained.

2.4 Human cell line

Human breast adenocarcinoma (MCF-7), human lung adenocarcinoma (A549), human promyelocytic leukaemia (HL-60), human prostate adenocarcinoma (PC-3), human non-tumourigenic breast (184B5) and human non-tumourigenic lung (NL 20) cell lines were purchased from American Type Culture Collection (ATCC), USA.

2.5 Chemicals and general consumables

Resource® Q ion exchange column, 2-D quant kit, 2-D clean-up kit, urea, thiourea, immobilized pH gradient (IPG) buffer (pH 3-10), linear immobilized pH gradient (IPG) strip (13 cm, pH 3-10), 3-[(3 cholamidopropyl) dimethylammonio]-1-propanesulfonate (CHAPS), dithiothreitol (DTT), iodoacetamide (IAA), protease inhibitor mix, and dry

strip cover fluid were purchased from GE Healthcare, Amersham Biosciences AB, Sweden.

Spectra™ broad range protein ladder, PageRuler™ prestained protein ladder, GeneRuler™ 1 kb DNA ladder, Pierce® silver stain for mass spectrometry kit, 20X Tris buffer saline with Tween® 20, 1-Step 3,3',5,5'-tetramethylbenzidine (TMB)-blotting, and goat anti-mouse IgG secondary antibody HRP conjugate were purchased from Thermo Scientific, Waltham, USA.

Cell culture medium; MEGM™ mammary epithelial cell growth medium (MEGM bullet kit) and Ham's F12 medium were purchased from LONZA, Basel, Switzerland.

Iscove's Modified Dulbecco's Medium (IMDM) was purchased from American Type Culture Collection (ATCC), USA.

Foetal bovine serum, RPMI-1640 and 0.25% trypsin-EDTA were purchased from Biowest, Nuaillé, France.

Dehydrated bacteria culture media (Mueller-Hinton broth, nutrient agar and nutrient broth) were purchased from Oxoid Ltd, Cambridge, UK.

Cefotaxime, kanamycin, tetracycline, vancomycin and penicillin antibiotics were purchased from Duchefa Biochemie B.V, Haarlem, Netherlands.

Bovine serum albumin (BSA), L-leucine, L-glutamine, trypan blue dye, o-dianisidine, horseradish peroxidase, catalase, acrylamide, N-N'-methylene bisacrylamide, Trizma® base (Tris-HCl), sodium dodecyl sulphate (SDS), dimethyl sulfoxide (DMSO), ammonium persulphate, β-mercaptoethanol, coomassie brilliant blue G-250, coomassie brilliant blue R-250, magnesium chloride hexahydrate ($MgCl_2 \cdot 6H_2O$), calcium chloride dehydrate ($CaCl_2 \cdot 2H_2O$), orange G, glycerol, ammonium bicarbonate (NH_4HCO_3),

sodium thiosulphate, potassium ferricyanide, triton-X, ethylenediaminetetraacetic acid (EDTA), permount, RNase I, phenol:chloroform:isoamyl alcohol (25:24:1), sodium acetate, eosin Y disodium salt, methyl green, harris haematoxylin, 3-(N-morpholino)propanesulfonic acid (MOPS) (free acid), formamide, and N,N,N',N'-tetramethylethylenediamine (TEMED) were purchased from Sigma Aldrich Chemical Company, MO, USA.

Trypsin gold (mass spectrometry grade), caspase-Glo® 3/7, caspase-Glo® 8, caspase-Glo® 9, and P450-Glo™ CYP1A1 assay kits were purchased from Promega, Madison, USA.

Cytochrome *c* (human) EIA kit was purchased from Enzo Life Sciences, Farmingdale, New York.

Tween® 20, ortho-phosphoric acid, 3,(4,5-dimethythiazol-2-yl)-2,3-diphenyl tetrazolium bromide (MTT), doxorubicin, and iso-propanol were purchased from Merck, Darmstadt, Germany.

Monoclonal anti-Hsc 70, monoclonal anti-Grp 75, and monoclonal anti-beta actin were purchased from Abcam®, Cambridge, UK.

Matrigel™, and PE Annexin V Apoptosis Detection Kit I were purchased from BD Biosciences, California, USA.

RNeasy® mini kit was purchased from Qiagen, Hilden, Germany.

Illumina® TotalPrep RNA amplification kit was purchased from Ambion, California, US.

HumanRef-8 v2 expression BeadChips was purchased from Illumina, San Diego, CA.

High capacity RNA-to-cDNA™ kit, TaqMan® gene expression master mix, TaqMan® gene expression assays, and beta actin were purchased from Applied Biosystems, CA, USA.

OxiSelect™ intracellular ROS assay kit (green fluorescence) was purchased from Cell Biolabs, CA, USA.

Agarose, TRIzol® reagent, DNase I, and PVDF iBlot™ gel transfer stacks were purchased from Invitrogen™, Grand Island, USA.

GelRed™ nucleic acid gel stain (10,000X in water) was purchased from Biotium, Hayward, CA.

ApopTag® plus peroxidase *in situ* apoptosis detection kit, proteinase K, and C18 ZipTip® were obtained from Millipore, MA, USA.

Glycine, phosphate buffered saline (PBS) tablet, and bromophenol blue were purchased from MP Biomedicals, LLC, United States.

Narketan®-10 (100 mg/mL) was purchased from Vetoquinol, UK.

Ilium xylazil-20 (20 mg/mL) was purchased from Troy laboratories, Australia.

N-butanol, acetic acid glacial, xylene, hydrogen peroxide, chloroform, 37% formaldehyde (12.3 M), acetonitrile, and formic acid were purchased from J.T. Baker Center Valley, PA, USA.

Sodium chloride, ethanol and methanol were purchased from J. Kollin Corporation, Germany.

2.6 L-amino acid oxidase assay

L-amino acid oxidase (LAAO) activity was determined according to Bergmeyer (1983). To 925 μL of substrate (containing 0.34 mM L-leucine and 81 μg of o-dianisidine in 100 mM Tris-HCl buffer, pH 8.5), 50 μL of 0.0075% horseradish peroxidase and 25 μL of the sample were added to initialize the reaction. Increase in absorbance at 436 nm was recorded. One unit of enzyme activity was defined as the oxidation of 1 μmol of L-leucine per min. Molar absorption coefficient of the reaction product was 8.31×10^{-3} M^{-1} cm^{-1}.

2.7 Purification of king cobra venom L-amino acid oxidase

King cobra venom L-amino acid oxidase (OH-LAAO) was purified using a method modified from Tan and Saifuddin (1989). Lyophilized king cobra venom (20 mg in 200 μL) was fractionated by Resource® Q high performance liquid chromatography (HPLC) (Shimadzu, Japan) previously equilibrated with 20 mM Tris-HCl, pH 9.0. Elution was carried out using a linear gradient of NaCl in 20 mM Tris-HCl, at a flow rate of 1 mL/min. The gradient program used was: 100% buffer A (20 mM Tris-HCl, pH 9.0) for 5 min, followed by a linear 0 - 60% buffer B (20 mM Tris-HCl, pH 9.0, 0.5 M NaCl) for another 50 min and finally 100% buffer B for 5 min. The UV absorbance of the eluate was monitored at 280 nm. Fractions exhibiting LAAO activity were pooled and stored at 4 °C.

2.8 Buffer exchange

Buffer exchange was carried out using vivaspin® 15R (30,000 molecular weight cut-off) (Sartorius Stedim Biotech, Goettingen, Germany) according to the manufacturer's protocol. In brief, purified OH-LAAO in the elution buffer (20 mM Tris-HCl, pH 9.0,

0.5 M NaCl) was first concentrated using vivaspin® by centrifugation at 3,000 x g for 30 min at 4 °C. The concentrated sample was then washed three cycles with PBS by centrifugation at 3,000 x g for 30 min.

2.9 Protein concentration determination

2.9.1 Protein concentration determination by Bradford method

Protein concentration was determined by Bradford (1976) method. The calibration curve was constructed using bovine serum albumin (BSA) ranging from 0 to 60 µg. One hundred microlitres of the sample/BSA was added to 5 mL of the Bradford reagent [prepared as described in Appendix II (A)]. The absorbance was measured at 595 nm using 1.5 mL cuvette placed in the 1 cm light path spectrophotometer (Cary 50 Conc, Varian, Australia). Specific activity of the pure OH-LAAO was determined by the formula below:

$$\text{Specific activity of LAAO (µmol/min/mg protein)} = \frac{\text{Enzyme activity (µmol/min/mL)}}{\text{Protein content (mg/mL)}}$$

2.9.2 Protein concentration determination using 2-D quant kit

Protein concentration was determined using 2-D quant kit according to the manufacturer's protocol (GE Healthcare, Sweden) with slight modifications. Briefly, 100 µL of the precipitant was mixed with the protein sample or BSA standard and incubated at room temperature for 3 min. Co-precipitant (100 µL) was then added into the mixture. After centrifugation at 10,000 x g for 5 min, the supernatant was discarded. Copper solution (20 µL) and milli-Q® water (80 µL) were pipetted on top of the pellet and vortexed until it is fully dissolved. Subsequently, 200 µL of the working color reagent (mixture of 100 parts of color reagent A with 1 part of color reagent B) was added into each tube and incubated at room temperature for 20 min. Absorbance reading

of each sample was taken at 460 nm using Model 680 microplate reader (Bio-Rad, Hercules, CA). Standard curve was constructed by plotting the absorbance reading at 460 nm versus amount of the BSA standard used (BSA ranging from 0 to 12 µg). Protein concentration for each sample was calculated using the constructed standard curve.

2.10 Sodium dodecyl sulphate polyacrylamide gel electrophoresis

Formulations of solutions or reagents for Sodium dodecyl sulphate polyacrylamide gel electrophoresis (SDS-PAGE) are shown in Table 2.1. The homogeneity of OH-LAAO was assessed by 12.5% (w/v) SDS-PAGE according to Laemmli (1970). Sodium dodecyl sulphate polyacrylamide gel electrophoresis was conducted using 4-gel Mini-PROTEAN® Tetra Cell (Bio-Rad, Hercules, CA). The molecular weight of the enzyme was determined by Spectra™ broad range protein ladder (Thermo Scientific, USA), as calibration standards (molecular mass 10 - 260 kDa). The $\log_{10}$ molecular weight of the standard proteins was plotted against their respective R_f to obtain a calibration curve.

Table 2.1: Formulations of solutions or reagents for sodium dodecyl sulphate polyacrylamide gel electrophoresis

Solution/reagent	**Formulations**
Solution A	29.2% (w/v) acrylamide, 0.8% (w/v) N-N'-methylene bisacrylamide
Solution B	1.5 M Tris-HCl, 0.4% sodium dodecyl sulphate (SDS) (w/v), pH was adjusted to 8.8
Solution C	10% (w/v) ammonium persulphate (freshly prepared)
Solution D	0.5 M Tris-HCl containing 0.4% sodium dodecyl sulphate (w/v), pH was adjusted to 6.8
Sample incubation buffer	62 mM Tris-HCl, 2.3% (w/v) sodium dodecyl sulphate, 10% (v/v) glycerol, 5% β-mercaptoethanol and 0.005% bromophenol blue, pH was adjusted to 6.8
Electrophoresis buffer	0.025 M Tris-HCl, 0.129 M glycine and 0.1% (w/v) sodium dodecyl sulphate
Fixing solution	40% (v/v) methanol, 10% (v/v) acetic acid and 50% water
Staining solution	0.2% (w/v) coomassie brilliant blue R-250 in the fixing solution
Destaining solution	5% (v/v) methanol and 7% (v/v) acetic acid in water

2.10.1 Preparation of 12.5% resolving gel and 4% stacking gel

Formulations of resolving gel and stacking gel are shown in Table 2.2. Solution mixtures for resolving gel were gently swirled and rapidly poured into the gel cassette until a level which sufficient for the comb to be inserted. Water was then overlaid on top of the gel solution. The gel was allowed to stand at room temperature for 20 - 30 min for polymerization to occur.

After polymerization of resolving gel, water was carefully removed. Solution mixtures for stacking gel were layered on top of the resolving gel and the comb was inserted immediately. Polymerization occurred within 10 - 15 min.

Table 2.2: Compositions of resolving and stacking gels

Solution	**12.5% resolving gel (mL)**	**4% stacking gel (mL)**
Milli-Q® water	4.5	6.1
Solution A	7.5	1.4
Solution B	6	-
Solution C	-	2.5
Ammonium persulphate	0.1	0.2
TEMED	0.01	0.01

2.10.2 Preparation of protein sample under denaturing and reduce condition

Protein samples (20 µg) were mixed with sample incubation buffer at an equal ratio for a maximum volume of 20 µL. Sample mixtures were boiled at 70 - 80 °C for 5 - 10 min and chilled on ice.

2.10.3 Running condition

Gel cassettes were assembled onto the electrophoresis tank according to the manufacturer's instructions (Bio-Rad, Hercules, CA). Sample mixtures were loaded onto the wells of the stacking gel. Electrophoresis was carried out at a constant voltage of 90 V for approximately 2 h.

2.10.4 Fixing, staining and destaining

Electrophoresis was stopped when the front dye reached half centimetre to the bottom of the gel. To prevent diffusion of the protein bands, gels were treated with fixing solution for 10 min with mild shaking. After fixing, gels were transferred into the staining solution for another 10 - 15 min and finally destained in the destaining solution until the background is cleared.

2.11 Formaldehyde agarose (FA) gel electrophoresis

Formulations of buffers for formaldehyde agarose (FA) gel electrophoresis are shown in Table 2.3. Solution mixtures for 1.2% FA gel was heated using a microwave oven until the agarose is melted and cooled under the running tap water. Nine hundred microlitres of formaldehyde and two microlitres of GelRed™ (Biotium, CA) were then added into the mixtures and mixed. Solution mixtures were poured onto the gel tray and the comb was inserted immediately. When the gel has solidified, it was transferred to the gel tank

(ENDURO 7.10 Horizontal Gel Box, Labnet International Inc. Woodbridge, USA) and equilibrated in 1X FA gel running buffer prior to electrophoresis.

The RNA samples were prepared by mixing one volume of 5X RNA loading buffer with four volumes of RNA samples. The mixtures were incubated at 65 °C for 5 min and immediately chilled on ice. Samples were loaded onto the wells of FA gel previously equilibrated with 1X FA gel running buffer. Electrophoresis was carried out at a constant voltage of 80 V for 20 - 30 min. Image acquisition was done using gel documentation system (Infinity-3026, Vilber Lourmat, France).

Table 2.3: Formulations of buffers for formaldehyde agarose gel electrophoresis

Buffers	**Compositions**
10X FA gel buffer	200 mM 3-(N-morpholino)propanesulfonic acid (MOPS), 50 mM sodium acetate, 10 mM EDTA. pH was adjusted to 7.0.
1X FA gel running buffer	100 mL of 10X FA gel buffer, 20 mL of 37% formaldehyde (12.3 M), 880 mL of RNase-free water.
5X RNA loading buffer	16 µL of saturated aqueous bromophenol blue solution, 80 µL of 500 mM EDTA (pH 8.0), 720 µL of 37% formaldehyde (12.3 M), 2 mL of 100% glycerol, 3.084 mL of formamide, 4 mL of 10X FA gel buffer. Top-up with RNase-free water to 10 mL and tored at 4°C.
1.2% FA gel	0.6 g agarose, 5 mL of 10X FA gel buffer and 45 mL of RNase-free water.

2.12 Cell culture

2.12.1 The cell lines

2.12.1.1 Human breast adenocarcinoma, MCF-7 (ATCC® HTB-22™)

The MCF-7, human breast adenocarcinoma cell line was isolated from a pleural effusion of a 69-year-old Caucasian female patient with metastatic breast cancer. The cell line was named after the Michigan Cancer Foundation-7, an institute in Detroit where the cell line was established by Soule and associates in 1973 (Soule *et al*., 1973). The adherent epithelial-like MCF-7 was grown in RPMI-1640 medium supplemented with L-glutamine and 10% (v/v) foetal bovine serum. The popularity of MCF-7 is largely due to its sensitivity to hormones through the expression of oestrogen receptor (ER), making it an ideal cell line for hormone response study (Levenson and Jordan, 1997).

2.12.1.2 Human lung adenocarcinoma, A549 (ATCC® CCL-185™)

Human lung adenocarcinoma, A549 was isolated through the explants culture of lung carcinomatous tissue from a 58-year-old Caucasian male (Giard *et al*., 1973). The A549 cells grow as monolayer, adherent to the cell culture flask. The cells were grown in RPMI-1640 medium supplemented with L-glutamine and 10% (v/v) foetal bovine serum.

2.12.1.3 Human non-tumourigenic breast, 184B5 (ATCC® CRL-8799™)

The 184B5 cell line was established from normal mammary epithelium tissue obtained from a normal reduction mammoplasty. Stampfer and Bartley (1985) established the transformed immortalized cell line by exposing the rapidly growing primary cells derived from mammary tissue to benzo(α)pyrene. The cell line grown as adherent,

monolayer in MEGM™ mammary epithelial cell growth medium (MEGM bullet kit) supplemented with 10% (v/v) foetal bovine serum.

2.12.1.4 Human non-tumourigenic lung, NL 20 (ATCC® CRL-2503™)

An immortalized, human non-tumourigenic lung cell line (NL 20) was obtained from autopsy samples of normal bronchus tissue. The cell line was established by transfection with the origin of replication-defective SV40 large T plasmid, p129 (Schiller and Bittner, 1995). The cells were grown as adherent in Ham's F12 medium supplemented with 10% (v/v) foetal bovine serum.

2.12.1.5 Human prostate adenocarcinoma, PC-3 (ATCC® CRL-1435™)

Human prostate adenocarcinoma, PC-3 cell line was derived from a bone metastasis of a grade IV prostatic adenocarcinoma from a 62-year-old Caucasian male. The cells do not respond to androgens, glucocorticoids, or epidermal or fibroblast growth factors (Kaighn *et al*., 1979). This cell line grown as adherent-epithelial like in complete RPMI-1640 medium supplemented with 10% (v/v) foetal bovine serum.

2.12.1.6 Human promyelocytic leukaemia, HL-60 (ATCC® CCL-240™)

Human promyelocytic leukaemia cell line, HL-60 was derived from a 36-year-old Caucasian female with acute promyelocytic leukaemia by leukopheresis (Collins *et al*., 1977). The HL-60 cells are predominantly a neutrophilic promyelocyte with prominent nuclear or cytoplasmic asynchrony (Gallagher *et al*., 1979). This cell line proliferates as a suspension culture in ATCC-formulated Iscove's Modified Dulbecco's Medium (IMDM) supplemented with 10% (v/v) foetal bovine serum.

2.12.2 Cell line maintenance

Different cell lines were grown in their respective media: RPMI-1640 for MCF-7, A549, and PC-3 cells; MEGM™ mammary epithelial cell growth medium (MEGM bullet kit) for 184B5 cells, Iscove's Modified Dulbecco's Medium (IMDM) for HL-60 cells and Ham's F12 medium for NL 20 cells. The medium were supplemented with 10% (v/v) foetal bovine serum. Cells were cultured in a humidified atmosphere with 95% air and 5% CO_2 at 37 °C. Inverted microscope (CK2 Olympus, Japan) was used to check the confluency and any contamination of the cell cultures.

2.12.3 Sub-culture

2.12.3.1 Sub-culturing of adherent cells

Sub-culture was performed when the cells reached the confluency of about 80 - 90%. Spent medium was removed and the cells were washed twice with phosphate buffered saline (PBS) prior for the trypsinization with an adequate volume of 0.25% trypsin-EDTA. Cells were incubated at 37 °C for 5 - 10 min to allow detachment of the cells. Complete cell culture medium was added onto the trypsinized cells to inactivate the trypsin. Cells were then spun down at 1,500 rpm for 5 min at 25 °C and the pellet was resuspended with culture medium. Desired amount of cell suspension was seeded onto the cell culture flask containing fresh medium.

2.12.3.2 Sub-culturing of suspension cells

Suspension cells (HL-60) were collected and spun down at 2,000 rpm for 10 min at 25 °C. Cell pellet was resuspended with fresh culture medium. Cells at desired density were seeded onto the cell culture flask.

2.12.4 Cryopreservation and thawing of cells

For cryopreservation, cell pellet was collected by centrifugation at 1,500 rpm for 5 min at 25 °C and resuspended with complete growth medium containing 5% dimethyl sulfoxide (DMSO). One millilitre of the cell suspension was aliquoted into the 2 mL cryovials and stored overnight at -80 °C. For long term storage, the cryopreserved cells were stored in the vapour phase of the liquid nitrogen.

Cryopreserved cells were thawed instantly in the pre-heated 37 °C water bath, spun down at 1,500 rpm for 5 min and resuspended with culture medium. Cell suspension was transferred into a cell culture flask containing complete growth medium and incubated in a humidified atmosphere with 95% air and 5% CO_2 at 37 °C.

2.12.5 Cell counting

Cell counting was performed using Neubauer-improved haemocytometer (Marienfeld, Lauda-Königshofen). Cells were spun down at 1,500 rpm for 5 min and adequate volume of culture medium was added to resuspend the cells. Ten microlitres of the cell suspension was gently mixed with 90 µL of the trypan blue dye. Subsequently, the cell mixture (10 µL) was loaded into the counting chamber placed under the coverslip by capillary action. Haemocytometer were observed under inverted light microscope (CK2 Olympus, Japan) at 200X magnifications and the 16 corner squares were focused. The viable cells (unstained by trypan blue) that fall within the 4 sets of the 16 corner squares and any position on the upper and left hand side boundary line were counted using hand tally counter. Cell concentration was calculated as follows:

$$\text{No. of cells/mL} = \frac{\text{No. of viable cells counted}}{4} \text{ X Dilution factor (10) X } 10^4$$

CHAPTER 3

ANTIBACTERIAL ACTION OF KING COBRA (*Ophiophagus hannah)* VENOM L-AMINO ACID OXIDASE (OH-LAAO) AGAINST SEVERAL STRAINS OF CLINICALLY ISOLATED BACTERIA

INTRODUCTION

The emergence of multidrug-resistant bacteria has drawn major attention among healthcare and medical practitioners ever since the introduction of penicillin in the late 1920s (Zainol *et al*., 2013). Although multidrug-resistant *Pseudomonas aeruginosa, acinetobacter sp., Staphylococcus aureus* and *E. faecium* are the best known therapeutic challenges among the gram-negative and gram-positive bacteria, resistance to the most potent antibiotics has been extended to members of the *Enterobacteriaceae* family of gram-negative bacteria, such as *Klebsiella sp., Escherichia coli*, and *enterobacter sp.* (Arias and Murray, 2009). In Malaysia, *P. aeruginosa, S. aureus, K. pneumoniae,* and *E. coli* were the most common healthcare-associated pathogens isolated from patients with nosocomial infection (Hughes *et al*., 2005; Rozaidi *et al*., 2001).

The used of currently available antimicrobial agents in the treatment of bacteria infectious diseases is becoming more challenging due to emergence of several antibiotic-resistance microbial. Therefore, it is important to search for a new potent antibacterial agent in order to supplement the currently increasingly ineffective antibiotics. Snake venom LAAO has been shown to exhibit potent antibacterial activity against both gram-negative and gram-positive bacteria. Compare to the pathogens, human host cells or normal flora are less sensitive to oxidative damage caused by H_2O_2 or other ROS, which implies that snake venom LAAOs may selectively kill bacterial strains without causing significant damage to the host (Guo *et al*., 2012). Therefore, this enzyme may be a promising alternative anti-microbial agent in treating bacterial infection diseases. In this chapter, the antibacterial activity of king cobra venom LAAO (OH-LAAO) was examined against several strains of clinical isolates Gram-positive and Gram-negative bacteria using broth microdilution assay. Its antibacterial potency was compared with some common antibiotics such as cefotaxime, kanamycin,

tetracycline, vancomycin and penicillin. Binding activity of OH-LAAO on bacteria cells was also carried out in order to study the mode of antibacterial action of the enzyme.

METHODS

3.1 Bacteria growth and preparation of inoculums suspensions

Bacteria from frozen suspensions were grown on the nutrient agar plates [prepared as described in Appendix II (B)] and passaged twice prior to susceptibility testing. Isolated colonies were selected from an agar plate culture and transferred with a wire loop into a tube containing 5 mL of the nutrient broth medium [prepared as described in Appendix II (C)]. Broth cultures were incubated at 37 °C until it achieved the turbidity of 0.5 McFarland (1 to 2 x 10^8 CFU/mL). The turbidity of the cultures was measured at 625 nm using 1 cm light path spectrophotometer (Cary 50 Conc, Varian, Australia). The absorbance reading of 0.08 - 0.1 at 625 nm was corresponding to 0.5 McFarland (National Committee for Clinical Laboratory Standards, NCCLS, 2000).

3.2 Broth microdilution assay and effect of catalase

Broth microdilution assay was carried out according to the protocol described by National Committee for Clinical Laboratory Standards, NCCLS (2000). In brief, inoculums suspensions were diluted with 2X Mueller-Hinton broths [prepared as described in Appendix II (D)] to a final concentration of 1×10^6 CFU/mL. Bacterial suspensions (50 μL) were incubated in 96-well plate in the presence of 50 μL of different concentrations of sterilized OH-LAAO ranging from 0.049 to 100 μg/mL or antibiotics ranging from 0.031 to 64 μg/mL using 2-fold serial dilutions to yield the appropriate bacterial density of 5×10^5 CFU/mL. The plates were incubated at 37 °C. After 24 h incubation, MIC (minimum inhibitory concentration) end points were determined by visual inspection. The end point was reached when the cultures were completely transparent. Susceptibility of *E. coli* ATCC 25922 to tetracycline was chosen as quality control and its acceptable quality control limit is MIC of 0.5 - 2 μg/mL (National Committee for Clinical Laboratory Standards, NCCLS, 2000).

Minimum inhibitory concentration was taken as the lowest concentration of antimicrobial agent that inhibited visible growth of the bacteria (n = 3). To evaluate the effect of catalase on the antibacterial action of the enzyme, the same assay was carried out in the presence of 1 mg/mL catalase.

3.3 Bacteria-binding activity of king cobra venom L-amino acid oxidase

Bacteria-binding activity of OH-LAAO was examined according to Kitani *et al*. (2008) with slight modifications. Two Gram-positive bacteria (*S. aureus* and *S. epidermidis*) and two Gram-negative bacteria (*E. coli* and *P. aeruginosa*) were chosen for this study. Bacteria were grown in nutrient broth at 37 °C. Cells were collected by centrifugation at 2,000 × g for 15 min, washed twice with PBS, and adjusted to 1×10^9 CFU/mL using 2X Mueller-Hinton broth. Bacterial suspensions (500 µL) were incubated with 500 µL of OH-LAAO (1 µg/mL) at 37 °C for 1, 3, 5 and 24 h. After the incubation time, mixture was filtered using 0.20 µm syringe filter and the enzyme activity of the filtrate was measured. The binding potency of the enzyme is inversely proportional to the enzyme activity of the filtrate. Relative LAAO activity in percentage was calculated using the formula below:

$$\text{Relative LAAO activity } (\%) = \frac{\text{LAAO activity in the filtrate}}{\text{LAAO activity of the control}} \text{X } 100\%$$

RESULTS

3.4 Purification of king cobra venom L-amino acid oxidase

Figure 3.1 shows the chromatogram of the purification of OH-LAAO using single step Resource® Q ion exchange high performance liquid chromatography. Fractions constituting peak-7 which exhibited LAAO activity were pooled and designated as pure OH-LAAO. The purified enzyme was homogeneous as judged by SDS-PAGE, with a molecular mass of approximately 65 kDa, which is in agreement with the previous report (Tan and Saifuddin, 1989). Specific activity of the purified OH-LAAO was 437.7 μmol/min/mg.

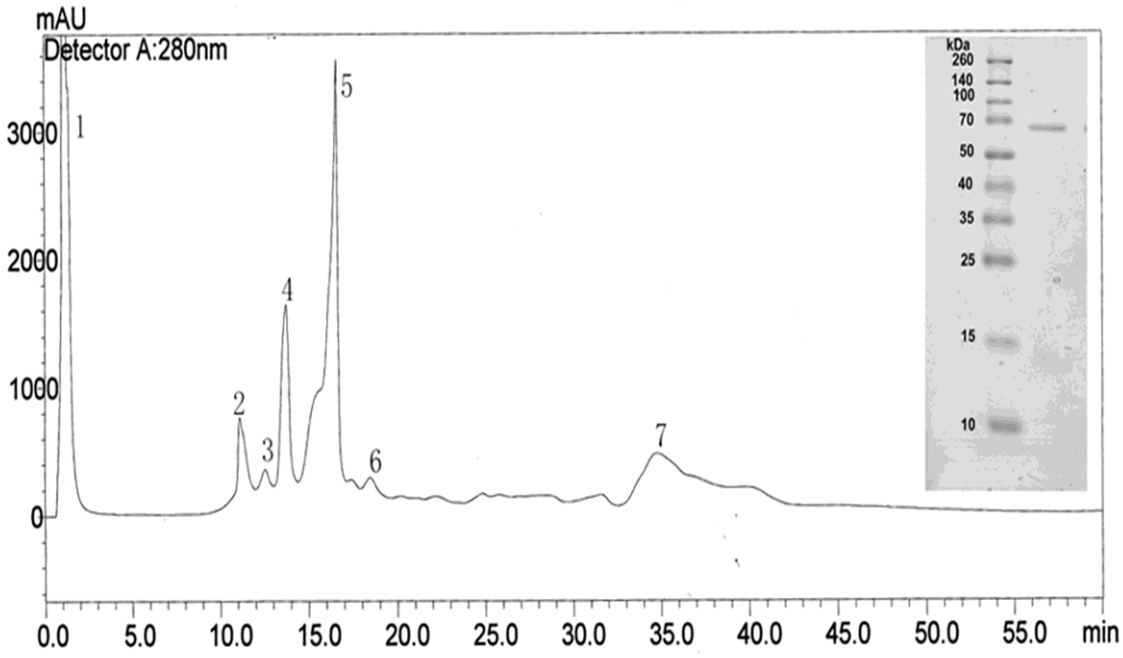

Figure 3.1: Purification of king cobra venom L-amino acid oxidase by Resource® Q ion exchange chromatography. King cobra (*Ophiophagus hannah*) venom (20 mg in 200 µL) was injected into the Resource® Q anion exchange column pre-equilibrated with 20 mM Tris-HCl, pH 9.0. Elution was carried out with a linear gradient of 0 - 0.3 M NaCl. Seven major protein peaks were obtained. Peak-7 was the pure OH-LAAO. Insert: SDS-PAGE of molecular weight markers (left, Spectra™ broad molecular weight protein ladder, Molecular mass 10 - 260 kDa) and fraction of peak-7 (right).

3.5 Antibacterial action of king cobra venom L-amino acid oxidase

Table 3.1 shows the minimum inhibitory concentration (MIC) of OH-LAAO against clinically isolated Gram-positive bacteria (*S. aureus* and *S. epidermidis*) and Gram-negative bacteria (*K. pneumonia*, *P. aeruginosa*, and *E. coli*), as well as *E. coli* ATCC 25922. For comparison, the MICs of some common antibiotics against both Gram-negative bacteria (cefotaxime, kanamycin and tetracycline) and Gram-positive bacteria (cefotaxime, vancomycin and penicillin) were also determined. The MIC of tetracycline against the standard *E. coli* ATCC 25922 was 2 μg/mL, which is within the acceptable quality control limit of 0.5 - 2 μg/mL. For comparison, the MIC values were also expressed in μM.

Results show that OH-LAAO is a potent antibacterial agent, effectively inhibiting both the growth of Gram-positive and Gram-negative bacteria examined. Its MICs against the Gram-positive bacteria *S. aureus* and *S. epidermidis* were 0.78 and 1.56 μg/mL, respectively. Its MICs against the Gram-negative bacteria *K. pneumonia, P. aeruginosa* and *E. coli,* ranged from 25 to 100 μg/mL. On a molar basis, MICs of OH-LAAO ranged from 0.006 μM to 0.800 μM, against both the Gram-positive and Gram-negative bacteria. The antibacterial action of OH-LAAO against all bacteria tested was abolished in the presence of 1 mg/mL of catalase (MIC > 100 μg/mL).

Under the same experimental conditions, MICs of the antibiotics (cefotaxime, kanamycin and tetracycline) against the three Gram-negative bacteria ranged from 0.06 μg/mL to > 64.00 μg/mL, whereas the MICs of the antibiotics (cefotaxime, vancomycin and penicillin) against the two Gram-positive bacteria ranged from < 0.031 μg/mL to 2.0 μg/mL.

Table 3.1: Antibacterial activities of king cobra venom L-amino acid oxidase in comparison to antibiotics

Bacteria	Antibiotic/LAAO	MIC (µg/mL)	MIC (µM)
Gram-negative			
Klebsiella pneumonia	Cefotaxime	0.060	0.130
	Kanamycin	4.000	6.900
	Tetracyclin	4.000	9.000
	LAAO	50.000	0.400
	LAAO+catalase	>100.000	>0.800
Pseudomonas aeruginosa	Cefotaxime	16.000	35.100
	Kanamycin	64.000	109.800
	Tetracyclin	64.000	144.000
	LAAO	25.000	0.200
	LAAO+catalase	>100.000	>0.800
Escherichia coli	Cefotaxime	>64.000	>140.500
	Kanamycin	16.000	27.500
	Tetracyclin	4.000	9.000
	LAAO	50.000	0.400
	LAAO+catalase	>100.000	>0.800
Escherichia coli ATCC 25922	Cefotaxime	0.060	0.130
	Kanamycin	8.000	13.700
	Tetracyclin	2.000	4.500
	LAAO	100.000	0.800
	LAAO+catalase	>100.000	>0.800
Gram-positive			
Staphylococcus aureus	Cefotaxime	1.000	2.000
	Vancomycin	0.500	0.340
	Penicillin	<0.030	<0.090
	LAAO	0.780	0.006
	LAAO+catalase	>100.000	>0.800
Staphylococcus epidermidis	Cefotaxime	2.000	4.400
	Vancomycin	0.500	0.340
	Penicillin	0.060	0.180
	LAAO	1.560	0.012
	LAAO+catalase	>100.000	>0.800

Minimum inhibitory concentration (MIC) of OH-LAAO and common antibiotics against several clinically isolated Gram-negative and Gram-positive bacteria were examined using broth microdilution assay. The end points were determined by visual inspection after 24 h incubation. The MICs values were expressed in µg/mL and µM from 3 independent experiments.

3.6 Bacteria-binding activity of king cobra venom L-amino acid oxidase

Table 3.2 shows the binding activity of OH-LAAO to bacteria cells. At a bacteria concentration of 5×10^8 cells/mL and OH-LAAO concentration of 0.5 μg/mL (3.8×10^{-12} mol/mL, molecular weight of OH-LAAO = 130 kDa), the enzyme binds effectively to all 4 bacteria tested. The binding activity was time-dependent and reached a plateau after 5 h incubation. At 24 h, approximately 40% of the OH-LAAO in the incubation mixture was bound to the two Gram-positive bacteria, *S. aureus* and *S. epidermidis*, and 25% was bound to the two Gram-negative bacteria, *E. coli* and *P. aeruginosa*.

Table 3.2: Bacterial cell binding activity of king cobra venom L-amino acid oxidase

Time (h)	**Relative LAAO activity (%) of the filtrate of bacterial suspension treated with OH-LAAO for 0 to 24 h.**			
	S.aureus	***S. epidermidis***	***E.coli***	***P.aeruginosa***
0	88.8 ± 3.5%	93.9 ± 3.7%	94.6 ± 2.4%	93.2 ± 4.0%
1	75.5 ± 4.0%	84.2 ± 3.8%	88.5 ± 4.7%	85.0 ± 5.1%
3	64.2 ± 3.6%	73.1 ± 3.1%	76.6 ± 5.8%	82.3 ± 3.0%
5	62.3 ± 3.3%	61.3 ± 4.4%	75.9 ± 5.2%	76.6 ± 4.8%
24	60.5 ± 2.3%	62.7 ± 3.7%	75.2 ± 4.8%	77.3 ± 4.1%

The incubation mixture consists of bacterial cell suspension (5×10^8 cells) and 0.5 μg/mL OH-LAAO in 2X Mueller-Hinton broth, incubated at 37 °C. The incubation mixture was filtered using 0.20 μm syringe filter; LAAO activity of the filtrate was measured. The results (mean ± S.D, n = 3) were expressed as the ratio of LAAO activity in the filtrate to that of the control (LAAO in incubation mixture without the bacteria), in percentage. Statistical analysis was performed using one-way analysis of variance (one-way ANOVA), followed by Tukey's post hoc multiple comparison test. Relative LAAO activities after 1 h incubation were all significantly different from control ($P < 0.05$).

DISCUSSION

3.7 Comparison of the antibacterial activity of king cobra venom L-amino acid oxidase with common antibiotics

Skarnes (1970) was the first to report the bactericidal activity of LAAO isolated from *C. adamanteus* venom. Subsequently, bactericidal activities of LAAO from various snake venoms have been reported (Ciscotto *et al*., 2009; Alves *et al*., 2011; Tõnismägi *et al*., 2006; Vargas *et al*., 2013; Zhong *et al*., 2009). Stiles *et al*. (1991) reported that *in vitro* antibacterial effects of LAAOs isolated from Australian elapid, *Pseudoechis australis* were 17.5 to 70.0 times more potent than tetracycline (on a molar basis). Therapeutic potential of the antibacterial agent is important to be evaluated by comparing its potency to that of common antibiotics. Hence, the antibacterial activity of king cobra venom LAAO (OH-LAAO) was carried out using the standardized broth microdilution assay according to the protocol described by National Committee for Clinical Laboratory Standards, NCCLS (2000). Its therapeutic potential was evaluated by comparing to the potency of five common antibiotics.

The present study demonstrated that OH-LAAO is indeed a potent antibacterial agent when compared to the common antibiotics. On a molar basis, the antibacterial activity of OH-LAAO against all bacteria tested is far more potent than most of the antibiotics examined. For example, the MIC of OH-LAAO against Gram-positive *S. epidermidis* was 0.012 µM which is far more potent than cefotaxime (MIC = 4.400 µM), vancomycin (MIC = 0.340 µM) and penicillin (MIC = 0.180 µM). Against the Gram-negative *P. aeruginosa*, the enzyme has a MIC of 0.2 µM, whereas the MICs for the antibiotics cefotaxime, kanamycin and tetracyclin against the same bacterium were 35.1 µM, 109.8 µM and 144.0 µM, respectively (Table 3.1). On a weight basis, the MICs of OH-LAAO against the two Gram-positive bacteria were comparable to the antibiotics

tested, except for penicillin, which was far more potent than the OH-LAAO. On the same (weight) basis, however, the MICs of the OH-LAAO against Gram-negative bacteria were generally higher than the antibiotics tested, except against the clinically isolated of *P. aeruginosa*, where the enzyme has a MIC (25 μg/mL), comparable to the three antibiotics tested (16 - 64 μg/mL) (Table 3.1).

Antibacterial activities of many different snake venom LAAOs have been reported (Table 3.3). Unfortunately, it is difficult to quantitatively compare the antibacterial potency of these LAAOs with the OH-LAAO, mainly because different methods of antibacterial assay were used. Of these, only three reported MICs of the enzyme using the standard broth microdilution assay according to NCCLS. Torres *et al*. (2010) reported that LAAO isolated from *B. marajoensis* has a MIC of 50 μg/mL against *S. aureus*. However, the enzyme was ineffective against *Candida albicans* (MIC > 200 μg/mL) and *P. aeruginosa* (MIC > 200 μg/mL). Zhong *et al*. (2009) reported that the MICs of *D. russellii siamensis* LAAO for *S. aureus*, *P. aeruginosa* and *E. coli* were 9 μg/mL, 144 μg/mL and 288 μg/mL, respectively. Vargas *et al*. (2013) demonstrated that the LAAO isolated from *Crotalus durissus cumanensis* effectively inhibiting the growth of Gram-positive *S. aureus* and Gram-negative *A. baumannii* and the MICs were 8 μg/mL and 16 μg/mL, respectively. In comparison, OH-LAAO is more potent against these same organisms. The antibacterial action of OH-LAAO is diminished by the catalase (1 mg/mL); suggesting that the antibacterial action of the enzyme is mainly due to the H_2O_2 generated during the oxidative deamination process. This is in agreement with previous reports (Rodrigues *et al*., 2009; Stábeli *et al*., 2007; Stiles *et al*., 1991; Tõnismägi *et al*., 2006; Toyama *et al*., 2006; Vargas *et al*., 2013).

The present results show that OH-LAAO was more potent against the Gram-positive bacteria than the Gram-negative bacteria tested. This is in agreement with the selectivity of antibacterial action of LAAOs of *B. marojoensis*, *D. russellii siamensis*, *C. durissus*

cascavella, B. atrox, C. durissus cumanensis and *T. mucrosquamatus*. On the other hand, LAAOs from *B. pauloensis, B. alternates, V. lebetina, N. oxiana* and *P. australis* were more active against Gram-negative than the Gram-positive bacteria, whereas LAAOs from *A. halys* and *B. moojeni* inhibited Gram-positive and Gram-negative bacteria almost equally (Table 3.3). These differences in the selectivity of the antibacterial action of these LAAOs are probably due to the differences in bacteria binding activity of the enzymes.

Table 3.3: The antibacterial actions of some snake venom L-amino acid oxidases

Venom source of LAAO	Antibacterial actions	Reference
Crotalus adamanteus	Almost equally active against Gram-negative *P. aeruginosa* and *E. coli*	(Skarnes, 1970)
Crotalus durissus cascavella	More active against Gram-positive *Staphylococcus mutans* than Gram-negative *Xanthomonas axonopodis pv passiflorae*	(Toyama *et al*., 2006)
Agkistrodon halys	Almost equally active against Gram-negative *E. coli* and Gram-positive *Bacillus subtilis*	(Zhang *et al*., 2004)
Bothrops alternatus	Slightly active against Gram-negative *E.coli* than Gram-positive *B. subtilis*	(Stábeli *et al*., 2004)
Bothrops marajoensis	Most active against Gram-positive *S. aureus* (MIC = 50 µg/ml) than *C. albicans* (MIC > 200 µg/mL) and *P. aeruginosa* (MIC > 200 µg/mL)	(Torres *et al*., 2010)
Bothrops moojeni	Almost equally active against Gram-negative *E. coli, Salmonella typhimurium, P. aeruginosa* and Gram-positive *S. aureus*	(Stábeli *et al*., 2007)
Bothrops pauloensis	More active against Gram-negative *E. coli* than Gram-positive *S. aureus*	(Rodrigues *et al*., 2009)
Bothrops pirajai	Almost equally active against Gram-negative *E. coli* and *P. aeruginosa*	(Izidoro *et al*., 2006)
Trimeresurus jerdonii (now known as *Protobothrops jerdonii*)	Active against Gram-positive *Bacillus megaterilum* and *S. aureus* and Gram-negative *E. coli* and *P. aeruginosa*	(Lu *et al*., 2002)
Trimeresurus mucrosquamatus (now known as *Protobothrops mucrosquamatus*)	Most active against Gram-positivie *S. aureus*. Also active against Gram-negative *E. coli* and *Bacillus dysenteriae*	(Wei *et al*., 2003)
Vipera lebetina	More active against Gram-negative *E. coli* than Gram-positive *B. subtilis*	(Tõnismägi *et al*., 2006)

Table 3.3, continued

Venom source of LAAO	Antibacterial actions	Reference
Daboia russellii siamensis	Most active against Gram-positive *S. aureus* (MIC = 9 µg/mL) than Gram-negative *P. aeruginosa* (MIC = 144 µg/mL) and *E. coli* (MIC = 288 µg/mL)	(Zhong *et al*., 2009)
Naja naja oxiana (now Naja oxiana)	Slightly more active against Gram-positive *B. subtilis* than Gram-negative *E. coli*	(Samel *et al*., 2008)
Pseudechis australis	Most active against Gram-negative *A. hydrophila* than Gram-positive *B. subtilis* and *S. aureus*	(Stiles *et al*., 1991)
Crotalus durissus cumanensis	Active against Gram-positive *S. aureus* (MIC = 8 µg/mL) than Gram-negative *A. baumannii* (MIC = 16 µg/mL)	(Vargas *et al*., 2013)
Agkistrodon blomhoffii ussurensis	Active against *S. aureus*	(Sun *et al*., 2010)
Bothrops atrox	Slightly more active against Gram-positive *S. aureus* than Gram-negative *E. coli*	(Alves *et al*., 2011)

3.8 Bacteria-binding activity of king cobra venom L-amino acid oxidase

Although H_2O_2 has been demonstrated to play an important role in the bactericidal activity of OH-LAAO, it should be noted that the amount of H_2O_2 generated by a very small amount of the enzyme is insufficient to inhibit the growth of the bacteria tested. For example, the MIC of OH-LAAO against *S. aureus* and *S. epidermidis* were as low as 0.78 µg/mL and 1.56 µg/mL, respectively. Thus, a unique mechanism must have taken place in order for the OH-LAAO to elicit its potent antibacterial activity.

The present study showed that the OH-LAAO binds effectively to bacteria, and its binding is a time-dependent process: it reached saturation only after approximately 5 h of incubation at 37 °C. The results also demonstrated that the binding affinity of the enzyme was higher against the Gram-positive *S. aureus* and *S. epidermidis* than the Gram-negative *E. coli* and *P. aeruginosa*. The binding affinity of the enzyme against *S. aureus* was approximately the same as the other Gram-positive bacteria, *S. epidermidis* and that the binding affinity of the enzyme against the two Gram-negative bacteria, *E. coli* and *P. aeruginosa* was also comparable. The higher bacteria binding affinity of OH-LAAO to the Gram-positive bacteria than to the Gram-negative bacteria are consistent with the observed differences in the MICs reported in the present study, suggesting that bacterial binding affinity of the enzyme plays an important role in its antibacterial activity.

This finding is in agreement with the bacteria binding study of LAAO isolated from venom of *Agkistrodon halys*, as reported by Zhang *et al*. (2004). Using fluorescence detection method, they reported that AHP-LAAO could bind to the surfaces of *E. coli* and *B. subtilis* and that binding of AHP-LAAO to the bacteria enables production of highly localized concentration of H_2O_2 near to the binding sites that would be

sufficiently potent to kill the bacteria. Therefore, a very small amount of AHP-LAAO is able to elicit antibacterial activity.

Similar studies and conclusions have also been reported with LAAO isolated from other organisms. Ehara *et al*. (2002), for example, showed that Achacin (LAAO isolated from the giant snail, *Achatina fulica ferussac*) binds stronger to *S. aureus* than *E. coli*, consistent with the observed differences in MICs between the two bacteria. Kitani *et al*. (2008) also suggested that bacterial-binding plays an important role in the antibacterial activity of SSAP (LAAO isolated from the skin mucus of Rockfish *S. schlegelii*). Using Western blotting and bacterial-binding studies, they demonstrated that the differences in the MICs of SSAP against various bacteria could be correlated to the differences in affinity of the enzyme towards the bacteria.

Toyama *et al*. (2006), on the other hand, showed that the antibacterial activity of LAAO isolated from *C. durissus cascavella* snake venom induced bacterial membrane rupture and subsequently promote the releasing of its plasmatic content. As the estimated amount of H_2O_2 generated was sufficient to inhibit the bacterial growth, they suggested that the binding activity does not play an important role in inhibition of bacterial growth (Toyama *et al*., 2006). Vargas *et al*. (2013) using scanning electron microscopy method further demonstrated that treatment of *S. aureus* and *A. baumannii* with Cdc LAAO for 24 h induced morphological alterations which are correlated with membrane damage and deposition of debris on the bacteria cell surface. They suggested that the enzyme generated high level of H_2O_2 in the medium to cause the membrane damages (Vargas *et al*., 2013).

The discrepancy in the role of bacterial binding affinity of LAAOs in their antibacterial activity is presumably due to the differences of their antibacterial potency as well as the amount of the enzyme used in the study. For LAAOs with weaker antibacterial activity

(these are usually LAAO that could not bind effectively to the bacteria), large amount of the enzyme was used in the studies, and the enzyme was likely to exert its antibacterial effect by generating sufficiently high level of H_2O_2 in the medium to cause direct cytotoxic effect, whereas for LAAOs with very potent antibacterial activity, the enzyme could bind effectively to bacteria, and therefore even a very small amount of the enzyme that binds to the bacteria could generate highly localized H_2O_2 that could elicit effective antibacterial effect.

It is important to note that while the results demonstrated that the OH-LAAO is a very potent antibacterial agent, therapeutic application of the enzyme as an antibacterial agent will always have its limitations due to its relatively high production cost (either purified from venom or via cloning). However, understanding of the mode of antibacterial action of LAAO (as an efficient H_2O_2 generator) may lead to the design of new antibacterial drugs or new therapeutic approaches.

CHAPTER 4

ANTICANCER EFFECTS OF KING COBRA (*Ophiophagus hannah)* VENOM L-AMINO ACID OXIDASE (OH-LAAO)

INTRODUCTION

Cancer is a class of diseases in which a group of cells display uncontrolled growth (division beyond the normal limits), invasion (intrusion on and destruction of adjacent tissues), and sometimes metastasis (spread to other locations in the body via lymph or blood) (Smart, 2010). Cancer is the leading cause of death globally and accounted for 7.6 million deaths, which is around 13% of all deaths in 2008. The deaths are caused mainly by lung, stomach, liver, colorectal, breast, and cervical cancers. Deaths from cancer worldwide are projected to continue rising, with an estimated 13.1 million deaths in 2030 (WHO, 2013).

The high mortality rate of cancer was due to ineffectiveness of currently available cancer treatments and their potential to cause toxicity to normal cells, accompanied by a range of side effects such as vomiting, nausea and alopecia. Thus, there is a continuous need to search for potential natural-based therapeutic agents that exhibit potent cytotoxicity against cancer cells over the normal cells.

Snake venom LAAOs have been reported to exhibit cytotoxicity against various cancer cell lines and its cytotoxic action was believed to be via apoptosis-induction. Unlike other venom LAAOs, king cobra (*Ophiophagus hannah*) venom LAAO, has an unusual thermal stability and is not inactivated by freezing (Tan and Saifuddin, 1989). Due to these favourable properties, king cobra venom LAAO (OH-LAAO) has a greater potential, when compared to other venom LAAOs, to be developed as a cancer therapeutic agent. In this study, the cytotoxic actions of OH-LAAO against human tumourigenic cell lines were investigated, and its cytotoxicity and apoptosis induction activities were compared with the respective non-tumourigenic cell lines. Its potency as a cytotoxic agent was also compared with doxorubicin, a standard anticancer drug. In addition, the enzyme's anti-tumour effect in a PC-3 tumour xenograft mouse model

implanted in immunodeficient NU/NU mice and its toxicity on the vital organs were also investigated.

METHODS

4.1 Cytotoxicity assay

The cytotoxic effect of king cobra venom LAAO (OH-LAAO) and doxorubicin was determined by 3,(4,5-dimethythiazol-2-yl)-2,3-diphenyl tetrazolium bromide (MTT) method according to Ahn et al. (1997) with modifications. Briefly, 100 µL of the cells at their optimal density were seeded onto a 96-well microtitre plate (Table 4.1). After overnight incubation, serially diluted doxorubicin or purified OH-LAAO was added into each well. Following 24 or 72 h treatment, 20 µL of the MTT stock solution of 5 mg/mL in PBS was added. Cells were then incubated for a further 4 h in the dark. Seventy-five percent of the medium was aspirated out and an equal volume of dimethyl sulfoxide (DMSO) was added to solubilize the formazan crystals. The absorbance was measured with a Model 680 microplate reader (Bio-Rad, Hercules, CA) at 570 nm. Cell viability was calculated as follows:

$$\text{Cell viability } (\%) = \frac{\text{Average OD of treated cells} - \text{Average OD of blank}}{\text{Average OD of control cells} - \text{Average OD of blank}} \text{ X } 100\%$$

The half-maximal inhibitory concentration (IC_{50}) value was determined from the dose-response curve.

Table 4.1: Seeding density of cell lines in 96-well microtitre plate for 24 and 72 h treatment period

Cell line	**24 h (cells/well)**	**72 h (cells/well)**
MCF-7	10,000	1,000
A549	15,000	3,000
PC-3	12,000	5,000
HL-60	100,000	28,000
184B5	20,000	5,000
NL 20	20,000	5,000

4.2 Apoptosis analysis

Apoptosis effect of OH-LAAO was first screened on the human tumourigenic (MCF-7, A549, PC-3 and HL-60) and non-tumourigenic (184B5 and NL 20) cell lines using caspase-3/7, DNA fragmentation, and Phycoerythrin-Annexin V/7-Amino-Actinomycin D (PE-Annexin V/7-AAD) assays.

4.2.1 Caspase-3/7 assay

Caspase-3/7 activity was measured using Caspase-Glo® 3/7 assay kit (Promega, USA) according to the manufacturer's protocol. Briefly, cells at their optimal density (Table 4.1) were seeded onto white-walled 96-well microtitre plate. After overnight incubation, cells were treated with OH-LAAO at their respective IC_{50}. Following 72 h treatment, 100 µL of Caspase-Glo® 3/7 reagent containing DEVD sequence luminogenic substrate selective for caspase-3 and -7 was added into each well. The content of the wells was gently mixed with shaking for 2 min. The plate was then incubated in the dark for 1 h at room temperature. The luminescence of each sample was measured using Glomax-Multi Detection System (Promega, USA).

4.2.2 DNA fragmentation assay

DNA fragmentation assay was carried out as described by Lin *et al*. (2003) with some modifications. Briefly, human tumourigenic (MCF-7, A549, PC-3 and HL-60) and non-tumourigenic (184B5 and NL 20) cells were treated with OH-LAAO at their respective IC_{50} for 72 h. Controls were treated with PBS (vehicle). After treatment, cells were harvested using trypsin-EDTA, washed with PBS and spun down at 2,000 rpm for 5 min. Cell pellet was resuspended with 500 µL of PBS. This was followed by adding with 50 µL of lysis buffer [1 M Tris-HCI (pH 8.0), 0.5 M EDTA and 5% (v/v) TritonX-100] and incubated on ice for 30 min. After centrifugation at 10,000 x g for 30 min at

4 °C, cell lysate was collected from the supernatant. An equal volume of phenol/chloroform/iso-amyl alcohol (25:24:1) was then added and gently mixed for 5 min. After centrifugation, the top layer was collected and precipitated with an equal volume of iced-cold iso-propanol and 1/10 volume of 3 M sodium acetate (pH 5.2). Following 30 min incubation at -20 °C, the mixture was subjected to centrifugation at 10,000 x g for 30 min at 4 °C. The supernatant was discarded and the DNA pellet was allowed to air-dry for 10 min. DNA pellet was dissolved in an adequate volume of RNase I solution (10 mg/mL RNase I) and incubated at 37 °C for 30 min. DNA was subjected to 1.2% agarose gel (containing GelRed™) electrophoresis at a constant voltage of 90 V for 1 h. Image acquisition was performed using gel documentation system (Infinity-3026, Vilber Lourmat, France).

4.2.3 Phycoerythrin-Annexin V/7-Amino-Actinomycin D (PE-Annexin V/7-AAD) assay

PE-Annexin V/7-AAD assay was performed using PE annexin V apoptosis detection kit I (BD Biosciences, USA) according to the manufacturer's instructions. In brief, human tumourigenic (MCF-7, A549, PC-3 and HL-60) cells were treated with OH-LAAO at their respective IC_{50} values. The corresponding non-tumourigenic breast (184B5) and lung (NL 20) were treated with 0.04 µg/mL and 0.05 µg/mL of OH-LAAO, respectively (IC_{50} of MCF-7 and A549 respectively). After 72 h treatment, cells were trypsinized and washed twice with PBS. The number of cells (1×10^5 cells) was adjusted with 1X binding buffer to a final volume of 100 µL. Cells were stained with 5 µL of Annexin V conjugated to phycoerythrin (PE) and followed by 5 µL of 7-Amino-Actinomycin D (7-AAD). After incubation in the dark for 15 min at room temperature, 400 µL of 1X binding buffer was added into the mixture. Cells (10,000 events) were analysed using a FACSCanto™ II, and FACSDiva software version 6.1.3 (BD Biosciences, USA). Data

analyses were performed using FCS express 4 flow software (De Novo™ software, CA). Results were expressed in density plots and plotted as 7-AAD versus PE-Annexin V. Data was obtained from an average of two independent experiments from two separate measurements.

4.3 Apoptotic pathways induced by king cobra venom LAAO

The apoptotic cell death induced by OH-LAAO was studied in more detailed by examine the components of the apoptotic cascade that involved in the apoptosis. For this purpose, MCF-7 was used as a representative cell line in measuring the enzymatic activities of caspase-8 and caspase-9 as well as the expression level of cytochrome *c* in the cells treated with OH-LAAO.

4.3.1 Caspase-8 and caspase-9 assays

Caspase-8 and caspase-9 activities were determined using Caspase-Glo® 8 and Caspase-Glo® 9 assay kits, respectively according to the protocols described by the manufacturer (Promega, USA). Briefly, MCF-7 cells at 1,000 cells/well were seeded onto white-walled 96-well cell culture plate. After overnight incubation, cells were treated with 0.04 µg/mL of OH-LAAO (IC_{50} of OH-LAAO). Following 72 h treatment, 100 µL of the reconstituted Caspase-Glo® 8 or Caspase-Glo® 9 reagent was added into each well. The contents of the wells were gently mixed and incubated at room temperature for 1 h. The luminescence of each sample was measured with a Glomax-multi Detection System (Promega, USA).

4.3.2 Measurement the expression level of cytochrome *c*

4.3.2.1 Protein samples preparation

Cytochrome *c* levels in MCF-7 cells treated with OH-LAAO or PBS (vehicle) were measured using Cytochrome *c* (human) EIA kit according to the manufacturer's guideline (Enzo Life Sciences, New York). Cells were treated with 0.04 µg/mL of OH-LAAO for 72 h, harvested by trypsin-EDTA and washed twice with PBS. Cell pellet was then resuspended with digitonin cell permeabilization buffer, vortexed briefly and incubated on ice for 5 min. Subsequently, cell lysate was centrifuged at 1,000 x g for 5 min at 4 °C and the supernatant was collected as a cytosolic fraction. The remaining cell pellet was further lysed with radioimmunoprecipitation assay (RIPA) cell lysis buffer, vortexed, incubated on ice for another 5 min and spun down at 10,000 x g for 10 min at 4 °C. The supernatant was then collected as a subcellular or mitochondria fraction. Protein concentrations of the cytosolic and mitochondria fractions were determined using 2-D quant kit (GE Healthcare, Sweden), as described in general methods (Chapter 2, Section 2.9.2).

4.3.2.2 Determination of cytochrome *c* levels

One hundred microlitres of cytochrome *c* standards (ranging from 0 to 450 pg/mL) or protein samples (100 µg of cytosolic fraction protein or 30 µg of mitochondria fraction protein) were pipetted onto the 96-well ELISA plate provided by the manufacturer, and incubated at room temperature for 1 h with shaking. The wells were emptied and washed four times with 400 µL of washing solution. After washing, 100 µL of the yellow antibody was introduced into the wells and incubated for another 1 h with agitation. The contents of the wells were then discarded and washed again with the washing solution. Blue conjugate (100 µL) was added and incubated for 30 min. After washing for four times with washing solution, 100 µL of substrate solution was added

into the wells and incubated for another 45 min. Reaction was stopped by adding with 25 μL of the stop solution. The optical density of each sample was measured using a Model 680 microplate reader (Bio-Rad, Hercules, CA) at 415 nm with the reference wavelength of 570 nm.

4.4 Prostate adenocarcinoma (PC-3) tumour xenograft mouse model

Prostate adenocarcinoma cells (PC-3) were grown to 80-90% confluency and harvested using trypsin-EDTA. Cells were washed twice with PBS and followed by centrifugation at 2,000 rpm for 5 min. Cell pellet was resuspended in PBS and the number of viable cells was determined using trypan blue exclusion method and counted with a haemocytometer. Subsequently, cell suspension was mixed with an equal volume of Matrigel^{TM}. Under anaesthesia condition, each mouse was inoculated subcutaneously (s.*c.*) with 200 μL of the cells-Matrigel$^{™}$ mixture which contained approximately 0.6 x 10^7 cells. Mice were examined daily for tumour growth at the injection site. Tumour volumes (mm^3) were measured weekly using a digital calliper (Mitutoyo, Japan) and were calculated as (length x width x height x $\pi/6$) to approximate the volume of a spheroid. When the tumour volume reached about 100-200 mm^3 (usually 1 - 2 weeks after inoculation of the PC-3 cells), mice were randomly assigned into control (n = 6) and treated (n = 6) groups. Mice were treated intraperitonealy (*i.p.)* daily with either PBS (control group) or OH-LAAO (treated group) at a dose of 1 μg/g/day/200 μL for 8 weeks. Tumour volume (mm^3) and body weight of individual animals were monitored and recorded weekly over the 8-week treatment period.

4.5 Toxicity study of king cobra venom L-amino acid oxidase in tumour-bearing mice

4.5.1 Organs/tissues fixation

Mice from both OH-LAAO and vehicle-treated groups were sacrificed at the end of the 8 weeks study by cervical dislocation after anaesthetize with *i.p.* injection of a combination of ketamine and xylazine. Vital organs (lung, liver, heart, spleen, kidneys) and solid tumour tissues were harvested and fixed in 10% buffered formalin for 48 h.

4.5.2 Tissue processing

4.5.2.1 Dehydration and clearing

Tissues were placed into the tissue cassettes and dehydrated by submerging in an increasing concentration of ethanol for 1 h in each concentration, starting with 60% and progressing through 70%, 80%, 95%, and finally in two volume changes of absolute ethanol. After dehydration, tissues were rinsed with benzene.

4.5.2.2 Infiltration and embedding

Tissues were transferred into a mixture containing equal volume of benzene and melted paraffin wax and incubated at 60 °C for 1 h. The mixture of benzene and paraffin wax was discarded and the tissues were allowed to equilibrate in melted paraffin for another 45 min at 60 °C. This step was repeated with freshly melted paraffin. Tissue cassettes were then transferred into an embedding mold and filled with melted paraffin. Paraffin was allowed to solidify at room temperature.

4.5.2.3 Tissue sectioning and mounting on microscope slides

Paraffin-embedded tissues were sectioned at 5 µm thick using a microtome. Tissue sections were floated on a pre-heated 45 °C water bath until the sections are flattened. Tissue sections were then mounted on a clean silanized microscope slides. Excessive water or adhesive solution around the section area was drained with a paper towel. Subsequently, slides were placed on a pre-heated 40 °C platform until the sections are firmly fixed on the slides.

4.5.2.4 Clearing and rehydration of tissue sections

Tissue sections were dewaxed in two volume changes of xylene for 5 min each in a coplin jar. Tissue sections were then rehydrated by submerging in a decreasing concentration of ethanol for 2 min in each concentration, starting with 100% ethanol, followed by 85% and 70% and finally washed with milli-Q™ water for 1 min.

4.5.2.5 Haematoxylin and eosin staining

Rehydrated tissue sections were stained with Harris haematoxylin for 5 min, washed in two volume changes of milli-Q™ water for 30 sec in each wash and differentiated in acidic ethanol (70% ethanol containing a few drops of HCl). Tissue sections were then washed with milli-Q™ water and finally counter stained with Eosin Y, 0.5% aqueous for 5 min. Subsequently, tissue sections were dehydrated in 95% ethanol for 20 sec, followed by absolute ethanol for 30 sec and xylene for 1 min. Slides were removed from the coplin jars and tapped gently on the edge to remove the excess solvent. Cover-slip was mounted on top of the tissue section by a mounting medium (permount). Images were capture using light microscope equipped with camera (BX 51 Olympus, Japan).

4.6 TdT-mediated dUTP nicked-end labelling (TUNEL) immunohistochemical staining of tumour tissue

TdT-mediated dUTP nicked-end labelling (TUNEL) assay for the detection of apoptotic cells was performed using ApopTag® plus peroxidase *in situ* apoptosis detection kit according to the manufacturer's protocol (Millipore, USA). Briefly, tumour tissues were processed, sectioned at 5 μm thick, and mounted on the silanized slides (as described in Section 4.5.2). Tumour sections were treated with proteinase K (20 mg/mL) for 15 min, and followed by quench in 3% H_2O_2 (diluted with PBS) for 5 min. An adequate volume of the equilibration buffer was pipetted onto the tissue sections and incubated for 10 sec. Subsequently, tissue sections were incubated with terminal deoxynucleotidyl transferase (TdT) enzyme at 37 °C for 1 h in a humidified chamber. Tissue sections were then washed with the washing buffer and allowed to bind to anti-digoxigenin conjugate in a humidified chamber for another 30 min. Subsequently, slides were stained with 3, 3'-diaminobenzidine (DAB) peroxidase substrate for 5 min, washed in 3 volume changes of milli-Q™ water, and counter stained with 0.5% methyl green for 10 min. Finally, cover-slip was mounted on top of the tumour section using a mounting medium (permount). Slides were examined under light microscope (BX 51 Olympus, Japan) and the pictures of 5 random fields of view per section at 200X magnifications were taken. The percentage of apoptotic cells were scored as an average of the ratio of TUNEL-positive cells to the total number of cells present in each field.

4.7 Statistical analysis

Results for i*n vitro* studies; cytotoxicity, PE-annexin V/7-AAD, caspase-3/7, caspase-8, and caspase-9 activities as well as cytochrome *c* expression level were expressed as mean ± S.D. The *in vivo* anti-tumour activities were expressed as mean ± S.E.M. The significance of the differences of the means was determined by one-way ANOVA,

followed by Tukey's post hoc multiple comparison test. The statistical analysis was conducted using SPSS 17.0 (SPSS Inc., Chicago, IL, USA).

RESULTS

4.8 Cytotoxicity of king cobra venom L-amino acid oxidase

Cytotoxicity of king cobra venom LAAO (OH-LAAO) and doxorubicin (the commonly used chemotherapeutic drug) were investigated by MTT assay. As shown in Figure 4.1 and 4.2, the cytotoxic effects of both OH-LAAO and doxorubicin treatments in six cell lines examined were in dose- and time-dependent manner. Table 4.2 and Table 4.3 show the IC_{50} values of the OH-LAAO and doxorubicin in four human tumourigenic cell lines; MCF-7 (breast adenocarcinoma), A549 (lung adenocarcinoma), HL-60 (promyelocytic leukaemia) and PC-3 (prostate adenocarcinoma), as well as two human non-tumourigenic cell lines; 184B5 (non-tumourigenic breast) and NL 20 (non-tumourigenic lung) after 24 h and 72 h incubation.

The results showed that the enzyme was very potent against the four tumourigenic cell lines (MCF-7, A549, HL-60 and PC-3), with IC_{50} ranging from 0.05 to 0.15 μg/mL after 24 h incubation. The cytotoxicity was increased when the treatment prolonged to 72 h (IC_{50} of 0.04 - 0.07 μg/mL). Surprisingly, such cytotoxicity was not observed in non-tumourigenic breast (184B5) and lung (NL 20) cell lines, even after 72 h incubation; the IC_{50} was at least 3 to 4 times higher than that of their corresponding tumourigenic cell lines ($P < 0.05$). Treatment with 400 μg/mL of catalase (ROS scavenger) substantially reduced the cytotoxic effect of OH-LAAO ($P < 0.05$) (Table 4.2, Figure 4.1). The IC_{50} values in all cell lines examined were ranged from 0.37 - 0.90 μg/mL and 0.33 - 1.13 μg/mL after 24 h and 72 h incubation, respectively (Table 4.2).

For comparison, the IC_{50} values of doxorubicin, a standard anti-cancer chemotherapeutic agent against the same cell lines were also determined under the same experimental conditions as OH-LAAO treatment. As shown in Table 4.2 and Table 4.3, OH-LAAO's anti-proliferative effects were far more potent than that of doxorubicin,

with at least 9- to 92-folds lower IC_{50} (24 h treatment) when compared on the same tumourigenic cell lines. Doxorubicin has minimal selectivity against tumourigenic and non-tumourigenic cells: at 24 h incubation, it was essentially equally cytotoxic to both tumourigenic MCF-7 (IC_{50} of 0.70 µg/mL) and non-tumourigenic 184B5 (IC_{50} of 1.00 µg/mL) breast cells, and in fact even more cytotoxic to non-tumourigenic NL 20 (IC_{50} of 1.37 µg/mL) lung cells than the tumourigenic A549 (IC_{50} of 2.23 µg/mL) counterpart (Table 4.3).

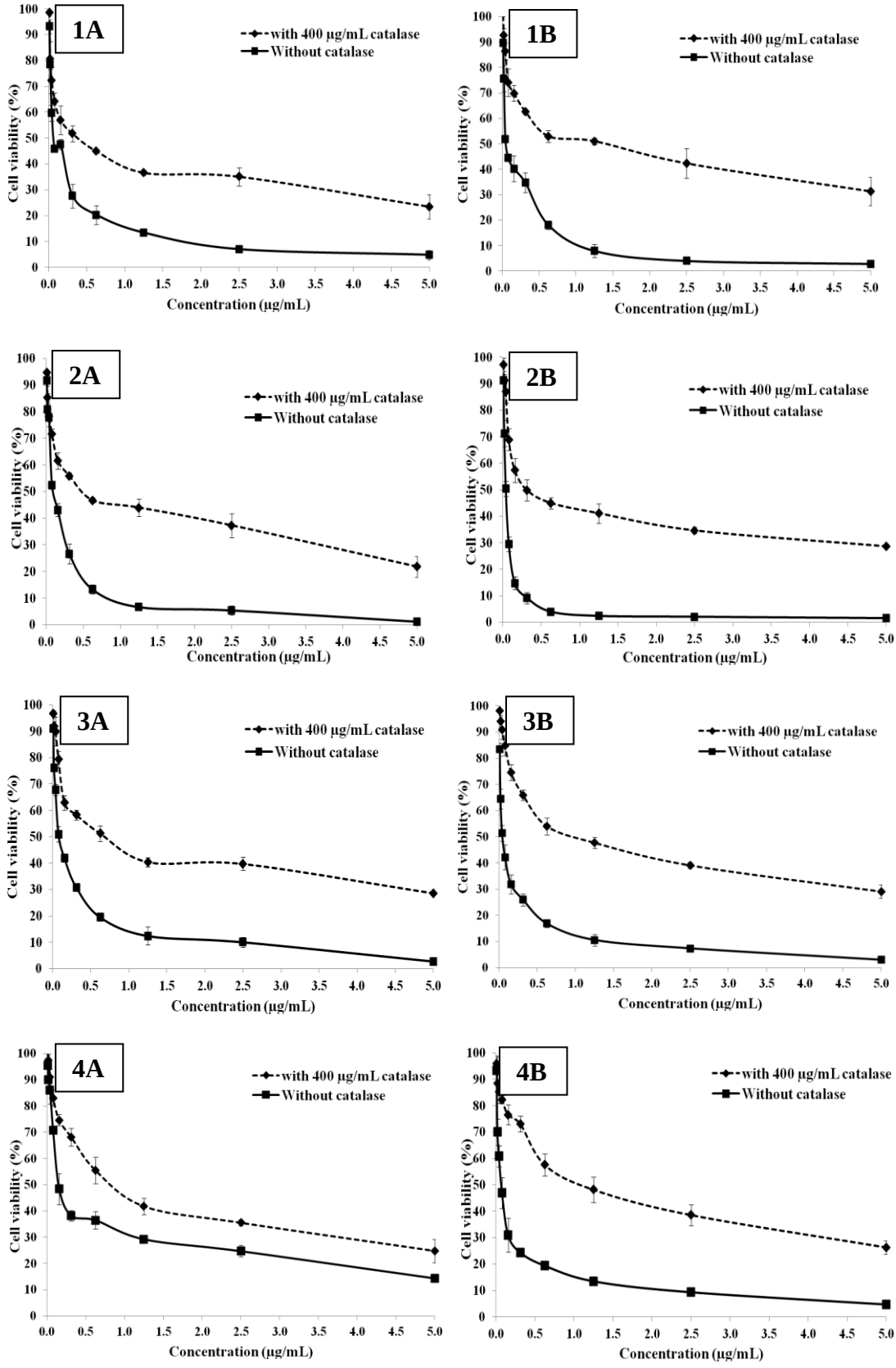
1A
1B
2A
2B
3A
3B
4A
4B
with 400 µg/mL catalase
Without catalase
Cell viability (%)
Concentration (µg/mL)

Figure 4.1, continued

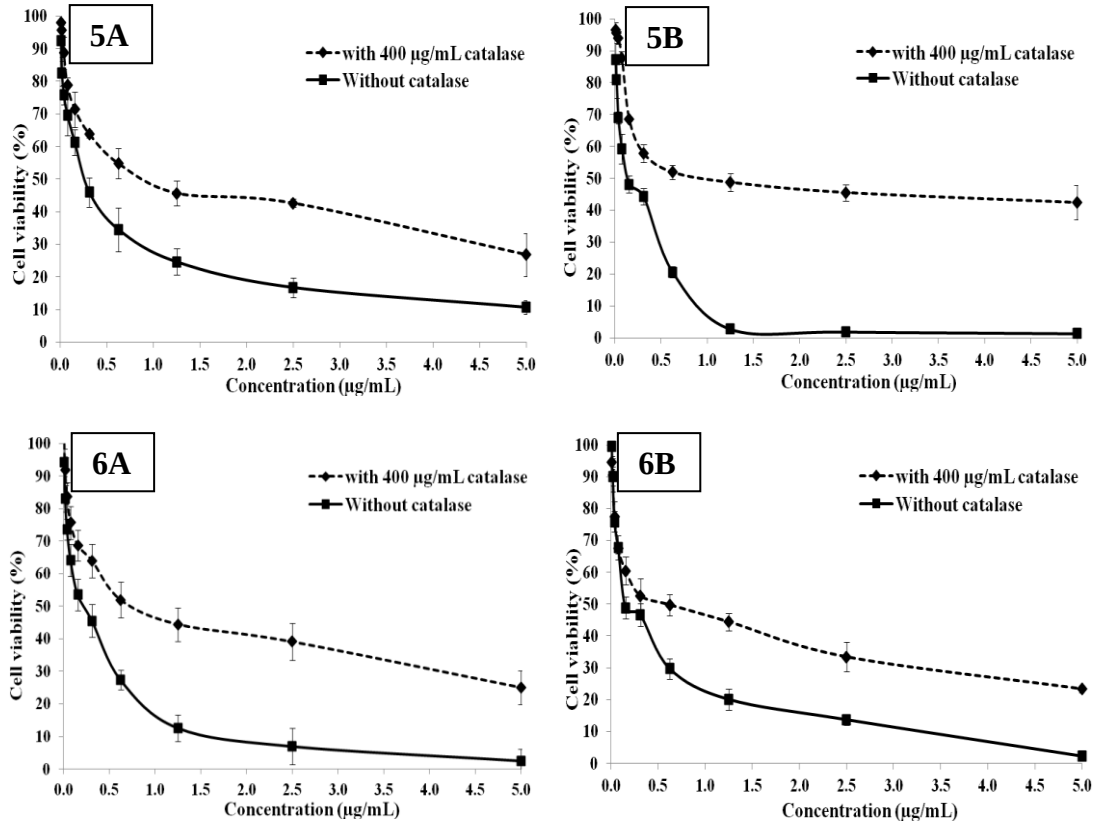

Figure 4.1: Effect of king cobra venom LAAO on viability of various human tumourigenic and non-tumourigenic cell lines. The tumourigenic (MCF-7, A549, PC-3 and HL-60) and non-tumourigenic (184B5 and NL 20) cells were treated with different concentrations of OH-LAAO (0.01 - 5.00 µg/mL) for 24 or 72 h, with or without catalase (400 µg/mL). The viability of the cells was measured by MTT assay. Results given are mean ± S.D (n = 3). Solid line —■—: without catalase; Broken line ---♦---: with catalase. 1A: MCF-7, 24 h treatment; 1B: MCF-7, 72 h treatment; 2A: A549, 24 h treatment; 2B: A549, 72 h treatment; 3A: PC-3, 24 h treatment; 3B: PC-3, 72 h treatment; 4A: HL-60, 24 h treatment; 4B: HL-60, 72 h treatment; 5A: 184B5, 24 h treatment; 5B: 184B5, 72 h treatment; 6A: NL 20, 24 h treatment; 6B: NL 20, 72 h treatment.

Table 4.2: Cytotoxic effect [IC_{50} (µg/mL)] of king cobra venom L-amino acid oxidase against human tumourigenic and non-tumourigenic cell lines

	IC_{50} (24 h Treatment)		IC_{50} (72 h Treatment)	
(µg/mL±SD)	without catalase	with catalase	without catalase	with catalase
MCF-7	0.05 ± 0.00	0.37 ± 0.10	0.04 ± 0.00	1.08 ± 0.48
A549	0.09 ± 0.01	0.48 ± 0.03	0.05 ± 0.00	0.33 ± 0.13
PC-3	0.08 ± 0.02	0.65 ± 0.13	0.05 ± 0.01	0.95 ± 0.28
HL-60	0.15 ± 0.05	0.80 ± 0.15	0.07 ± 0.02	1.13 ± 0.38
184B5	0.25 ± 0.05	0.90 ± 0.30	0.15 ± 0.05	1.05 ± 0.51
NL 20	0.22 ± 0.08	0.73 ± 0.28	0.18 ± 0.06	0.62 ± 0.35

Human tumourigenic cells (MCF-7, A549, PC-3 and HL-60) and non-tumourigenic cells (184B5 and NL 20) were treated with OH-LAAO for 24 h and 72 h, with or without catalase (400 µg/mL). Data are expressed as mean ± S.D (n = 3).

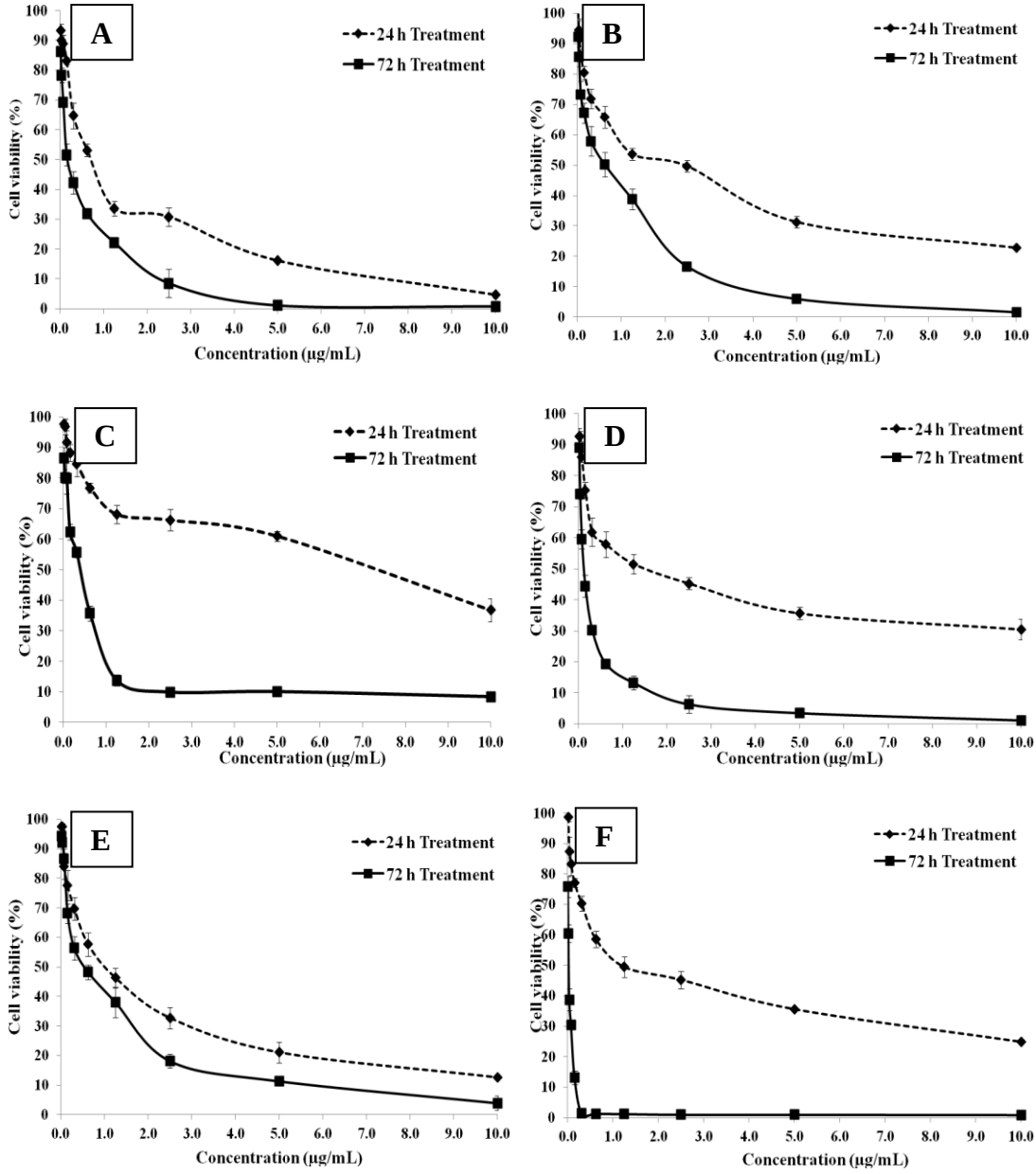

Figure 4.2: Effect of doxorubicin on viability of various human tumourigenic and non-tumourigenic cell lines. Cells were treated with different concentrations of doxorubicin (0.02 - 10.00 µg/mL for MCF-7, A549, PC-3, HL-60 and 184B5; 0.01 - 10.00 µg/mL for NL 20) for 24 or 72 h. The viability of the cells was measured by MTT assay under the same experimental conditions as for OH-LAAO. Results given are mean ± S.D (n=3). Broken line ---♦---: 24 h treatment; Solid line —■—: 72 h treatment. A: MCF-7, B: A549, C: PC-3, D: HL-60, E: 184B5, F: NL 20.

Table 4.3: Cytotoxic effect [IC_{50} (µg/mL)] of doxorubicin against human tumourigenic and non-tumourigenic cell lines

IC_{50} (µg/mL±SD)	24 h Treatment	72 h Treatment
MCF-7	0.70 ± 0.05	0.18 ± 0.03
A549	2.23 ± 0.57	0.63 ± 0.21
PC-3	7.33 ± 0.58	0.40 ± 0.00
HL-60	1.35 ± 0.41	0.10 ± 0.00
184B5	1.00 ± 0.27	0.48 ± 0.20
NL 20	1.37 ± 0.57	0.02 ± 0.00

Cells were treated with doxorubicin for 24 h and 72 h. Data are expressed as mean ± S.D (n = 3).

4.9 Apoptosis effect of king cobra venom L-amino acid oxidase

To examine whether the OH-LAAO exerts its cytotoxicity via induction of apoptosis, caspase-3/7 activities, formation of DNA fragmentation, and surface externalization of membrane phospholipid phosphatidylserine (PS) in human tumourigenic and non-tumourigenic cell lines following OH-LAAO treatment were examined.

4.9.1 Effect of king cobra venom L-amino acid oxidase on caspase-3/7 activities

Caspase-3/7 activities in both vehicle- and LAAO-treated tumourigenic (MCF-7, A549, PC-3 and HL-60) and non-tumourigenic (184B5 and NL 20) cells at their respective IC_{50} value were measured after 72 h treatment. As shown in Figure 4.3, caspase-3/7 activities were significantly increased in LAAO-treated cells, with at least 1.8-fold greater than in vehicle-treated (control) cells. The highest caspases activation (3.8-fold) was observed in PC-3 cells. Low levels of caspase-3/7 activities were also detected in the control cells, which was probably due to small numbers of cells undergoing normal apoptosis in the growing cell population.

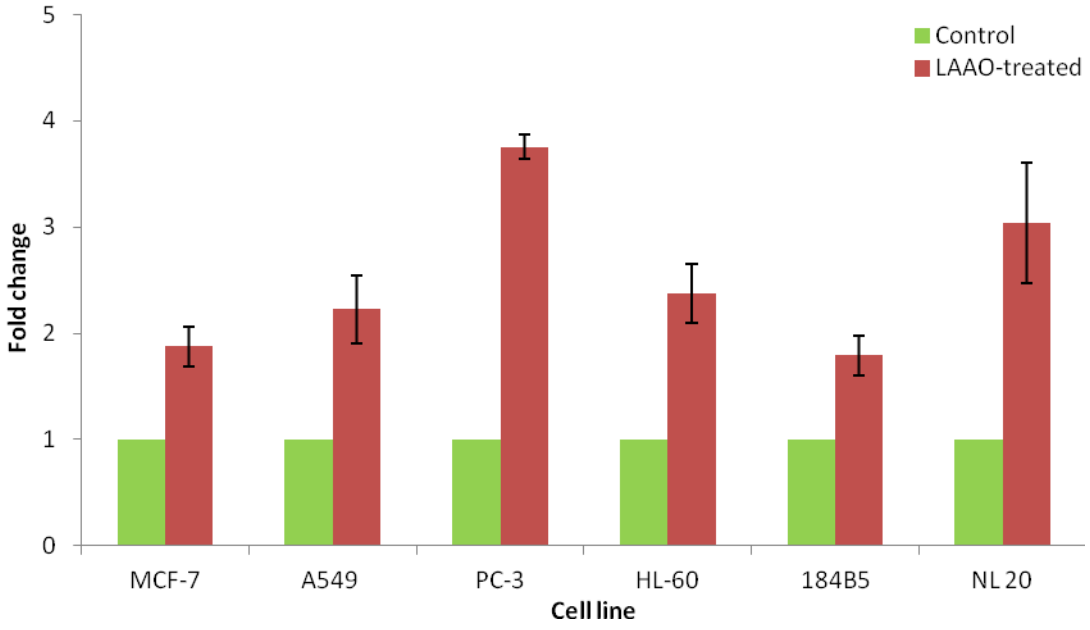

Figure 4.3: Caspase-3/7 activities of OH-LAAO treated cells. The following cell lines were treated with OH-LAAO at their respective IC_{50} dosage for 72 h: MCF-7, A549, PC-3, HL-60, 184B5 and NL 20 cells. Caspase-3/7 activities were determined using Caspase-Glo® 3/7 assay kit (n = 3). Fold change of the control is 1 and the error bars indicate S.D from three independent experiments. Statistical analysis was performed using one-way ANOVA, followed by Tukey's post hoc multiple comparison test. * $P < 0.05$ in the LAAO-treated versus control cells.

4.9.2 Effect of king cobra venom L-amino acid oxidase on nuclear fragmentation

The formation of DNA ladders in tumourigenic and non-tumourigenic cells were examined following OH-LAAO treatment at their respective IC_{50} value for 72 h. Figure 4.4 shows the presence of DNA fragments in MCF-7, A549, PC-3, HL-60, 184B5 and NL 20 cells as a result of OH-LAAO treatment. No DNA fragmentations were observed in the respective vehicle-treated (control) cells. Both increase in caspase-3/7 activities and the formation of DNA fragments indicated that OH-LAAO induced cell death via apoptosis.

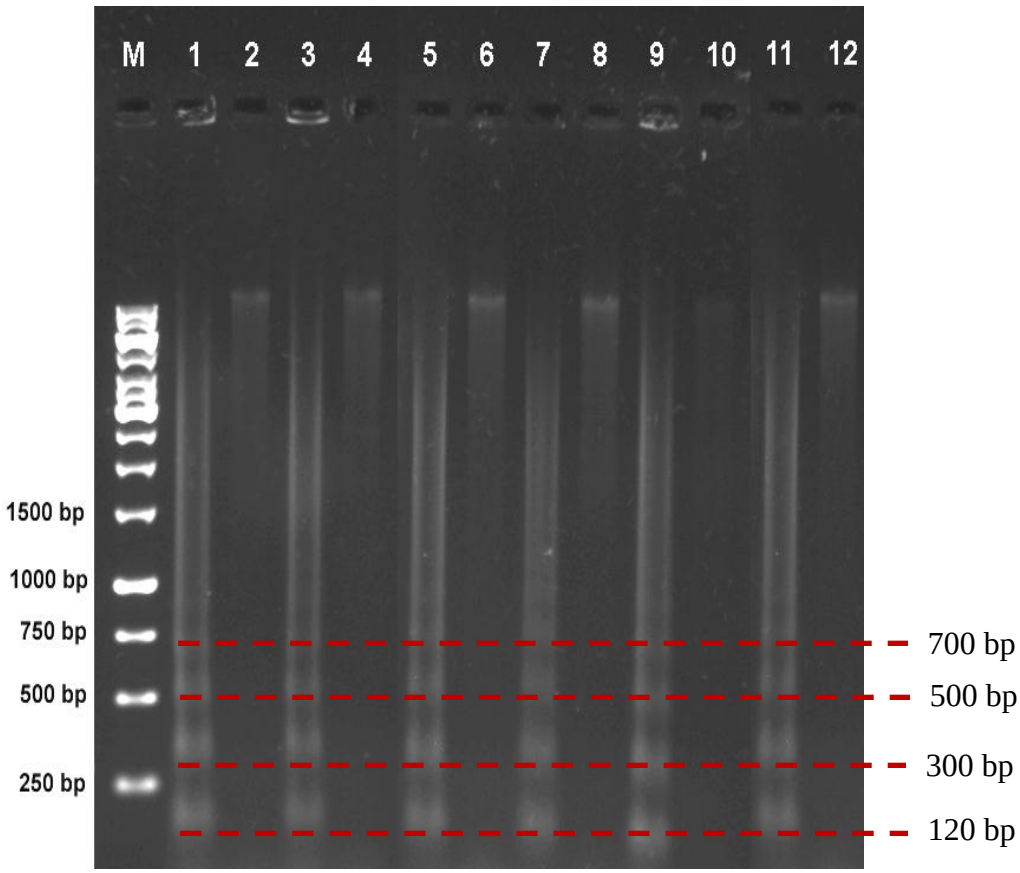

Figure 4.4: King cobra venom L-amino acid oxidase induced DNA fragmentations in tumourigenic and non-tumourigenic cells. Tumourigenic and non-tumourigenic cells were treated with OH-LAAO at their respective IC_{50} for 72 h. M: 1 kb DNA ladder, Lane 1: Treated MCF-7, Lane 2: MCF-7 control, Lane 3: Treated A549, Lane 4: A549 control, Lane 5: Treated PC-3, Lane 6: PC-3 control, Lane 7: Treated HL-60, Lane 8: HL-60 control, Lane 9: Treated 184B5, Lane 10: 184B5 control, Lane 11: Treated NL 20, Lane 12: NL 20 control. Red coloured lines indicate the estimated size of the DNA fragments.

4.10 The selectivity of cytotoxic and apoptosis effects of king cobra venom L-amino acid oxidase

The selectivity of cytotoxic action of OH-LAAO was demonstrated by PE-annexin V/7-AAD assay. The MCF-7 and 184B5 cells were treated with 0.04 µg/mL of OH-LAAO (IC_{50} value of MCF-7), A549 and NL 20 cells were treated with 0.05 µg/mL of OH-LAAO (IC_{50} of A549), whereas PC-3 and HL-60 cells were treated with 0.05 µg/mL and 0.07 µg/mL of OH-LAAO, respectively (their respective IC_{50}), for 72 h. Cells stained with PE-annexin V and 7-AAD were analysed using flow cytometry.

In tumourigenic MCF-7 cells, OH-LAAO treatment resulted in 35.9% cell death, compared to 16.9% in the non-tumourigenic counterpart (184B5) (Figure 4.5). Selective cytotoxic action of OH-LAAO was evident as the vehicle-treated cells only showed 4.5% and 11.4% of cell death, respectively, in MCF-7 and 184B5 cells. Similarly, a greater percentage cell death occurred in LAAO-treated A549 cells (34.6%) than in its non-tumorigenic counterpart, NL 20 cells (6.4%). In comparison, vehicle treated cells only showed 7.6% and 4.9%, of cell death respectively, for A549 and NL 20 cells (Figure 4.5) (data obtained from an average of 2- independent experiments).

Besides the selectivity, PE-annexin V/7-AAD data also suggest that LAAO-induced cell death in tumourigenic cells (MCF-7, A549, PC-3 and HL-60) is via induction of apoptosis, as a significant increased of early and late apoptotic cells of 30.8%, 21.0%, 24.7% and 34.2% were observed in the LAAO-treated MCF-7, A549, PC-3 and HL-60, respectively (Figure 4.5A and B minus the control).

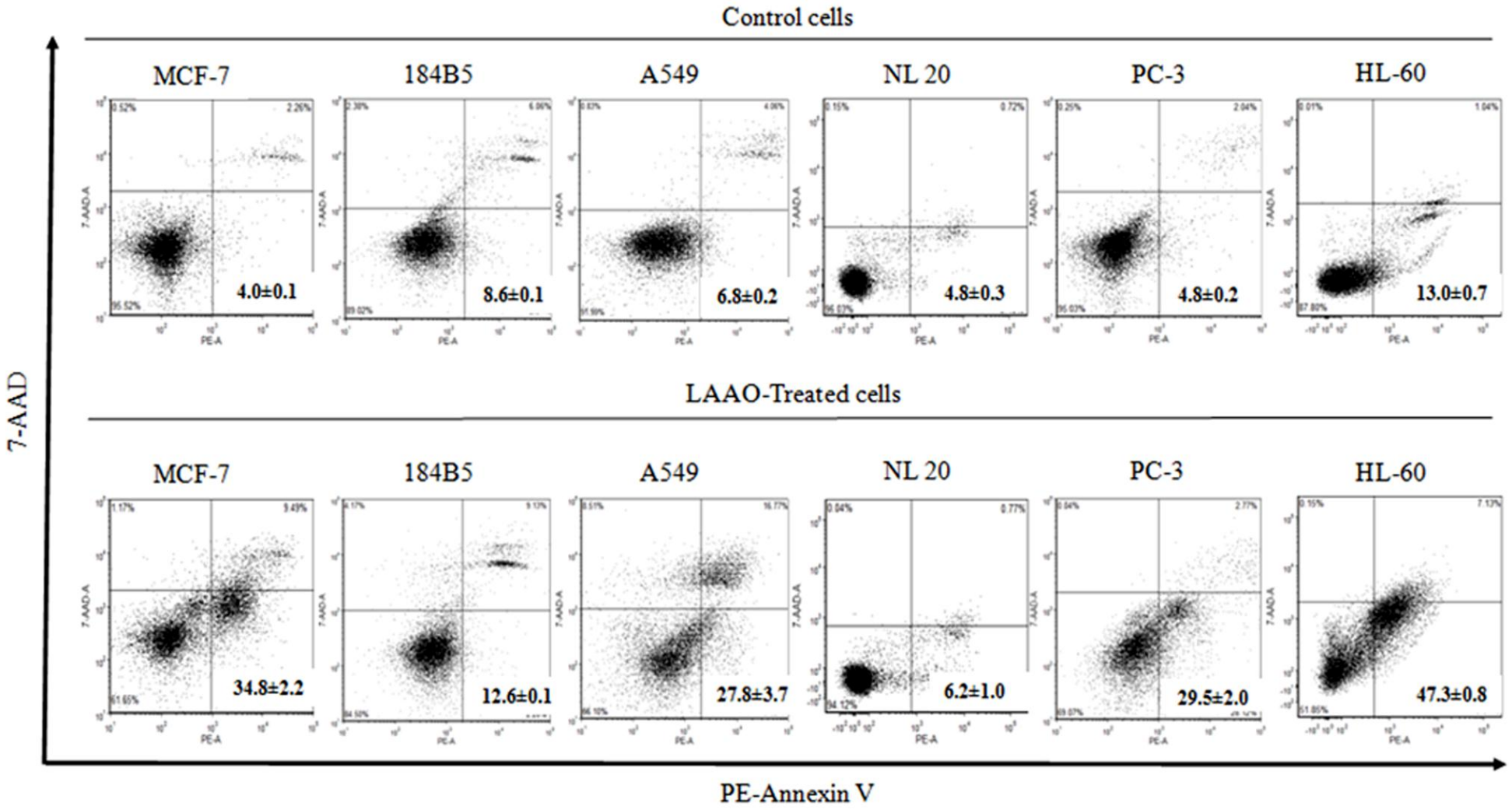
Control cells
MCF-7
184B5
A549
NL 20
PC-3
HL-60
4.0±0.1
8.6±0.1
6.8±0.2
4.8±0.3
4.8±0.2
13.0±0.7
LAAO-Treated cells
MCF-7
184B5
A549
NL 20
PC-3
HL-60
34.8±2.2
12.6±0.1
27.8±3.7
6.2±1.0
29.5±2.0
47.3±0.8
7-AAD
PE-Annexin V

Figure 4.5, continued

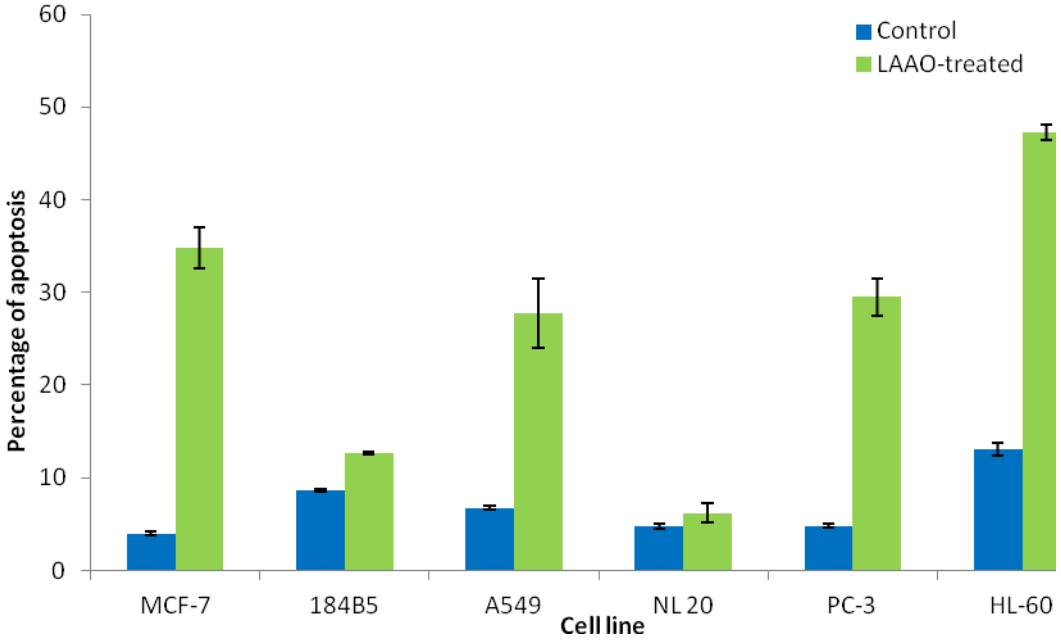

Figure 4.5: PE-Annexin V/7-AAD analysis of the effects of OH-LAAO treatment on tumourigenic and non-tumourigenic cell lines. (A) Flow cytometry analysis of PE Annexin V/7-AAD dual staining. The MCF-7 and 184B5 cells were treated with 0.04 µg/mL of OH-LAAO, A549 and NL 20 cells were treated with 0.05 µg/mL of OH-LAAO, whereas PC-3 and HL-60 cells were treated with 0.05 µg/mL and 0.07 µg/mL of OH-LAAO respectively, for 72 h. Cells (10,000 events) were analysed by fluorescent-activated cell scanner. The lower left quadrant contains the viable cells (Annexin V -; 7-AAD -), the upper left quadrant contains the damage population (Annexin V -; 7-AAD +), the upper right quadrant contains the late apoptotic cells (Annexin V +; 7-AAD +) and the lower right quadrant contains the early apoptotic cells (Annexin V +; 7-AAD -). X-axis indicates the number of PE-Annexin V stained cells. Y-axis indicates the number of 7-AAD stained cells. Total apoptotic cells (%) are shown in each figure. (B) Quantitative data of PE-Annexin V/7-AAD dual staining. Data is expressed in % of apoptotic cells (in lower right and upper right quadrants). All figures represent the mean ± S.D of duplicate analysis from 2-independent experiments. * $P < 0.05$ in the LAAO-treated versus control cells.

4.11 Apoptotic pathways induced by king cobra venom L-amino acid oxidase

To examine the components of the apoptotic cascade involved in king cobra venom LAAO-induced apoptotic cell death in MCF-7 cells, enzymatic activities of caspase-8 and caspase-9 as well as the expression level of cytochrome *c* were measured following 72 h OH-LAAO treatment at its IC_{50} value.

4.11.1 Effect of king cobra venom L-amino acid oxidase on caspase-8 and caspase-9 activities

Caspase-8 and caspase-9 activities in the control and LAAO-treated MCF-7 cells were measured using caspase-Glo® 8 and caspase-Glo® 9 assay kit, respectively. As shown in Figure 4.6, caspase-8 and caspase-9 activities in the treated cells were 3.3- and 4.7-fold, respectively greater than that in their corresponding control cells ($P < 0.05$).

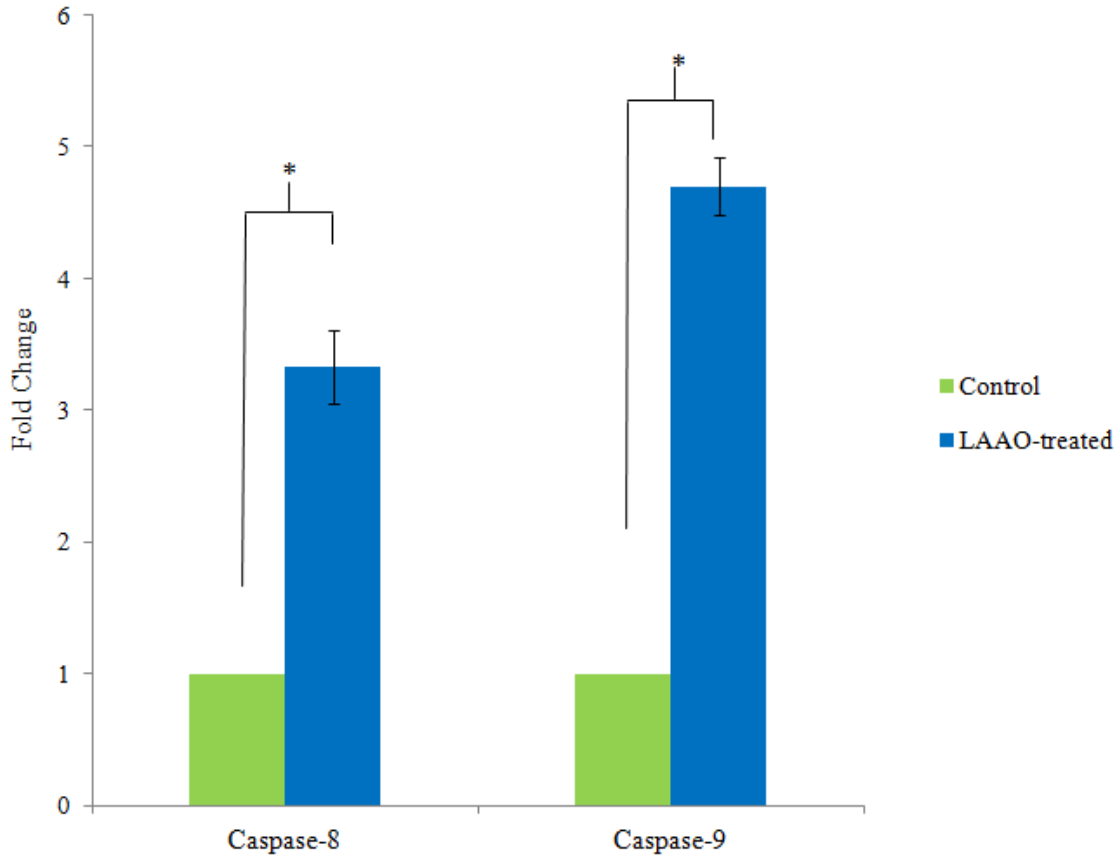

Figure 4.6: Caspase-8 and caspase-9 activities in LAAO-treated MCF-7 cells. The cells were treated with 0.04 µg/mL of OH-LAAO. The caspase activities were determined after 72 h incubation. Fold-change of the control is 1 and the error bars indicate the S.D from three independent experiments. Statistical analysis was performed using one-way ANOVA, followed by Tukey's post hoc multiple comparison test. * $P < 0.05$ in the LAAO-treated versus control cells.

4.11.2 Effect of king cobra venom L-amino acid oxidase on cytochrome *c* levels

Expression levels of cytochrome c in the vehicle- and LAAO-treated MCF-7 cells were determined using cytochrome *c* (human) EIA kit. After 72 h treatment with 0.04 µg/mL (IC_{50}) of OH-LAAO, proteins from both cytosolic and mitochondria fractions were extracted. The concentrations of the cytochrome *c* were determined. When compared to the controls, expression levels of cytochrome *c* in LAAO-treated cells were 1.6- and 3.3-fold higher in the cytosolic and mitochondria fraction, respectively ($P < 0.05$) (Figure 4.7).

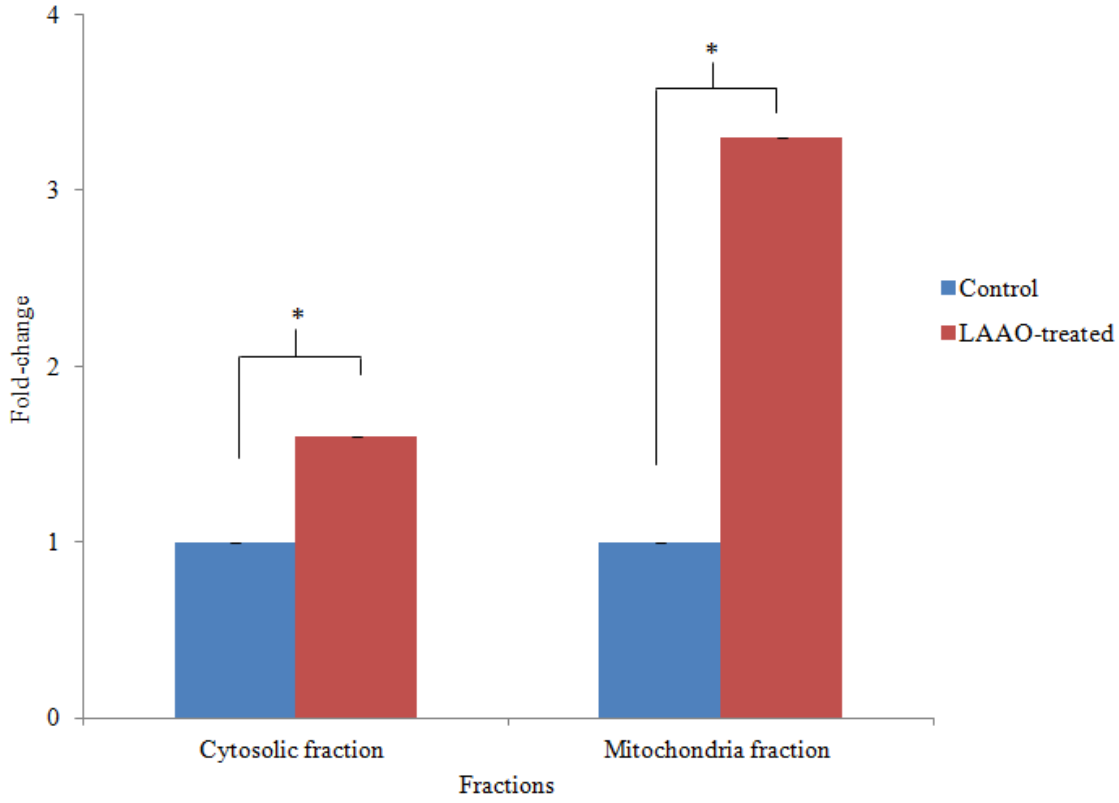

Figure 4.7: Expression levels of cytochrome *c* in MCF-7 cells in response to OH-LAAO treatment. MCF-7 cells were treated with 0.04 µg/mL of OH-LAAO for 72h. The expression levels of cytochrome *c* in both cytosolic and mitochondria fractions were determined and expressed as fold-change. The error bars indicate the S.D from three independent experiments. * $P < 0.05$ in the LAAO-treated versus control cells.

4.12 *In vivo* anti-tumour studies

4.12.1 *In vivo* anti-tumour effects of king cobra venom L-amino acid oxidase in PC-3 tumour xenograft mouse model

As shown in Figure 4.8, LAAO-treated tumours grew markedly slower than those treated with vehicle only. A significant difference in mean tumour size was seen between vehicle-treated and LAAO-treated group ($P < 0.01$), as early as 7 days post-treatment. By the 8^{th} week, tumours in control mice had grown to greater than 700% of the original size (size of the tumour at the start of treatment assigned as 100%), whereas for the OH-LAAO treated mice, the average tumour size was 300% of their original size ($P < 0.01$, between treated and control). All tumours were harvested at the end of the study (week 8) (Figure 4.9). One of the tumours achieved complete regression with no sign of tissue left for harvest (picture not shown).

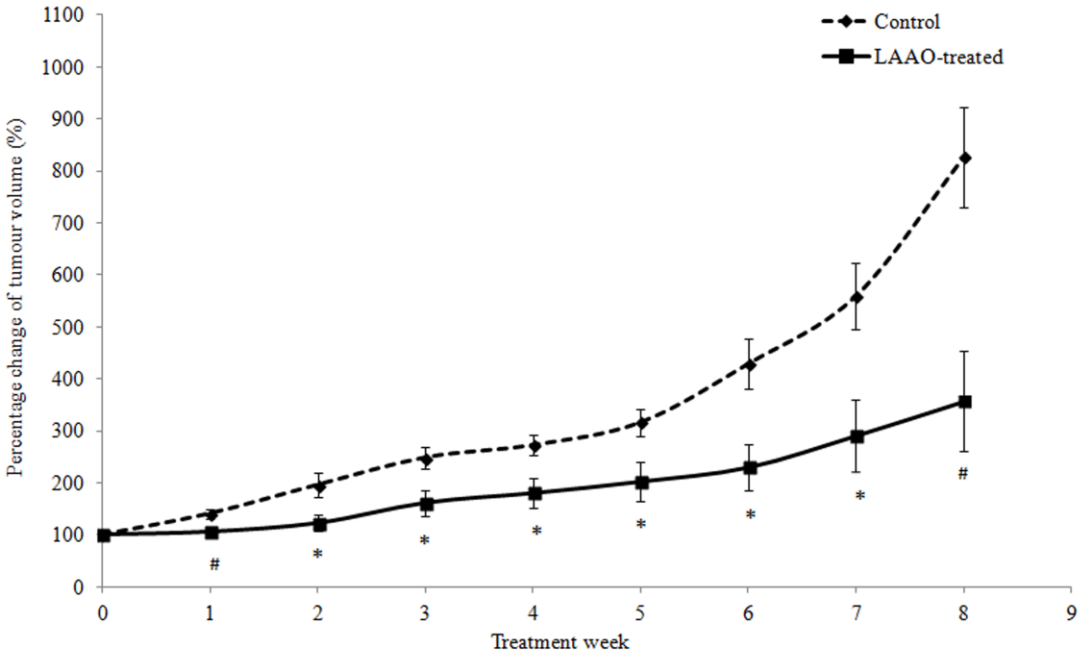

Figure 4.8: *In vivo* anti-tumour effect of OH-LAAO on solid PC-3 prostrate tumour in nude mice. Tumour-bearing nude mice were treated *i.p.* daily with either vehicle (control, broken line---♦---, n = 6) or OH-LAAO (1 μg/g/day/200 μL, solid line —■—, n = 6). Tumour volume was measured weekly. The percentage change of tumour volume was calculated after compare with those at week 0. Data was expressed as mean ± standard error of the mean. Statistical analysis was performed using one-way ANOVA, followed by Tukey's post hoc multiple comparison test ($P < 0.05$ for data points marked with *, $P < 0.01$ for data points marked with #).

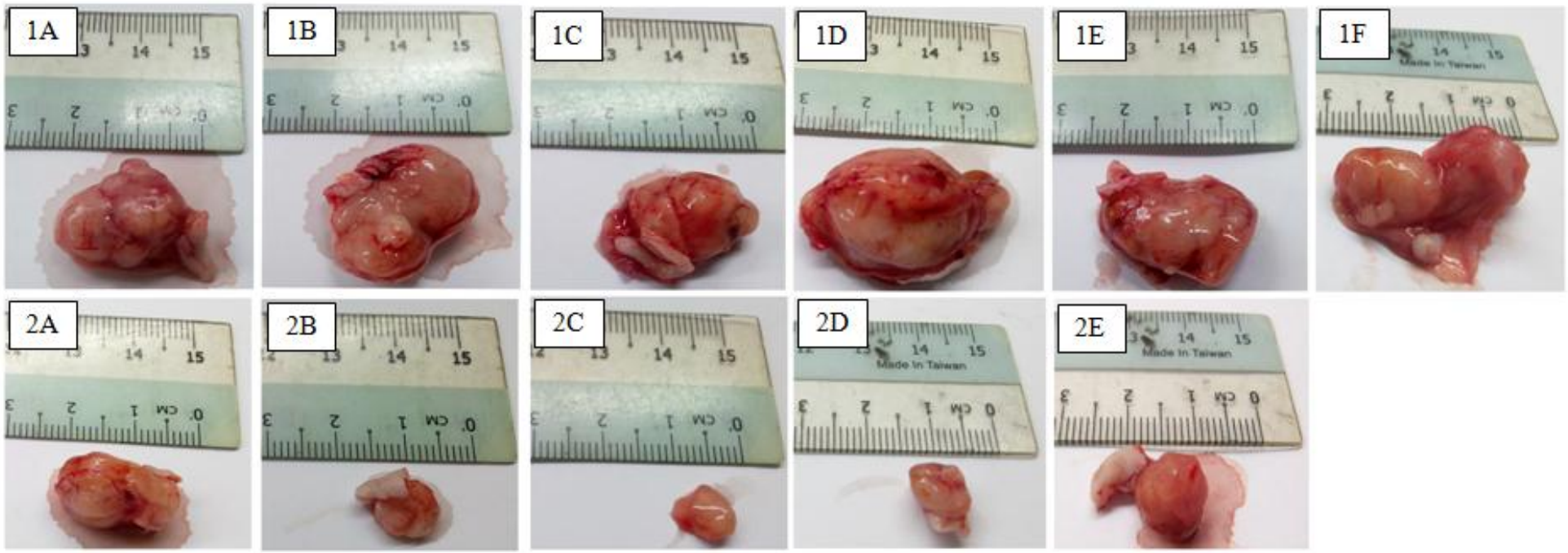

Figure 4.9: Suppression of tumour size in PC-3 tumour-bearing nude mice treated with OH-LAAO. Images showing tumours harvested at the end of 8th week treatment: control group (1A-F) and OH-LAAO treated group (2A-E). One of the tumours from the LAAO-treated group achieved complete regression, as no evidence of tumour tissue could be detected at the end of treatment period (picture not shown).

4.13 Toxicity study of king cobra venom L-amino acid oxidase in tumour-bearing mice

Histological examinations of the major organs harvested (heart, kidney, liver, lung and spleen) at the end of 8th week show that the OH-LAAO treatment did not cause any abnormal pathological changes when compared to those in vehicle-treated (Figure 4.10). Also, the body weight of the LAAO-treated group did not differ ($P > 0.05$) from the vehicle-treated mice throughout the treatment period (Figure 4.11).

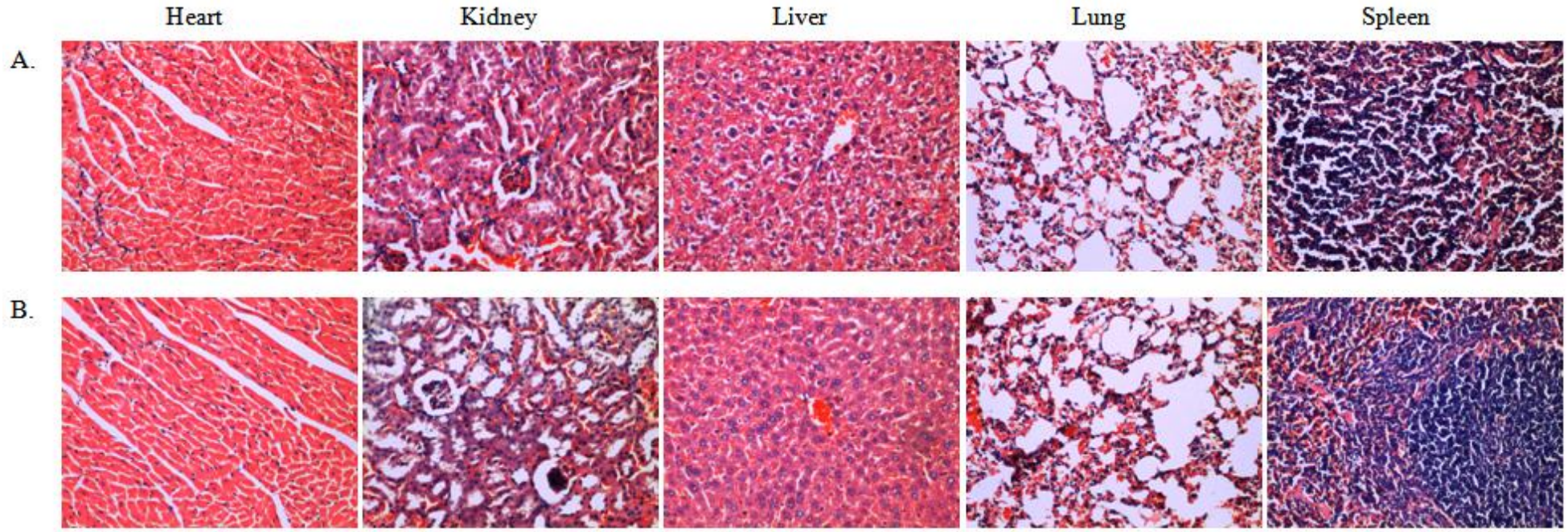

Figure 4.10: Histological sections of major organs of control and LAAO-treated mice. Haematoxylin and Eosin (H&E) stained sections (100X magnifications) of heart, kidney, liver, lung and spleen tissues of (A) vehicle-treated mice and (B) LAAO-treated mice. Intraperitoneal (*i.p.*) administration of 1 μg/g/200 μL of OH-LAAO daily for 8 weeks did not cause significant pathological changes in heart, kidney, liver, lung and spleen of the mice when compared to those in the vehicle-treated mice.

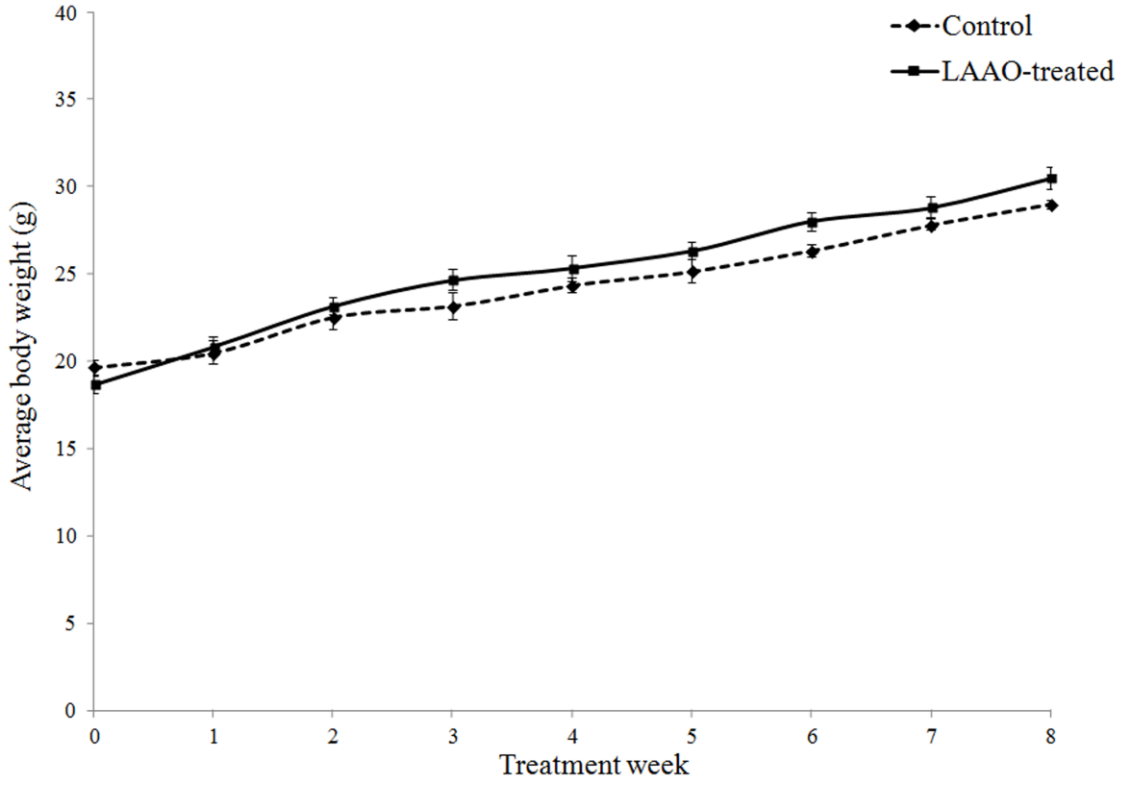

Figure 4.11: Changes in the body weight of mice in the control and LAAO-treated groups. Body weight of the mice in both control and LAAO-treated groups were determined weekly. There were no significant differences in the average body weight of the two groups over the 8-weeks treatment period ($P > 0.05$). Solid line —■—: LAAO-treated mice; Broken line ---♦---: Control mice. Data was expressed as mean ± standard error of the mean.

4.14 *In vivo* apoptosis effect of king cobra venom L-amino acid oxidase

To determine whether decreased in tumour volume is associated with apoptotic cell death induced by the enzyme, the extent of DNA fragmentation in the tumour cells were examined by TUNEL method. Representative tumour sections stained with TUNEL are shown in Figure 4.12 (A). Figure 4.12 (B) shows the average percentage of TUNEL-positive cells in the control and LAAO-treated tumour. The amount of apoptotic cells in the tumour section harvested from LAAO-treated mice was 26.7%. In contrast, tumour section from the control mice showed that the tumour predominantly consists of viable cells, with only few individual scattered cells (2.5%) stained positively with TUNEL [Figure 4.12 (A) and (B)].

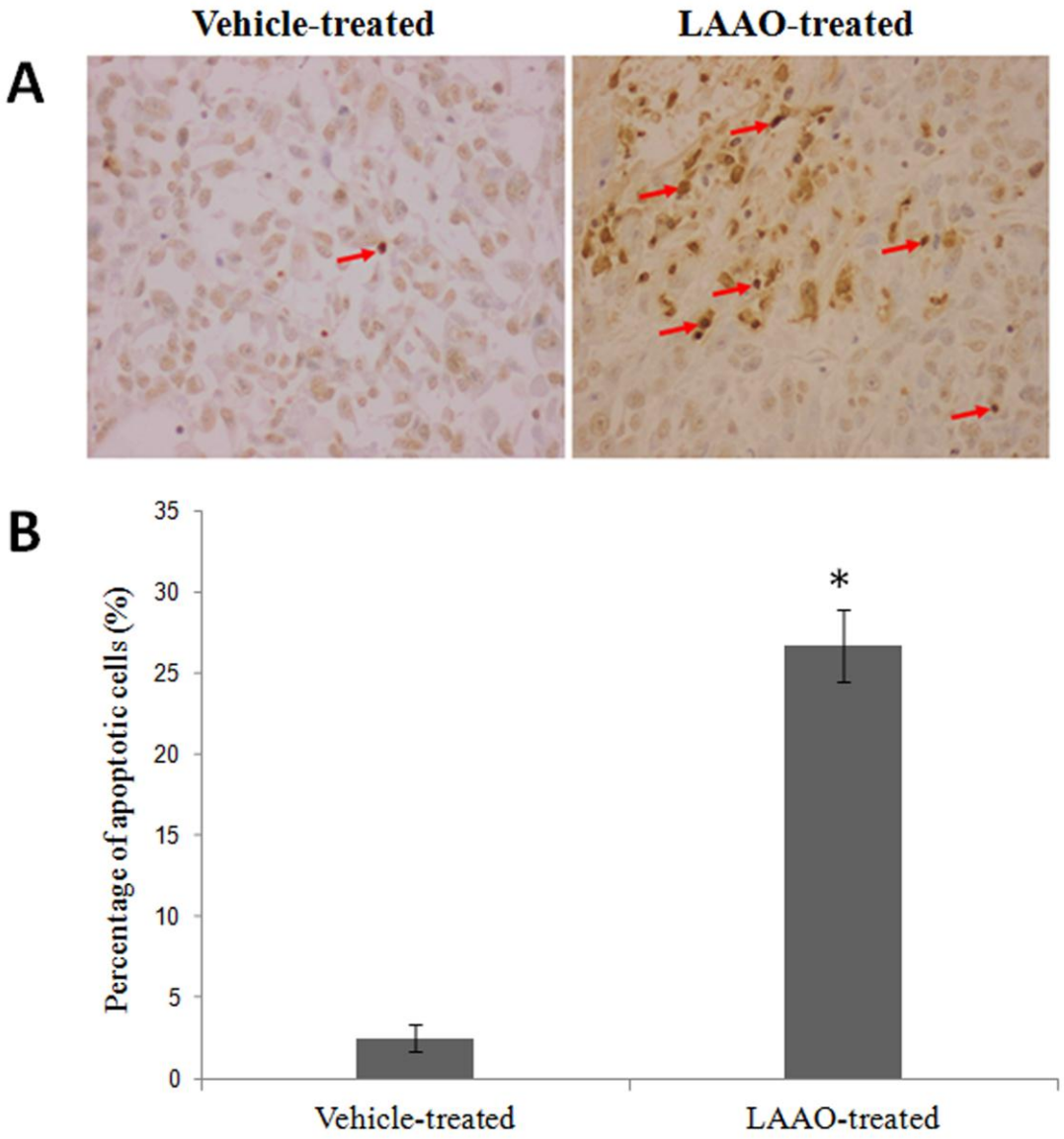

Figure 4.12: Apoptotic effect of L-amino acid oxidase in PC-3 solid tumour. (A) Representative TUNEL stained of tumour sections harvested from tumour-bearing nude mice treated with vehicle (PBS) and OH-LAAO (200X magnifications). Apoptotic cells were stained in dark brown (indicated by red arrows). (B) Average percentage of TUNEL-positive cells in tumour sections from the vehicle- and LAAO-treated mice. Data was expressed as mean ± standard error of the mean. * $P < 0.05$ in the LAAO-treated versus control group. Results showed that higher numbers of tumour cells underwent apoptosis in LAAO-treated mice compared to the vehicle-treated mice.

DISCUSSION

4.15 The *in vitro* cytotoxic action of king cobra venom L-amino acid oxidase

Results in the present study showed that the L-amino acid oxidase purified from Malaysian king cobra venom (OH-LAAO) is an extremely potent anti-proliferative agent against cancer cells, when compared with LAAO purified from other snake venoms including king cobra venom of unknown geographical origin reported by Ahn *et al*. (1997). The IC_{50} of OH-LAAO against MCF-7, A549, HL-60 and PC-3 cells (0.05 - 0.15 μg/mL) after 24 h incubation, were 28 to 1000 times more potent than those reported non-king cobra snake venom LAAOs (IC_{50} of 1.4 - 50 μg/mL), and were 3 to 12 times more potent than that of king cobra venom LAAO reported by Ahn *et al*. (1997) (Table 4.4). This may be due to intra-species variation as king cobras from different geographical regions may contain different forms of LAAO.

Interestingly, OH-LAAO exerts lower cytotoxicity in human non-tumourigenic cell lines (184B5 breast and NL 20 lung cells) when compared to their corresponding tumourigenic (MCF-7 and A549) cell lines, suggesting a selective cytotoxic property of the OH-LAAO against tumourigenic cells. The selectivity of the enzyme's cytotoxic action was demonstrated by the greater extent of cell death in tumourigenic MCF-7 (31.4%) and A549 (27%) cells than in the corresponding non-tumourigenic 184B5 (5.5%) and NL 20 (1.5%) cells, respectively as shown by PE-annexin V/7-AAD assay. The differential cytotoxicity could be due to the differences in the metabolism of the cells as well as the selective binding activity of the enzyme to tumourigenic versus non-tumourigenic cells. Such selectivity was not seen in standard anti-cancer drugs such as doxorubicin. Doxorubicin exerts stronger cytotoxicity against non-tumourigenic lung (NL 20) cells than its corresponding tumourigenic (A549) cells, though it was slightly

selective against the tumourigenic MCF-7 cells than the corresponding non-tumourigenic 184B5 cells.

Table 4.4: Anti-proliferative activities of some snake venom L-amino acid oxidases

Venom source of LAAO	Cell line and IC_{50} (µg/mL, incubation time)	Reference
Ophiophagus hannah (Malaysia)	Human breast adenocarcinoma (0.05 µg/mL, 24 h) Human lung adenocarcinoma (0.09 µg/mL, 24 h) Human prostate adenocarcinoma (0.08 µg/mL, 24 h) Human promyelocytic leukaemia (0.15 µg/mL, 24 h)	This work
Ophiophagus hannah (Unknown geographical origin)	Murine melanoma B16/F10 (0.17 µg/mL, 24 h) Human fibrosarcoma HT-1080 (0.60 µg/mL, 24 h) Chinese hamster ovary cells (0.30 µg/mL, 24 h) Murine epithelial cells Balb/3T3 (0.45 µg/mL, 24 h)	(Ahn *et al*., 1997)
Bungarus fasciatus	Human lung cancer A549 (24.00 µg/mL, 12 h)	(Wei *et al*., 2009)
Agkistrodon acutus	Human lung cancer A549 (10.00 µg/mL, 24 h)	(Zhang and Cui, 2007)
Agkistrodon acutus (ACTX-8)	Human cervical Hela (10.00 µg/mL, 48 h)	(Zhang and Wei, 2007)
Trimeresurus flavoviridis	Rat glioma C6 (1.90 µg/mL, 48 h) Human malignant glioma RBR 17T (2.48 µg/mL, 48 h) Human malignant glioma U251 (2.10 µg/mL, 48 h)	(Sun *et al*., 2003)
Bothrops atrox	Human leukaemia HL60 (~50.00 µg/mL, 24 h) Jurkat (~ 25.00 µg/mL, 24 h) Murine melanoma B16F10 (~25.00 µg/mL, 24 h) Rat pheochromocytoma PC12 (~25.00 µg/mL, 24 h)	(Alves *et al*., 2008)
Bothrops leucurus	Human gastric carcinoma MKN-45 (25.00 µg/mL or 0.41µM, 24 h) Human colon carcinoma RKO (2.40 µg/mL or 0.04 µM, 24 h) Human fibroblasts LL-24 (23.17 µg/mL or 0.38 µM, 24 h) Human adenocarcinoma HUTU (9.15 µg/mL or 0.15 µM, 24 h)	(Naumann *et al*., 2011)
Bothrops moojeni	Ehrlich ascites tumour cells (5.00 µg/mL, 1 h)	(Stábeli *et al*., 2007)
Trimeresurus stejnegeri	Human T cell leukaemia cells (C8166) (1.44 µg/mL or 24 nM, 72 h)	(Zhang *et al*., 2003)
Bothrops marajoensis	Murine macrophages (> 200.00 µg/mL, 24 h)	(Torres *et al*., 2010)
Lachesis muta	Human gastric adenocarcinoma AGS (22.70 µg/mL, 24 h) Human breast adenocarcinoma MCF-7 (1.41 µg/mL, 24 h)	(Bregge-Silva *et al*., 2012)
Agkistrodon acutus (ACTX-6)	Human lung cancer A549 (20.00 µg/mL, 24h)	(Zhang and Wu, 2008)

Snake venom LAAOs have been shown to induce apoptosis in cancer cells (Alves *et al*., 2008; Ande *et al*., 2006; Braga *et al*., 2008; Alves *et al*., 2011; Sun *et al*., 2003; Zhang and Wei, 2007). Recent study demonstrated an increase in caspase-3/7 activities in OH-LAAO treated cells, suggesting that the cytotoxic action of OH-LAAO is also due to the enzyme-induced apoptosis in the treated cells. The results showed clearly that for all 6 cell lines tested, caspase-3/7 activities were significantly increased over the basal level of the control cells. The formation of typical DNA fragments of oligonucleosomal size of about 180 - 200 bp by cleavage of the inhibitor of the caspase-activated DNase (ICAD) is one of the biochemical hallmarks of apoptosis in many cells (Bortner *et al*., 1995; Janicke, 2009). The formation of DNA fragments were also observed in the present study. Apparently, activation of caspase-3/7 leads to the typical DNA fragmentation pattern as observed on the agarose gel electrophoresis. The apoptotic mode of cell death was further demonstrated by surface externalization of membrane phospholipid phosphatidylserine (PS) using PE-Annexin V/7-AAD assay, in which increase of cells undergoing early and late apoptosis were detected. The increase in caspase-3/7 activities, surface externalization of membrane phospholipid phosphatidylserine (PS), and the formation of fragmented DNA in king cobra venom LAAO-treated cells all strongly supported that the enzyme exerts its cytotoxic action via induction of apoptosis.

It is well established that snake venom LAAOs induced cytotoxicity by the H_2O_2 liberated as a result of oxidative deamination reaction of the enzyme (Tan and Fung, 2009). This is also confirmed in the case of OH-LAAO, as the presence of catalase (a H_2O_2 scavenger), effectively reduced the cytotoxicity of the enzyme. This finding is in agreement with the suggestions by several other authors (Alves *et al*., 2008; Alves *et al*., 2011; Samel *et al*., 2006; Stábeli *et al*., 2007; Sun *et al*., 2003; Zhang and Wei, 2007; Zhang and Cui, 2007).

Apoptosis is initiated via two pathways: the extrinsic (death receptor-mediated) and intrinsic (mitochondria-mediated) apoptosis pathways. The extrinsic pathway is activated upon the binding of ligands to membrane death receptors, leading to activation of caspase-8 and the downstream procaspase-3, which eventually triggers cell execution (Crow *et al*., 2004). The intrinsic pathway involves loss of mitochondrial membrane potential, release of cytochrome *c* and other apoptogens into the cytosol and leading to procaspase-9 activation, which subsequently triggers the execution-phase of cell apoptosis by activating the effector procaspase-3 (Arya *et al*., 2007; Crow *et al*., 2004). Regardless of pathway initiated, both will eventually converge and activate the execution-phase of cell apoptosis (Lee *et al*., 2011).

Zhang and Wei (2007) reported that the cytotoxic action of LAAO isolated from *Agkistrodon acutus* snake venom involved activation of caspase-3 and -9, and that the apoptosis was accompanied by the release of cytochrome *c*, indicating involvement of the intrinsic pathway. Similarly, Alves *et al*. (2008) reported the induction of caspase-9 and caspase-3 in the cytotoxic action of *B. atrox* LAAO, again supporting the intrinsic pathway of apoptosis. On the other hand, Zhang and Cui (2007) reported that ACTX-6, a LAAO isolated from *Agkistrodon acutus* snake venom, could increase the activities of caspases-3, -8 and -9 in ACTX-6 treated cells. They also reported that the enzyme could induce mitochondrial-dependent apoptosis via regulations of Fas and FasL expression at the transcriptional level, suggesting the involvement of both intrinsic and extrinsic pathways of apoptosis.

In the same way, king cobra venom LAAO-induced apoptosis involve activation of caspase-8 and -9, supporting the involvement of both intrinsic and extrinsic apoptosis pathways. In addition, significantly increase expression levels of cytochrome *c* in both cytosolic and mitochondria fractions were also detected after 72 h treatment period.

This may due to the possibility that the initial leakage of cytochrome *c* itself acts as the feedback regulator that triggers the synthesis of this mitochondrial protein (Sanchez *et al*., 2001). Alternatively, it is possible that the synthesis and enrichment of the mitochondrial cytochrome *c* is the primary event that facilitates the release of cytochrome *c* into the cytosol (Sanchez *et al*., 2000; Sanchez *et al*., 2001). Nevertheless, these results are consistent with the involvement of both extrinsic and intrinsic pathways of apoptosis.

The apoptosis induced by OH-LAAO may be related to its action in releasing high local levels of H_2O_2 in the cancer cells. Ali *et al*. (2000) suggested that LAAOs can bind directly to the cell surface and generate a high concentration of H_2O_2 locally. Suhr and Kim (1996) and Torii *et al*. (1997) using fluorescence microscopy method demonstrated that the enzyme accumulated or bind to the cell surface and generate a high local concentration of H_2O_2. Similar mechanism presumably also occurs in the cytotoxic action of OH-LAAO, in view of its very high cytotoxic potency, as the amount of H_2O_2 generated by the minute amount of OH-LAAO would be too little to have any significant direct cytotoxic effect if the H_2O_2 is evenly distributed in the medium. Earlier, Ande *et al*. (2006) reported that the LAAO purified from *Calloselasma rhodostoma* venom induced cell death in Jurkat cells by necrosis caused by the generated H_2O_2 in the medium, and that apoptosis occurred only when the H_2O_2 concentration was lowered in the presence of catalase.

The apparent discrepancy regarding the cause of cell death induced by different LAAOs (whether apoptosis induced by local high concentration of H_2O_2 or necrosis by direct action of H_2O_2 in the medium) can be explained by comparing the cytotoxic potency (IC_{50} values) of the enzymes used. *Calloselasma rhodostoma* LAAO is a weak cytotoxic agent with IC_{50} of approximately 25 - 50 μg/mL against various cell lines

tested (Ande *et al*., 2006). Therefore, a very large amount of *C. rhodostoma* LAAO has to be used in the cytotoxicity experiments and resulting in a relatively large amount of H_2O_2 being generated in the medium. It was well established that large amounts of H_2O_2 can cause cell death by necrosis (Kannan and Jain, 2000). On the other hand, the cytotoxic action of king cobra venom LAAO (and many other venom LAAOs) is probably more than 250 times stronger than that of *C. rhodostoma* LAAO and the minute amount of H_2O_2 produced by approximately 0.1 μg/mL of king cobra venom LAAO (the amount of the enzyme used in cytotoxicity studies) is very unlikely to be able to cause cell necrosis, and hence apoptosis is the sole mechanism of cell death here.

4.16 *In vivo* anti-cancer effect of king cobra venom L-amino acid oxidase

In vivo studies using PC-3 tumour xenograft in nude mice showed that 8 weeks of OH-LAAO treatment at a dose of 1 μg/g (*i.p.*) markedly inhibited the growth of the solid tumour. The original rationale for choosing the dosage of 1 μg/g OH-LAAO for the *in vivo* anticancer was based on toxicity consideration. Tan and Saifuddin (1989) reported that the intravenous (*i.v.*) LD_{50} was 5 μg/g in mice. Indeed the 8-weeks treatment of OH-LAAO at the chosen dosage did not cause any significant pathological abnormalities in the major organs of the treated animals, nor did it cause any body weight reduction, compared to the vehicle-treatment mice throughout the treatment period. These observations, together with the high IC_{50} of OH-LAAO determined in non-tumourigenic breast and lung cells, strongly suggest that this enzyme is relatively non-toxic to normal tissues. These were in the agreement with the findings of Wei *et al*. (2009) and Bregge-Silva *et al*. (2012). Wei *et al*. (2009) reported that at dosage up to 50 μg, *Bungarus fasciatus* LAAO did not induce significant organ damage including lung, heart, kidneys, liver and spleen. Bregge-Silva *et al*. (2012) reported that 100 μg of *Lachesis muta* LAAO did not cause morphological changes in the heart, lung and

kidney tissues. However, Wei *et al*. (2007) reported that 50 μg of *Agkistrodon blomhoffii ussurensis* LAAO caused severe lung lesions after 6 and 24 h injections.

The dose of OH-LAAO chosen in the *in vivo* anti-tumour studies (1 μg/g body weight) was estimated to give a theoretical level of LAAO of about 5 μg/mL in the extracellular fluid (ECF) of the mice, assuming that ECF was 20% of body weight (Chapman *et al*., 2010), if all the injected LAAO were absorbed and distributed throughout the entire ECF compartment instantaneously. This level would far exceed the IC_{50} dose of PC-3 cells *in vitro* (0.08 μg/mL). However, it should be noted that absorption of injected LAAO is not likely to be instantaneous, and not all injected LAAO would be absorbed. Further, a certain quantity of LAAO may be degraded or excreted before it reaches the target cells. Also, the rate and ability of the LAAO to permeate the capillary wall and penetrate to the tumour cells are likely to be limited. Thus, the exact level of LAAO that the tumour cells in the treated mice are exposed to is likely to be much lower than 5 μg/mL. Nevertheless, at this dose of treatment, the LAAO in the circulation was shown to be able to inhibit growth of the tumour effectively, with no visible deleterious effect on the major organs nor reducing the body weight of the animals.

It is well established that many anti-cancer drugs cannot penetrate solid tumour tissue efficiently to reach the target cancer cells due to the tumour microenvironment (Minchinton and Tannock, 2006). This is particularly so for a large molecules such as snake venom LAAOs (with molecular weight of 130 kDa), which possess low diffusion coefficient. Present study demonstrated that despite the large molecular size, OH-LAAO could effectively inhibit solid tumour growth *in vivo*. Compared to the control, treatment with OH-LAAO caused 39% reduction on PC-3 tumour size in the nude mice ($P < 0.01$) after just one week of treatment. While substantial individual variation in anti-tumour effect was observed in the LAAO-treated mice during the 8-weeks

treatment, data also demonstrated that OH-LAAO could indeed effectively inhibit tumour growth *in vivo*. The ability of OH-LAAO to effectively inhibit the tumour growth is presumably due to its very high cytotoxicity as well as its ability to induce apoptotic cell death in the tumour cells as demonstrated by TUNEL staining on tumour sections.

Zhang and Wu (2008) reported that 10 days treatment with 1.5 μg/g of *Agkistrodon acutus* venom LAAO inhibited tumour growth of Hepatoma 22, Sarcoma 180 and Ehrlich ascites carcinoma tumours (established in Kun Ming mice) by 21.6%, 12.9% and 14.2%, respectively. In contrast, immunocompromised (nude) mice were used in this study and the OH-LAAO yielded greater level of growth inhibition, including one complete regression after 8-weeks treatment.

In conclusion, the selective cytotoxic action of OH-LAAO against tumourigenic, in contrast to non-tumourigenic cells and its capability to suppress solid PC-3 tumour growth in a tumour xenograft mouse model via apoptotic cell death without causing any significant toxic effect to the treated-mice suggest that the enzyme has the potential as an anti-cancer agent. However, its high molecular weight may hinder its penetration into the tumour cells; therefore further development in delivery system may be required. The enzyme is probably more effective against cancer cell suspensions such as leukaemias and ascites, than in solid tumours. Alternatively, the enzyme could be cloned and transfected to tumour cells to induce cell death *in situ*, an approach suggested by Sun *et al*. (2003).

CHAPTER 5

ALTERATIONS OF GENE EXPRESSIONS LEADING TO CELL DEATH INDUCED BY KING COBRA (*Ophiophagus hannah*) VENOM L-AMINO ACID OXIDASE (OH-LAAO)

INTRODUCTION

Gene expression is a process by which the information encoded in the gene is transformed into a functional gene product. The gene products are often proteins, but some are functional RNAs. Study of gene expression will assist in the understanding of cellular regulatory networks that are involved in response to various stimuli by looking at the alteration of gene transcription profiles. Analysis of gene expression patterns using microarray-based technology have been adopted in cancer research (Cooper, 2001; Grant *et al*., 2004; Kumar *et al*., 2012). Global gene expression study using microarray technology enables simultaneous measurement of the expression of thousands of genes in a high-throughput fashion and allows characterization of gene transcription profiles which reflect the changes in the biological processes within the cells.

King cobra venom L-amino acid oxidase (OH-LAAO) has been shown to induce apoptosis in various cancer cell lines and the apoptosis induction activity of the enzyme is via both intrinsic and extrinsic pathways as demonstrated by increase in caspase-9 and -8 activities, as well as increased cytochrome *c* levels in both cytosolic and mitochondria fractions in the LAAO-treated cells (Chapter 4). However, the molecular mechanism leading to cell death has not been investigated. This chapter describes the OH-LAAO induced alterations in gene expression in MCF-7 cells as examined by oligonucleotide microarray approach, to provide in-depth understanding of the molecular events leading to cell death induced by the enzyme.

METHODS

5.1 RNA samples preparation

5.1.1 Treatment of cells

In order to study the relationship between alterations of gene expression and mechanism of cell death induced by OH-LAAO, it is necessary to choose a non-toxic treatment dose. In this case, IC_{20} (0.015 µg/mL) was chosen as the dose for the treatment of MCF-7 cells. Human breast adenocarcinoma cells (MCF-7) were seeded onto 6-well plate and incubated overnight in 37 °C humidified incubator for the cells to attach. Cells were then treated with 0.015 µg/mL of OH-LAAO for 72 h.

5.1.2 Total RNA isolation

Total RNA was extracted using TRIzol® reagent according to the methods of Chomczynski and Sacchi (1987) and Chomczynski (1993). In brief, cell culture media was removed and the cells were washed twice with PBS. Cells were lysed in one millilitre of TRIzol® reagent by pipetting several times. The homogenized sample was incubated at room temperature for 5 min for complete dissociation of nucleoprotein complex. Chloroform (0.2 mL) was then added, incubated at room temperature for 3 min and subsequently centrifuged at 12,000 x g for 15 min at 4 °C. After centrifugation, the upper aqueous phase was transferred into a new tube. Three units of DNase I were added, mixed and incubated at 37 °C for 20 min. Iso-propanol (0.5 mL) was then added into the mixture and kept at -20 °C for 30 min. The mixture was centrifuged at 12,000 x g for 10 min at 4 °C and the supernatant was decanted. The RNA pellet was washed with one millilitre of 75% ice-cold ethanol and centrifuged at 12,000 x g for 5 min. The pellet was dried at 37 °C for 10 min and dissolved in nuclease-free water.

5.1.3 RNA clean-up

Isolated RNA was cleaned-up using RNeasy® mini kit according to the methods described by the manufacturer (Qiagen, Germany). In brief, volume of RNA was adjusted to 100 µL with nuclease-free water prior to RNA clean-up. The RNA sample was added with 350 µL of RLT buffer, followed by 250 µL of absolute ethanol and mixed well. The sample mixture (700 µL) was transferred into an RNeasy mini spin column placed onto the collection tube and centrifuged at 10,000 x g for 15 sec at 25 °C and the flow-through was discarded. Washing was performed twice by adding 500 µL of RPE buffer and centrifuged at 10,000 x g for 15 sec. Spin column was then placed onto the new collection tube and centrifuged at full speed for 1 min to ensure no ethanol is carried over during RNA elution. Finally, RNA was eluted by adding 50 µL of nuclease-free water into the spin column and spun at 10,000 x g for 1 min.

5.1.4 Quantitation of RNA

RNA samples were quantified using Nanodrop, software ND-1000 V3.7.1 (Thermo scientific, MA). Two microlitres of nuclease-free water was used as blank and the same volume of RNA samples were used for RNA quantitation. RNA samples with OD ratio of A260/A280 and A260/A230 greater than 1.8 were considered as good quality RNA and further subjected to formaldehyde denaturing agarose gel electrophoresis. Formaldehyde denaturing agarose gel electrophoresis was carried out as described in general methods (Chapter 2, Section 2.11).

5.2 Whole-genome gene expression direct hybridization assay

Oligonucleotide microarray was carried out by direct hybridization assay using HumanRef-8 v3.0 Expression BeadChips® (Illumina, San Diego, CA). Each gene chip contains more than 22,000 transcript probes. Sample labelling was performed using

Illumina® TotalPrep RNA amplification kit (Ambion, US) and the gene chip was scanned by Illumina Beadarray reader (Illumina, San Diego, CA).

5.2.1 First strand cDNA synthesis

All procedures for cRNA synthesis were carried out according to the protocols described by the manufacturer. Reverse transcription master mix was prepared at room temperature as follows:

T7 Oligo(dT) primer	1 µL
10X First strand buffer	2 µL
dNTP mix	4 µL
RNase inhibitor	1 µL
ArrayScript	1 µL

Reverse transcription master mix (9 µL) was mixed with 11 µL of 350 ng RNA sample. Reactions were initiated by incubation at 42 °C for 2 h and hold at 4 °C using PTC-100™ programmable thermal controller (MJ Research™, Inc., USA). The tubes were then placed on ice until preparation for second strand cDNA synthesis is ready.

5.2.2 Second strand cDNA synthesis

Master mix for second strand cDNA synthesis was prepared on ice as follows:

Nuclease-free water	63 µL
10X Second strand buffer	10 µL
dNTP mix	4 µL
DNA polymerase	2 µL
RNase H	1 µL

The master mix for second strand cDNA synthesis (80 µL) was mixed with 20 µL of the previously synthesized first strand cDNA. Mixtures were incubated in the thermal cycler programmed at 16 °C for 2 h and hold at 4 °C.

5.2.3 Purification of cDNA

The cDNA binding buffer (250 µL) was mixed with the synthesized cDNA sample. Mixtures were then transferred onto cDNA filter cartridge and centrifuging at 10,000 x g for 1 min at room temperature. Flow-through was discarded. Subsequently, cDNA filter cartridge was washed with 500 µL of the wash buffer by centrifuging at 10,000 x g for 1 min. The cDNA filter cartridge was then placed onto the cDNA elution tube and 20 µL of pre-heated nuclease-free water (55 °C) was applied onto the centre of the cDNA filter cartridge. The cDNA filter cartridge was incubated at room temperature for 5 min and followed by centrifugation at 10,000 x g for 1 min. A volume of approximate 17.5 µL of double-stranded cDNA was collected.

5.2.4 *In vitro* transcription to synthesize biotinylated cRNA

In vitro transcription master mix was prepared at room temperature as follows:

T7 10X reaction buffer	2.5 µL
T7 enzyme mix	2.5 µL
Biotin-NTP mix	2.5 µL

In vitro transcription master mix (7.5 µL) was mixed with 17.5 µL of the purified cDNA and incubated in thermal cycler programmed at 37 °C for 14 h and followed by hold at 4 °C. The reaction was stopped by adding 75 µL of nuclease-free water.

5.2.5 Purification and quantitation of cRNA

The cRNA binding buffer (350 µL) was mixed with 100 µL of the biotinylated cRNA sample. Two hundred fifty microlitres of 100% ethanol was then added into the mixture. The mixtures were transferred into the cRNA filter cartridge and centrifuged at 10,000 x g for 1 min. Subsequently, cRNA filter cartridge was washed with 650 µL of wash buffer by centrifugation at 10,000 x g for 1 min. The flow-through was discarded. One hundred microlitres of pre-heated nuclease-free water (55 °C) was applied onto the centre of the filter cartridge and the cartridge was incubated at room temperature for 2 min. Finally, cRNA was collected by centrifugation at 10,000 x g for 2 min. The purified cRNA samples were quantified using Nanodrop as described in this chapter (Section 5.1.4).

5.2.6 BeadChip hybridization

Prior to hybridization, 5 µL of 750 ng cRNA sample was heated at 65 °C for 5 min and cooled to room temperature. Ten microlitres of hybridization buffer (HYB) was mixed with the pre-heated cRNA sample. Hybridization chamber gasket was assembled into the hybridization chamber and the humidifying buffer reservoirs were filled with 200 µL of humidity control buffer. BeadChip was placed into a hybridization chamber insert and 15 µL of the cRNA sample mixtures were loaded onto the centre of the inlet port. The hybridization chamber insert containing sample-laden BeadChip was then placed into the hybridization chamber. BeadChip hybridization chamber was placed into the Illumina hybridization oven (Illumina, San Diego, CA) pre-equilibrated at 58 °C. The samples were allowed to hybridize for 18 h at 58 °C.

5.2.7 Washing and blocking

After hybridization, BeadChip hybridization chamber was removed from the hybridization oven. BeadChip was submerged into the diluted E1BC wash buffer and the cover-seal was removed. BeadChip was then quickly transferred to the slide rack and submerged into 250 mL of the E1BC wash buffer. Subsequently, BeadChip was incubated for 10 min in 1X high-temperature wash buffer that was pre-heated at 55 °C on the previous day in hybex microarray incubation system (SciGene, USA). First room temperature wash was performed by submerging the BeadChip into the fresh E1BC wash buffer for 10 min with shaking. BeadChip was then washed with 100% ethanol for 10 min followed by second room temperature wash with E1BC wash buffer for 2 min. BeadChip was then incubated in 4 mL of E1 block buffer for 10 min on the wash tray that was placed on a rocker mixer.

5.2.8 Staining and signal detection

BeadChip was stained with streptavidin-Cy3 (stock of 1 mg/mL) diluted in 2 mL of E1 block buffer with a 1:1,000 dilution. After staining, third room temperature wash was performed by submerging the BeadChip into the E1BC wash buffer for 5 min with shaking. BeadChip was then dried by centrifugation at 1,400 rpm for 4 min at room temperature and scanned by Illumina BeadArray reader (Illumina, San Diego, CA) at a scan factor of 0.6. The primary data was saved as an “idat” file.

5.2.9 Microarray data analysis

The initial quality controls (housekeeping, sample labelling, array hybridization, signal generation and negative control) of the BeadChip were checked using GenomeStudioV2010.1 software (Illumina, San Diego, CA). The generated “txt” file was imported and further analysed using GeneSpring GX 11.0 software (Agilent

Technologies, Inc., Santa Clara, CA). Those genes that displaying fold-change greater than 1.5 and Anova *P*-value < 0.05 were considered as significantly deregulated genes. These genes were classified according to their biological functions as described by Liu *et al*. (2003), using PubMed database provided by National Centre for Biotechnology information (NCBI, http://www.ncbi.nlm.nih.gov/).

5.3 Real-time polymerase chain reaction (RT-PCR)

In order to validate the microarray results, genes from different biological function groups in particularly related to apoptosis, autophagy, cell adhesion/migration, cell cycle arrest, heat shock protein, oxidative stress, proteolysis and signalling pathway/ signal transduction were chosen for RT-PCR validation (Table 5.1). Newly isolated RNA was used for RT-PCR validation, which was performed using TaqMan® gene expression assay.

Table 5.1: Selected genes for validation of microarray analysis using RT-PCR

Category of gene	Gene symbol	Gene full name	TaqMan® gene expression assay number
Apoptosis	BMF	Bcl2 modifying factor	Hs00372937_m1
	IGFBP3	Insulin-like growth factor binding protein 3	Hs00181211_m1
	PLEKHF1	Pleckstrin homology domain containing, family F member 1	Hs00759096_s1
	PPARG	Peroxisome proliferator-activated receptor gamma	Hs01115513_m1
Autophagy	SQSTM1	Sequestosome 1	Hs00177654_m1
Cell adhesion/migration	IGFBP5	Insulin-like growth factor binding protein 5	Hs01052296_m1
Cell cycle arrest	MLF1	Myeloid leukaemia factor 1	Hs00223695_m1
Heat shock protein	HSPD1	Heat shock 60kDa protein 1 (chaperonin)	Hs01036753_g1
Oxidative stress	ANG	Angiogenin, ribonuclease, RNase A family, 5	Hs04195574_sH
	CYP1A1	Cytochrome P450, family 1, subfamily A, polypeptide 1	Hs01054797_g1
	CYP1B1	Cytochrome P450, family 1, subfamily B, polypeptide 1	Hs02382916_s
	GPX2	Glutathione peroxidase 2	Hs01591589_m1
	MGST1	Microsomal glutathione S-transferase 1	Hs00220393_m1
Proteolysis	SERPINA3	Serpin peptidase inhibitor, clade A (alpha-1 antiproteinase, antitrypsin), member 3	Hs00153674_m1
	SERPINA5	Serpin peptidase inhibitor, clade A (alpha-1 antiproteinase, antitrypsin), member 5	Hs00167244_m1
	SPINT1	Serine peptidase inhibitor, Kunitz type 1	Hs00173678_m1
Signalling pathway/signal transduction	P2RY6	Pyrimidinergic receptor P2Y, G-protein coupled, 6	Hs00602548_m1
	TFG	TRK-fused gene	Hs02832013_g1

5.3.1 Reverse transcription of RNA to cDNA

Reverse transcription was performed using high capacity RNA-to-cDNA™ kit according to the manufacturer's instruction (Applied Biosystems, USA). One microgram of the total RNA was used for each 20 µL reaction. Reagents for reverse transcription were mixed as follows:

2X RT buffer	10 µL
20X RT enzyme mix	1 µL
RNA + nuclease-free water	9 µL

Reaction was initiated by incubation in PTC-100™ programmable thermal controller (MJ Research™, Inc., USA) programmed at 37 °C for 60 min, followed by 95 °C for 5 min and hold at 4 °C. Synthesized cDNA for RT-PCR application was stored at -20 °C.

5.3.2 RT-PCR TaqMan® assay

The reaction mixtures were mixed as follows:

2X TaqMan® gene expression master mix	10 µL
20X TaqMan® gene expression assay	1 µL
cDNA template (10 ng) + nuclease-free water	9 µL

Amplification was performed at 50 °C for 2 min and 95 °C for 10 min followed by 40 cycles at 95 °C for 15 sec and 60 °C for 1 min per cycle using StepOnePlus™ RT-PCR system (Applied Biosystems, USA). The comparative Ct method was used to determine the relative expression between control and treated sample, using beta actin as a normalization control.

5.4 Measurement of cytochrome P450 activities

Combination of CYP1A1 and CYP1B1 enzyme activities in the control and LAAO-treated MCF-7 cells were measured using P450-Glo™ CYP1A1 assay kit according to the manufacturer's instruction (Promega, USA). In brief, MCF-7 cells at the seeding density of 1,000 cells per well were seeded onto white-walled 96-well cell culture plate. After overnight seeding at 37 °C, cells were treated with OH-LAAO at its IC_{50} value (0.04 µg/mL) for 72 h. Spent medium was replaced with 50 µL of the fresh medium containing 100 µM Luciferin-CEE substrate. Cells were incubated for another 3 h at 37 °C, 5% CO_2. Subsequently, an equal volume of reconstituted Luciferin detection reagent (50 µL) was added into each well and mixed. The plate was allowed to equilibrate at room temperature for 20 min and the luminescence of each sample was measured with glomax-multi detection system (Promega, USA).

5.5 Measurement of intracellular reactive oxygen species (ROS) activity

Intracellular ROS activity, a parameter to measure intracellular H_2O_2 level was determined using OxiSelect™ intracellular ROS assay kit according to the manufacturer's guidelines (Cell Biolabs, USA). An oxidation sensitive 2', 7'-dichlorodihydrofluorescin diacetate (DCFH-DA) method was used in this assay. In brief, DCFH-DA is diffused into the cells and deacetylated by cellular esterases to non-fluorescent 2', 7'-dichlorodihydrofluorescin (DCFH), which will be rapidly oxidized to a highly fluorescent 2', 7'-dichlorodihydrofluorescein (DCF) by ROS (H_2O_2) generated in the treatment.

Human breast tumourigenic (MCF-7) cells at the seeding density of 25,000 cells per well were seeded onto black-walled 96-well cell culture plate. After overnight incubation at 37 °C, medium was removed and the cells were gently washed with PBS. Cells were then treated with 100 µL of 1X DCFH-DA solution (diluted in serum-free

medium) for 1 h at 37 °C. Medium containing DCFH-DA was discarded and the cells were gently washed with PBS. Subsequently, cells were treated with 0.03 µg/mL and 0.05 µg/mL of OH-LAAO for 24 h. Following treatment, cells were washed with PBS and 100 µL of 1X cell lysis buffer (diluted in the medium) was added into each well to lyse the cells. Contents of the wells were gently mixed for 5 min in the dark. The fluorescent intensity of each sample was measured with glomax-multi detection system (Promega, USA) at 460 nm excitation/515-585 nm emission.

RESULTS

5.6 Isolation of RNA

Total RNA for microarray and RT-PCR analyses were isolated using TRIzol® reagent and followed by clean-up with RNeasy® mini columns. The isolated RNA was highly purified (OD ratio of A260/A280 and A260/A230 ranged from 1.8 to 2.0, as determined by Nanodrop; Table 5.2) as well as of high quality as judged by formaldehyde agarose gel electrophoresis (Figure 5.1).

Table 5.2: Purity and concentration of the isolated RNA for microarray and RT-PCR analyses

RNA Sample	OD Ratio		Concentration (µg/mL)
	A260/A280	A260/A230	
Microarray			
Control sample 1	1.85	2.00	289.00
Treated sample 1	1.91	1.93	325.00
Control sample 2	1.90	1.84	277.00
Treated sample 2	1.94	1.90	302.9
Control sample 3	2.00	1.91	313.2
Treated sample 3	1.84	1.93	298.3
RT-PCR			
Control sample 1	2.02	1.86	258.40
Treated sample 1	2.02	1.87	267.10
Control sample 2	1.98	1.85	252.90
Treated sample 2	1.87	2.02	257.00
Control sample 3	1.80	1.92	205.80
Treated sample 3	1.88	1.90	268.80

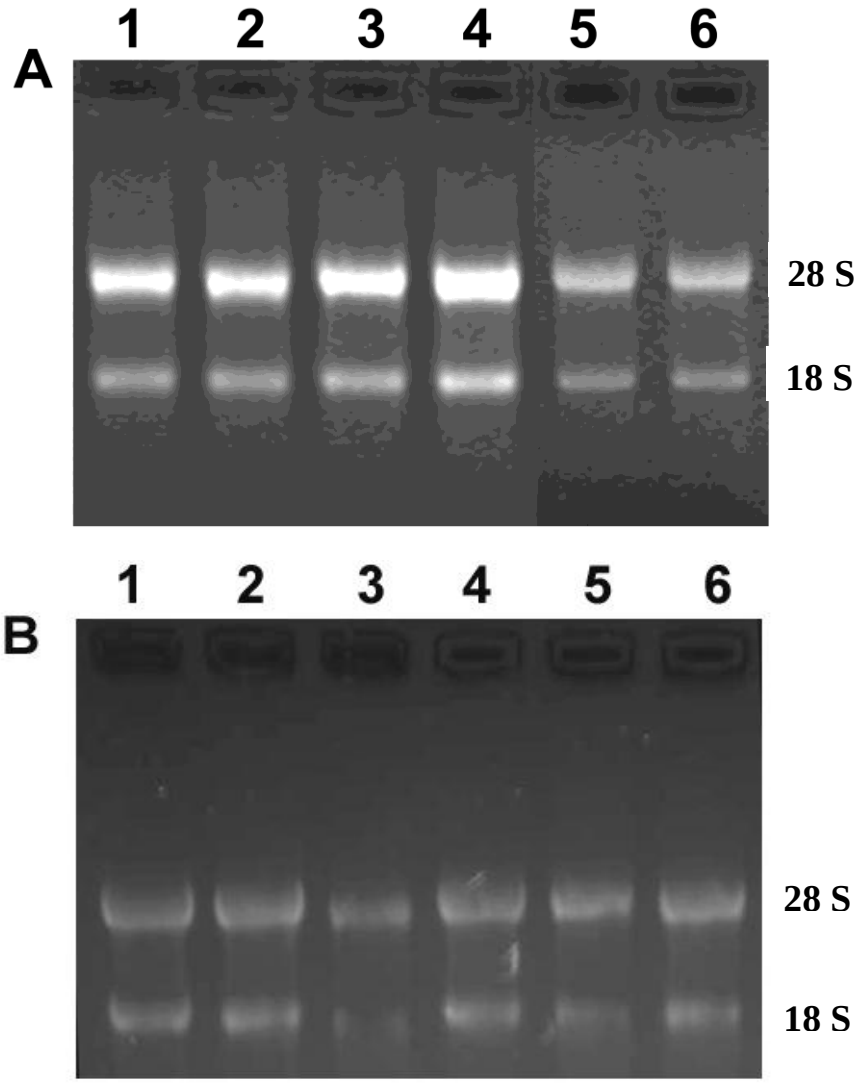

Figure 5.1: Electrophoresis of the isolated RNA on 1.2% denaturing formaldehyde agarose gel. Total RNA isolated from MCF-7 cells were separated on 1.2% denaturing formaldehyde agarose gel electrophoresis at a constant voltage of 80 V for 20 - 30 min using 1X MOPS running buffer. Two distinct bands (28 S and 18 S) for all the RNA samples were clearly seen on the gel images. (A) Formaldehyde agarose gel electrophoresis of total RNA isolated for microarray analysis. Lane 1: control sample 1; Lane 2: control sample 2; Lane 3: control sample 3; Lane 4: treated sample 1; Lane 5: treated sample 2; Lane 6: treated sample 3. (B) Formaldehyde agarose gel electrophoresis of total RNA isolated for RT-PCR analysis. Lane 1: control sample 1; Lane 2: control sample 2; Lane 3: control sample 3; Lane 4: treated sample 1; Lane 5: treated sample 2; Lane 6: treated sample 3.

5.7 Gene expression analysis of MCF-7 cells treated with LAAO

5.7.1 Alterations of gene expression profile of MCF-7 cells using microarray analysis

Gene expression analysis was carried out using HumanRef-8 v3.0 Expression BeadChip® which contains more than 22,000 transcript probes in each gene chip. Changes of 1.5-fold or greater in gene expression (*P*-value < 0.05) were considered as significant. A total of 178 genes showed significant difference in expression following OH-LAAO treatment. Of these 178 genes, 84 (47.2%) were down-regulated, and 94 (52.8%) were up-regulated. Table 5.3 shows the 178 genes and the fold changes as a result of OH-LAAO treatment. The 178 genes were classified into 27 categories according to their main biological functions: angiogenesis (3 genes), apoptosis (4 genes), autophagy (1 gene), carbohydrate metabolism (1 gene), cell adhesion or migration (9 genes), cell cycle arrest (2 genes), cellular organization (8 genes), detoxification (4 genes), DNA replication and cell cycle (4 genes), growth factor activity (1 gene), heat shock protein (1 gene), heme metabolism (2 genes), hormonal activity (2 genes), immune response (7 genes), inflammatory response (4 genes), ion or molecule transport (16 genes), lipid metabolism (5 genes), nervous system (9 genes), nucleic acid metabolism (1 gene), osteomuscular system (4 genes), oxidative stress (4 genes), oxidoreductase activity (4 genes), protein synthesis, modification and transport (9 genes), proteolysis (9 genes), signalling pathway or signal transduction (16 genes), steroid metabolism (3 genes), and others (45 genes).

Genes that are related to cytotoxic action of OH-LAAO include 27 genes found in the following categories: apoptosis, autophagy, cell cycle arrest, DNA replication and cell cycle, heat shock protein, oxidative stress, proteolysis and signalling pathway or signal transduction.

Among these genes, the following genes which have been reported as pro-apoptotic regulator were grouped under categories of apoptosis, heat shock protein and signalling pathway or signal transduction: Bcl-2 modifying factor, insulin-like growth factor binding protein 3, pleckstrin homology domain containing (family F), peroxisome proliferator-activated receptor gamma, heat shock 60 kDa protein 1, caveolin 1 (caveolae protein), and pirin. Of these 7 pro-apoptotic genes, 6 were up-regulated and 1 down-regulated.

Genes that may be involved in cell death were grouped under categories of cell cycle arrest (myeloid leukaemia factor 1, up-regulated, it suppresses cell cycle; cyclin-dependent kinase inhibitor 2B, which functions to arrest cell cycle progress, down-regulated), DNA replication and cell cycle (betacellulin, and RET proto-oncogene, positively regulate cell cycle, were down-regulated; kruppel-like factor 10 that suppresses cell cycle, was up-regulated; dual specificity phosphatise 5, negative regulation of cellular proliferation, was down-regulated) and proteolysis (5 protease genes were up-regulated and 4 protease inhibitor genes were down-regulated).

All the four genes that may be involved in oxidative stress were up-regulated: cytochrome P450 (families A and B), glutathione peroxidise 2, and microsomal glutathione S-transferease. Particularly noteworthy is the 6- to 34-fold up-regulation of the two cytochrome P450 family 1 genes, CYP1A1 and CYP1B1, respectively.

It is also interesting to note that gene sequestosome 1 that is involved in autophagy was also up-regulated as a result of OH-LAAO treatment (Table 5.4).

Table 5.3: Functional clustering of 178 genes exhibiting 1.5-fold or greater changes in expression in MCF-7 cells following king cobra venom L-amino acid oxidase treatment

Category of gene	Gene name	Fold change	Gene name	Fold change	Gene name	Fold change
Angiogenesis	ANG (Angiogenin, ribonuclease, RNase A family, 5)	2.5	EPHA2 (Ephrin receptor A2)	-1.6	VEGFA (Vascular endothelial growth factor A)	1.5
Apoptosis	BMF (Bcl2 modifying factor)	1.7	IGFBP3 (Insulin-like growth factor binding protein 3)	2.2	PLEKHF1 (Pleckstrin homology domain containing, family F member 1)	1.9
	PPARG (Peroxisome proliferator-activated receptor gamma)	2.5				
Autophagy	SQSTM1 (Sequestosome 1)	1.5				
Carbohydrate metabolism	PDK4 (Pyruvate dehydrogenase kinase, isozyme 4)	1.5				
Cell adhesion/migration	CELSR2 (Cadherin, EGF LAG seven-pass G-type receptor 2 (flamingo homolog, Drosophila)	-1.8	CLDN9 (Claudin 9)	-1.6	CLSTN2 (Calsyntenin 2)	1.6
	IGFBP5 (Insulin-like growth factor binding protein 5)	-1.9	ITGB4 (Integrin, beta 4)	-1.5	JUB (Jub, ajuba homolog)	-1.5
	LAMA3 (Laminin, alpha 3)	2.6	TGM2 (Transglutaminase 2)	-1.7	THBS1 (Thrombospondin 1)	-1.6

Category of gene	Gene name	Fold change	Gene name	Fold change	Gene name	Fold change
Cell cycle arrest	CDKN2B (Cyclin-dependent kinase inhibitor 2B (p15, inhibits CDK4)	-1.6	MLF1 (Myeloid leukaemia factor 1)	1.6		
Cellular organization	GSN (Gelsolin)	-1.7	KRT6A (Keratin 6A)	-4.1	KRT8 (Keratin 8)	-1.5
	KRT80 (Keratin 80)	-1.5	KRT81 (Keratin 81)	-2.3	KRT86 (Keratin 86)	-2.3
	SPTBN1 (Spectrin, beta, non-erythrocytic 1)	1.5	TUBB6 (Tubulin, beta 6)	-1.6		
Detoxification	ALDH1A3 (Aldehyde dehydrogenase 1 family, member A3)	2.8	ALDH3A1 (Aldehyde dehydrogenase 3 family, member A1)	7.5	AOX1 (Aldehyde oxidase 1)	-1.5
	UGT1A6 (UDP glucuronosyltransferase 1 family, polypeptide A6)	3.2				
DNA replication and cell cycle	BTC (Betacellulin)	-1.5	DUSP5 (Dual specificity phosphatase 5)	-1.9	KLF10 (Kruppel-like factor 10)	1.5
	RET (Ret proto-oncogene)	-1.8				
Growth factor activity	GDF15 (Growth differentiation factor 15)	1.6				
Heat shock protein	HSPD1 (Heat shock 60kDa protein 1 (chaperonin)	1.5				
Heme metabolism	FECH (Ferrochelatase)	1.6	HMOX1 (Heme oxygenase (decycling) 1)	1.7		

Category of gene	Gene name	Fold change	Gene name	Fold change	Gene name	Fold change
Hormonal activity	DIO2 (Deiodinase, iodothyronine, type II)	-2.2	TFF3 (Trefoil factor 3, intestinal)	-1.7		
Immune response	C20orf114 (Chromosome 20 open reading frame 114)	3.8	IL4R (Interleukin 4 receptor)	-1.5	IRF1 (Interferon regulatory factor 1)	1.6
	LGALS3BP (Lectin, galactoside-binding, soluble, 3 binding protein)	1.5	PTGER4 (Prostaglandin E receptor 4 (subtype EP4)	2.2	S100A14 (S100 calcium binding protein A14)	-2.4
	SUSD2 (Sushi domain containing 2)	-1.6				
Inflammatory response	ANXA1 (Annexin A1)	-2.8	S100A13 (S100 calcium binding protein A13)	-1.7	S100A8 (S100 calcium binding protein A8)	-2.1
	S100A9 (S100 calcium binding protein A9)	-1.6				
Ion or molecule transport	ABCG1 (ATP-binding cassette, sub-family G (WHITE), member 1)	-1.5	ABCG2 (ATP-binding cassette, sub-family G (WHITE), member 2)	1.6	CLIC3 (Chloride intracellular channel 3)	-1.9
	KCNK2 (Potassium channel, subfamily K, member 2)	1.7	LCN2 (Lipocalin 2)	1.7	MCOLN2 (Mucolipin 2)	1.5
	OSTalpha (Organic solute transporter alpha)	1.5	S100A16 (S100 calcium binding protein A16)	-2.0	S100A6 (S100 calcium binding protein A6)	-1.5
	SLC25A29 (Solute carrier family 25)	-1.5	SLC3A2 (Solute carrier family 3)	2.0	SLC44A1 (Solute carrier family 44, member 1)	1.6
	SLC7A11 (solute carrier family 7 (anionic amino acid transporter light chain)	1.8	SLC7A5 (solute carrier family 7 (amino acid transporter light chain, L system), member 5)	2.5	SLCO2A1 (Solute carrier organic anion transporter family, member 2A1)	-1.8

Category of gene	Gene name	Fold change	Gene name	Fold change	Gene name	Fold change
Ion or molecule transport	STRA6 (Stimulated by retinoic acid gene 6 homolog)	1.9				
Lipid metabolism	ACOT11 (Acyl-CoA thioesterase 11)	1.7	ACOX2 (Acyl-CoA oxidase 2, branched chain)	-1.7	DEGS2 (Degenerative spermatocyte homolog 2, lipid desaturase)	-1.7
	SCD (Stearoyl-CoA desaturase (delta-9-desaturase)	-1.8	SREBF1 (Sterol regulatory element binding transcription factor 1)	-1.6		
Nervous system	AHNAK (AHNAK nucleoprotein)	-1.6	FAM5B (Family with sequence similarity 5, member B)	-1.5	GABBR2 (Gamma-aminobutyric acid (GABA) B receptor, 2)	-1.6
	GLDN (Gliomedin)	2.6	GM2A (GM2 ganglioside activator)	1.5	NAB2 (NGFI-A binding protein 2 (EGR1 binding protein 2)	-1.7
	NAV2 (Neuron navigator 2)	-2.9	NEDD9 (Neural precursor cell expressed, developmentally down-regulated 9)	1.9	PCP4 (Purkinje cell protein 4)	-1.6
Nucleic acid metabolism	PRPS1 (Phosphoribosyl pyrophosphate synthetase 1)	1.7				
Osteomuscular system	BMP1 (Bone morphogenetic protein 1)	-1.6	MGP (Matrix Gla protein)	-3.6	PNKD (Paroxysmal nonkinesigenic dyskinesia)	-1.7
	TMSB4X (Thymosin beta 4, X-linked)	-1.6				

Category of gene	Gene name	Fold change	Gene name	Fold change	Gene name	Fold change
Others	AGR2 (Anterior gradient homolog 2)	-1.9	ANKRD29 (Ankyrin repeat domain 29)	2.3	ASS1 (Argininosuccinate synthase 1)	-1.7
	C15orf48 (Chromosome 15 open reading frame 48)	-2.1	C1orf112 (Chromosome 1 open reading frame 112)	1.6	C1QTNF6 (C1q and tumor necrosis factor related protein 6)	-1.5
	C20orf186 (Chromosome 20 open reading frame 186)	1.7	C9orf61 (Chromosome 9 open reading frame 61)	-1.6	CCDC83 (Coiled-coil domain containing 83)	-1.9
	EPS8L1 (EPS8-like 1)	-1.6	FAM105A (Family with sequence similarity 105, member A)	1.7	FAM123A (Family with sequence similarity 123A)	2.2
	FAM174B (Family with sequence similarity 174, member B)	2.0	FTHL11 (Ferritin, heavy polypeptide-like 11)	1.7	FTHL12 (Ferritin, heavy polypeptide-like 12)	1.5
	FTHL2 (Ferritin, heavy polypeptide-like 2)	1.6	FTHL3P (Ferritin, heavy polypeptide 1 pseudogene 3)	1.7	H19 (H19, imprinted maternally expressed transcript)	-2.8
	HS3ST3A1 (Heparan sulfate (glucosamine) 3-O-sulfotransferase 3A1)	-1.7	IER5L (Immediate early response 5-like)	-1.5	LACTB (Lactamase, beta)	1.6
	LMCD1 (LIM and cysteine-rich domains 1)	2.1	LRIG3 (Leucine-rich repeats and immunoglobulin-like domains 3)	1.5	LYPD1 (LY6/PLAUR domain containing 1)	-1.4
	MEST (Mesoderm specific transcript homolog)	1.6	MSMB (Microseminoprotein, beta)	-1.5	MYEOV (Myeloma overexpressed)	-1.9

Category of gene	Gene name	Fold change	Gene name	Fold change	Gene name	Fold change
Others	NBPF1 (Neuroblastoma breakpoint family, member 1)	2.1	OXTR (Oxytocin receptor)	-1.5	PLAC1 (Placenta-specific 1)	-1.7
	PPL (Periplakin)	-1.5	RAI14 (Retinoic acid induced 14)	1.7	RHOBTB3 (Rho-related BTB domain containing 3)	-1.5
	SAT1 (Spermidine/spermine N1-acetyltransferase 1)	1.5	SCUBE2 (Signal peptide, CUB domain, EGF-like 2)	1.8	SELL (Selectin L)	2.5
	SERTAD4 (SERTA domain containing 4)	-1.5	SH3BGRL2 (SH3 domain binding glutamic acid-rich protein like 2)	1.5	SPOCK1 (Sparc/osteonectin, cwcv and kazal-like domains proteoglycan)	-2.1
	TFPI (Tissue factor pathway inhibitor (lipoprotein-associated coagulation inhibitor)	1.7	TLE6 (Transducin-like enhancer of split 6 (E(sp1) homolog, Drosophila)	1.5	TMTC3 (Transmembrane and tetratricopeptide repeat containing 3)	1.5
	TSKU (Tsukushin)	3.0	VTCN1 (V-set domain containing T cell activation inhibitor 1)	2.1	ZNF365 (Zinc finger protein 365)	-1.8
Oxidative stress	CYP1A1 (Cytochrome P450, family 1, subfamily A, polypeptide 1)	33.9	CYP1B1 (Cytochrome P450, family 1, subfamily B, polypeptide 1)	6.1	GPX2 (Glutathione peroxidase 2 (gastrointestinal)	2.2
	MGST1 (Microsomal glutathione S-transferase 1)	1.5				
Oxidoreductase activity	DHRS3 (Dehydrogenase/reductase (SDR family 3)	2.7	LOXL1 (Lysyl oxidase-like 1)	-1.6	NQO1 (NAD(P)H dehydrogenase, quinone 1)	2.0

Category of gene	Gene name	Fold change	Gene name	Fold change	Gene name	Fold change
Oxidoreductase activity	TXNRD1 (thioredoxin reductase 1)	2.5				
Protein synthesis, modification and transport	ELF5 (E74-like factor 5 (ets domain transcription factor)	2.0	FHL2 (Four and a half LIM domains 2)	-1.5	PARP4 (Poly (ADP-ribose) polymerase family, member 4)	1.7
	RAB31 (RAB31, member RAS oncogene family)	-1.5	RNASE4 (Ribonuclease, RNase A family, 4)	1.7	ST3GAL1 (ST3 beta-galactoside alpha-2,3-sialyltransferase 1)	1.7
	TIPARP (TCDD-inducible poly(ADP-ribose) polymerase)	2.3	UPK3B (Uroplakin 3B)	1.7	XPOT (Exportin, tRNA (nuclear export receptor for tRNAs)	1.5
Proteolysis	ADAM19 (ADAM metallopeptidase domain 19)	1.7	APH1B (Anterior pharynx defective 1 homolog B)	1.5	LXN (Latexin)	2.2
	OTUB2 (OTU domain, ubiquitin aldehyde binding 2)	1.5	SCPEP1 (Serine carboxypeptidase 1)	1.5	SERPINA1 (Serpin peptidase inhibitor, clade A (alpha-1 antiproteinase, antitrypsin), member 1)	-1.7
	SERPINA3 (Serpin peptidase inhibitor, clade A (alpha-1 antiproteinase, antitrypsin), member 3)	-1.9	SERPINA5 (Serpin peptidase inhibitor, clade A (alpha-1 antiproteinase, antitrypsin), member 5)	-1.6	SPINT1 (Serine peptidase inhibitor, Kunitz type 1)	-1.6
Signalling pathway/signal transduction	AHRR (Aryl-hydrocarbon receptor repressor)	1.5	ARHGDIB (Rho GDP dissociation inhibitor (GDI) beta)	-1.8	CALML5(Calmodulin-like 5)	-2.3

Category of gene	Gene name	Fold change	Gene name	Fold change	Gene name	Fold change
Signalling pathway/signal transduction	CAV1 (Caveolin 1, caveolae protein, 22kDa)	-1.8	DKK1 (Dickkopf homolog 1 (Xenopus laevis)	-1.5	FLRT3 (Fibronectin leucine rich transmembrane protein 3)	1.9
	GPER (G protein-coupled estrogen receptor 1)	-1.5	GPR126 (G protein-coupled receptor 126)	-1.7	P2RY6 (Pyrimidinergic receptor P2Y, G-protein coupled, 6)	1.7
	PANX2 (Pannexin 2)	1.8	PIR (Pirin, iron-binding nuclear protein)	1.5	PMEPA1 (Prostate transmembrane protein, androgen induced 1)	-1.7
	RAP1GAP (RAP1 GTPase activating protein)	1.5	S100A10 (S100 calcium binding protein A10)	-1.5	SIPA1L2 (Signal-induced proliferation-associated 1 like 2)	1.5
	TFG (TRK-fused gene)	1.7				
Steroid metabolism	AKR1C2 (Aldo-keto reductase family 1, member C2 (dihydrodiol dehydrogenase 2; bile acid binding protein; 3-alpha hydroxysteroid dehydrogenase, type III)	2.7	AKR1C3 (Aldo-keto reductase family 1, member C3 (3-alpha hydroxysteroid dehydrogenase, type II)	3.2	UGT2B7 (UDP glucuronosyltransferase 2 family, polypeptide B7)	2.3

Genes with significantly changes in expression are classified into 27 categories according to their main biological function. Fold change values that are negative indicate down-regulation, while positive values indicate up-regulation, *i.e*, increase in expression in relative to the control cells. Data were obtained from triplicate analyses (n = 3).

Table 5.4: Summary of 27 genes involved in the cytotoxic action of king cobra venom L-amino acid oxidase

Gene name/ Category of gene	Function	Fold change
Apoptosis		
BMF (Bcl2 modifying factor)	Bind to Bcl2 proteins and function as an apoptotic activator	1.7
IGFBP3 (Insulin-like growth factor binding protein 3)	Positive regulation of apoptotic process	2.2
PLEKHF1 (Pleckstrin homology domain containing, family F member 1)	Induce apoptosis via lysosomal-mitochondrial pathway	1.9
PPARG (Peroxisome proliferator-activated receptor gamma)	Activation of cysteine-type endopeptidase activity involved in apoptosis	2.5
Autophagy		
SQSTM1 (Sequestosome 1)	Facilitate protein degradation by autophagy	1.5
Cell cycle arrest		
CDKN2B (Cyclin-dependent kinase inhibitor 2B (p15, inhibits CDK4)	Cell growth regulator that inhibits cell cycle G1 progression	-1.6
MLF1 (Myeloid leukaemia factor 1)	Suppress CDKN1B/p27Kip1 progression and induces cell cycle arrest	1.6
DNA replication and cell cycle		
BTC (Betacellulin)	Promotes cell proliferation	-1.5
DUSP5 (Dual specificity phosphatase 5)	Negative regulation of cellular proliferation and differentiation	-1.9
KLF10 (Kruppel-like factor 10)	Acts as transcriptional repressor and inhibits growth of cancer cells	1.5
RET (RET proto-oncogene)	Positive regulations of cell cycle	-1.8
Heat shock protein		
HSPD1 (Heat shock 60kDa protein 1 (chaperonin)	Involve in caspase-3 maturation	1.5

Table 5.4, continued

Gene name/ Category of gene	Function	Fold change
Oxidative stress		
CYP1A1 (Cytochrome P450, family 1, subfamily A, polypeptide 1)	Enhances the oxidative stress by producing ROS	33.9
CYP1B1 (Cytochrome P450, family 1, subfamily B, polypeptide 1)	Enhances the oxidative stress by producing ROS	6.1
GPX2 (Glutathione peroxidase 2 (gastrointestinal)	Response to oxidative stress	2.2
MGST1 (Microsomal glutathione S-transferase 1)	Response to oxidative stress	1.5
Proteolysis		
ADAM19 (ADAM metallopeptidase domain 19)	Involves in membrane protein ectodomain proteolysis	1.7
APH1B (Anterior pharynx defective 1 homolog B)	Functions in membrane protein intracellular domain proteolysis	1.5
LXN (Latexin)	Acts as protease	2.2
OTUB2 (OTU domain, ubiquitin aldehyde binding 2)	Involves in proteolysis	1.5
SCPEP1 (Serine carboxypeptidase 1)	Involves in proteolysis	1.5
SERPINA1 (Serpin peptidase inhibitor, clade A (alpha-1 antiproteinase, antitrypsin), member 1)	Acts as protease inhibitor	-1.7
SERPINA3 (Serpin peptidase inhibitor, clade A (alpha-1 antiproteinase, antitrypsin), member 3)	Negative regulation of proteolysis	-1.9
SERPINA5 (Serpin peptidase inhibitor, clade A (alpha-1 antiproteinase, antitrypsin), member 5)	Inhibits protease activity	-1.6
SPINT1 (Serine peptidase inhibitor, Kunitz type 1)	Protease inhibitors	-1.6
Signalling pathway/signal transduction		
CAV1 (Caveolin 1, caveolae protein, 22kDa)	Involve in apoptotic signaling pathway	-1.8
PIR (Pirin, iron-binding nuclear protein)	Modulation of NFκB pathway	1.5

5.7.2 Verification of microarray gene expression data using RT-PCR

A total of 18 genes with altered expression from the various biological function groups were subjected to RT-PCR for validation, using TaqMan® gene expression assay. The selected genes were ANG (angiogenin, ribonuclease, RNase A family, 5), BMF (Bcl2 modifying factor), CYP1A1 (cytochrome P450, family 1, subfamily A, polypeptide 1), CYP1B1 (cytochrome P450, family 1, subfamily B, polypeptide 1), GPX2 (glutathione peroxidase 2), HSPD1 (heat shock 60 kDa protein 1), IGFBP3 (insulin-like growth factor binding protein 3), IGFBP5 (insulin-like growth factor binding protein 5), MGST1 (microsomal glutathione S-transferase 1), MLF1 (myeloid leukaemia factor 1), P2RY6 (pyrimidinergic receptor P2Y, G-protein coupled, 6), PLEKHF1 (pleckstrin homology domain containing, family F member 1), PPARG (peroxisome proliferator-activated receptor gamma), SERPINA3 (serpin peptidase inhibitor, clade A Alpha-1 antiproteinase, antitrypsin, member 3), SERPINA5 (serpin peptidase inhibitor, clade A alpha-1 antiproteinase, antitrypsin, member 5), SPINT1 (serine peptidase inhibitor, Kunitz type 1), SQSTM1 (sequestosome 1) and TFG (TRK-fused gene).

The relative expression of each gene was obtained by comparative Ct method after normalizing against the beta actin as internal control. Figure 5.2 shows the expression patterns of the selected 18 genes using RT-PCR, as compared to that determined by microarray analysis. The highest expression of genes was CYP1A1, with the fold-change of 29.0 and 33.9 as determined by RT-PCR and microarray, respectively. The results show that the expression patterns and the fold-change determined by the two approaches are in agreement and comparable to each other, thereby validating the microarray analysis.

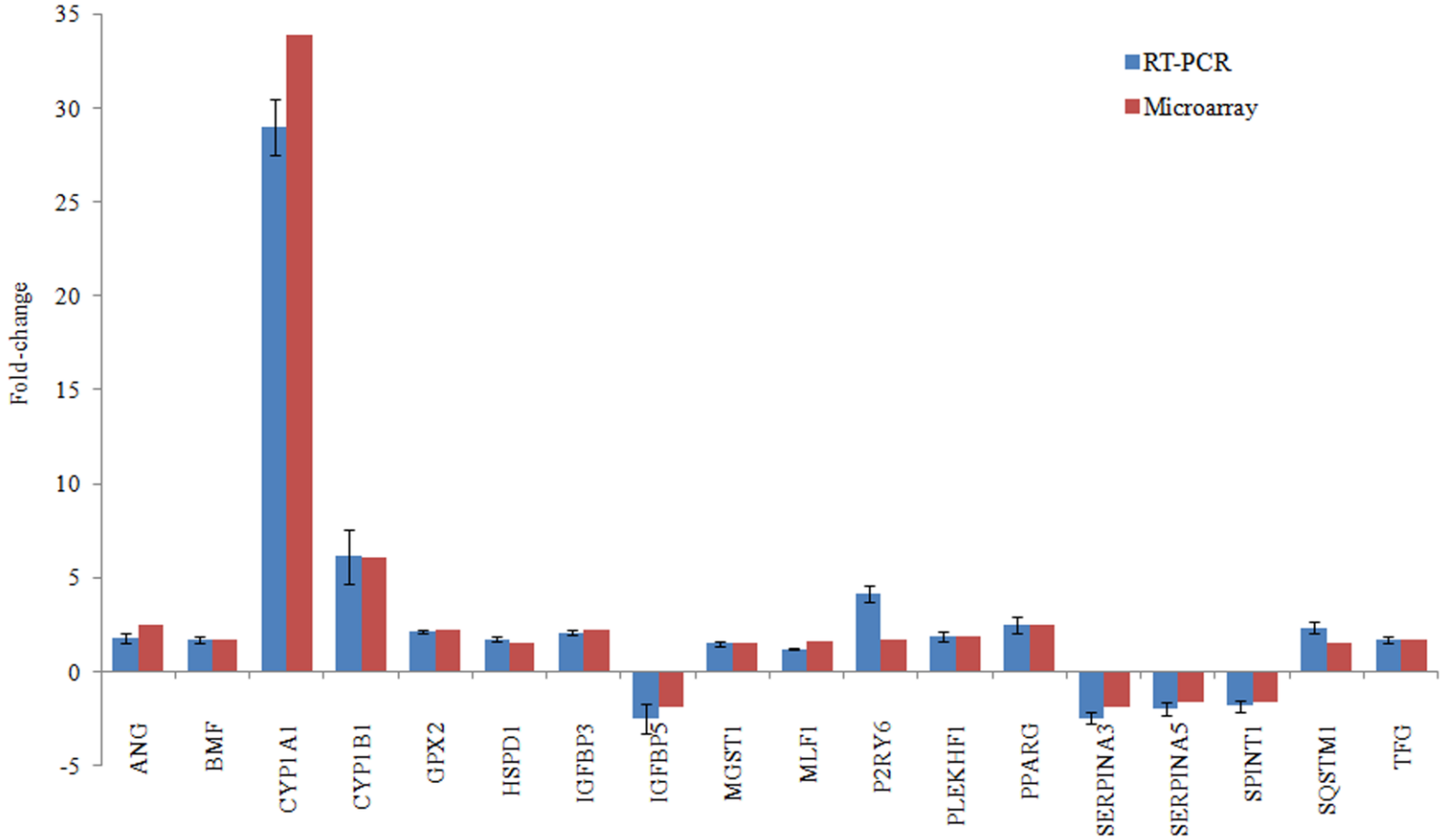

Figure 5.2: Expression patterns of the selected 18 genes determined by microarray and RT-PCR. RT-PCR was performed in triplicate and the results were expressed as fold-change ± S.D.

5.8 Intracellular reactive oxygen species (ROS) activity induced by king cobra venom L-amino acid oxidase

To further investigate the involvement of H_2O_2 or ROS in the cytotoxic action of OH-LAAO, intracellular ROS level in LAAO- and vehicle-treated MCF-7 cells were determined. MCF-7 cells pre-loaded with DCFH-DA were treated with two different concentrations of OH-LAAO: IC_{20} (0.03 µg/mL) and IC_{50} (0.05 µg/mL) for 24 h. The fold-change of the ROS activity in LAAO-treated cells was determined in relative to the control (PBS-treated) cells. As shown in Figure 5.3, OH-LAAO treatment significantly increased the intracellular ROS activity in the MCF-7 cells: the intracellular ROS activity in the cells treated with 0.03 µg/mL and 0.05 µg/mL of OH-LAAO increased by 2.7- and 4.2-fold, respectively.

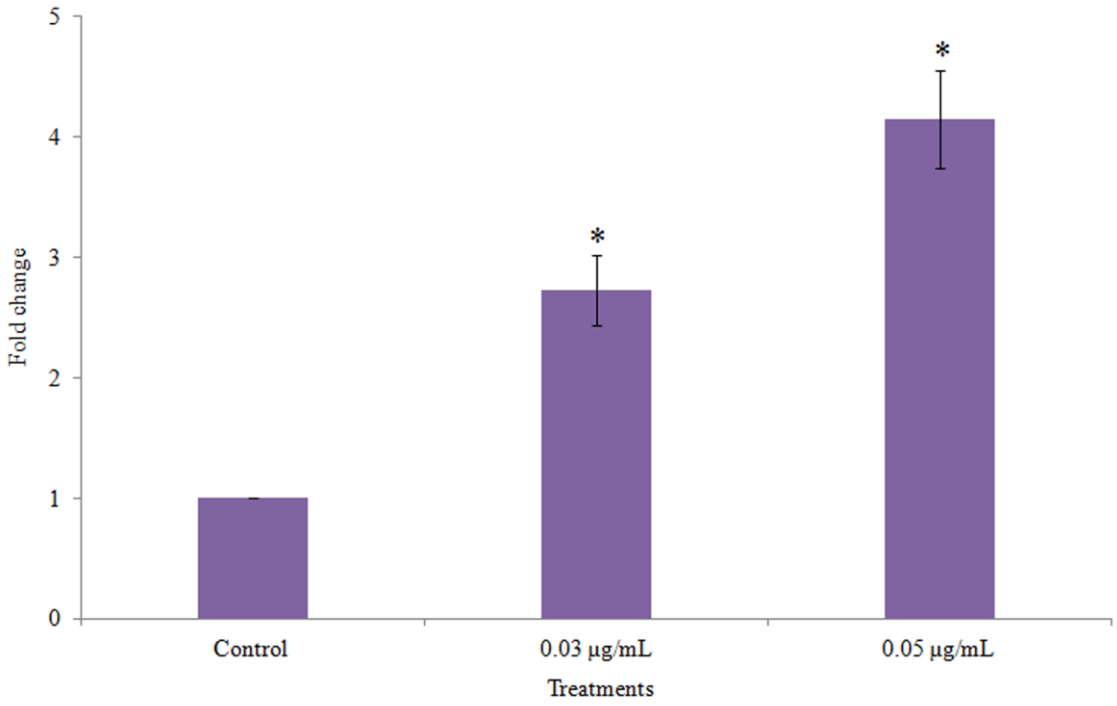

Figure 5.3: Intracellular reactive oxygen species (ROS) activity in MCF-7 cells treated with king cobra venom L-amino acid oxidase. The MCF-7 cells pre-loaded with DCFH-DA were treated with IC_{20} (0.03 µg/mL) and IC_{50} (0.05 µg/mL) of OH-LAAO for 24 h. The fluorescent intensity of each sample was measured at the excitation wavelength of 460 nm and emission wavelength of 515 - 585 nm. Results were expressed as fold-change in relative to the control. Error bars indicate the S.D of three independent experiments. Statistical analysis was performed using one-way ANOVA, followed by Tukey's post hoc multiple comparison test. * $P < 0.05$ in the LAAO-treated versus control cells.

5.9 Enzyme activities of CYP1A1 and CYP1B1 in king cobra venom LAAO-treated cells

Total activities of CYP1A1 and CYP1B1 in king cobra venom LAAO-treated cells were determined using P450-Glo™ CYP1A1 assay kit. The luminescence of each sample was measured after 72 h treatment with 0.04 µg/mL (IC_{50}) of OH-LAAO. As shown in Figure 5.4, the combination of CYP1A1 and CYP1B1 enzyme activities in LAAO-treated cells were 2.3-fold greater than that in the vehicle-treated cells ($P < 0.05$).

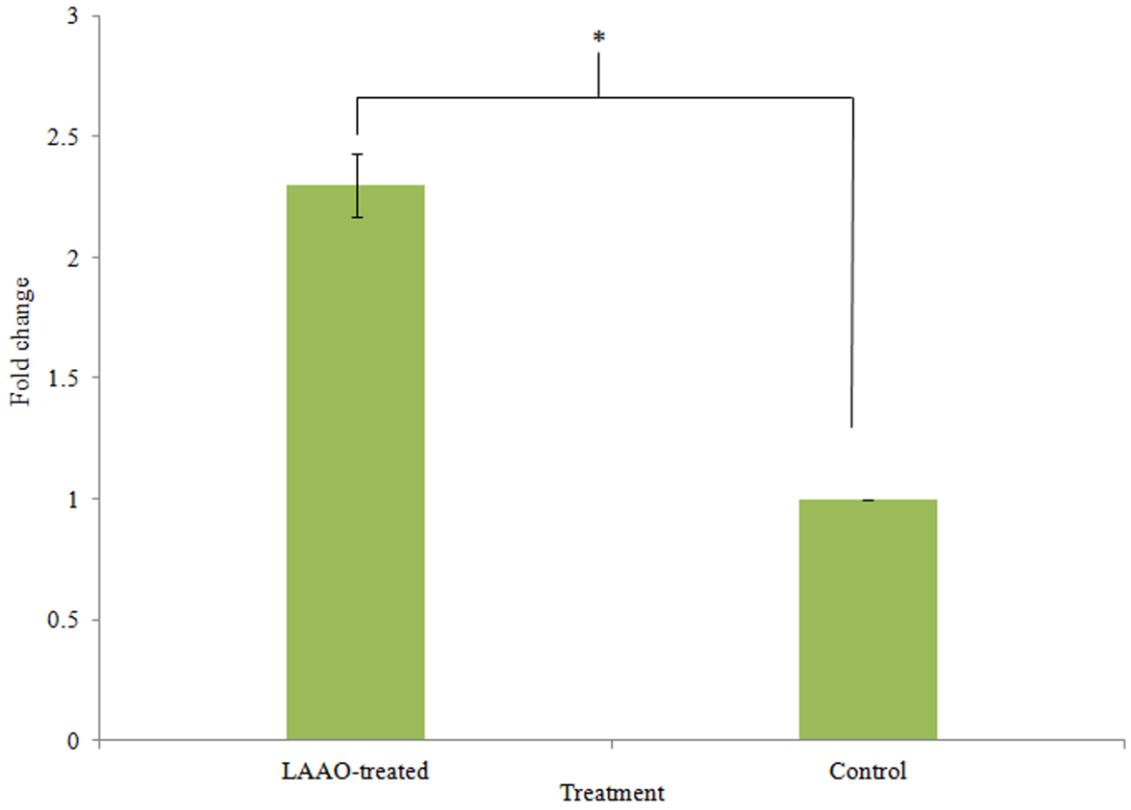

Figure 5.4: Total CYP1A1 and CYP1B1 activities in MCF-7 cells treated with king cobra venom L-amino acid oxidase. Cells were treated with 0.04 µg/mL of OH-LAAO for 72 h. The enzymes activities were determined using P450-Glo™ CYP1A1 assay kit (n = 3). The fold-change of the control is 1 and the error bar indicates the S.D. * $P < 0.05$ in the LAAO-treated versus control cells.

DISCUSSION

Snake venom LAAOs have been shown to induce apoptosis in various cancer cells (Ahn *et al*., 1997; Braga *et al*., 2008; Alves *et al*., 2011; Samel *et al*., 2006, see also chapter 4). Zhang and Cui (2007) reported that ACTX-6, a LAAO isolated from *Agkistrodon acutus* venom, could increase the activities of caspase-3, -8 and -9 in ACTX-6 treated cells, suggesting that both pathways of apoptosis are involved. In chapter 4, we also demonstrated that caspase-8 and -9 activities were significantly increased in LAAO-treated MCF-7 cells, indicating that OH-LAAO also mediates its cytotoxicity via both intrinsic and extrinsic apoptosis pathways.

It has been established that the apoptosis is the result of LAAO-induced oxidative stress (Tan and Fung, 2009). Under normal physiological conditions, cells maintain redox homeostasis through generation and elimination of reactive oxygen/nitrogen species. The presence of high levels of exogenous H_2O_2 liberated by LAAO could result in oxidative stress to the cell, which may disrupt the redox homeostasis, causing apoptosis (Kannan and Jain, 2000; Trachootham *et al*., 2008). What then are the molecular events triggered by the oxidative stress that lead to activation of apoptosis?

In the present study, the OH-LAAO induced alterations in gene expression in MCF-7 cells was investigated by oligonucleotide microarray approach, to provide deeper understandings of the molecular events leading to cell deaths induced by the enzyme. Microarray analysis showed that the oxidative stress induced by H_2O_2 liberated during the enzymatic reaction of OH-LAAO resulted in the alterations of expression of 178 genes, out of which at least 27 genes are involved in apoptosis and cell death (Table 5.4). Half (14 out of 27) of these gene expression alterations were also validated by RT-PCR (Comparing Table 5.4 and Figure 5.2). The 27 genes with altered expressions are as follows:

- Four genes related to the activation of apoptosis, including Bcl-2 modifying factor (BMF), insulin-like growth factor binding protein 3 (IGFBP3), pleckstrin homology domain containing family F (PLEKHF1) and peroxisome proliferator-activated receptor gamma (PPARG) were up-regulated. The involvement of BMF and PLEKHF1 also suggest the involvement of mitochondria-mediated pathway.

- Heat shock 60 kDa protein 1 (HSPD1), which is involved in caspase-3 maturation, was up-regulated and indicative of activation of apoptosis.

- Caveolin 1 (CAV1) and pirin (PIR) genes are involved in apoptotic signalling pathway and modulation of NFκB pathway, respectively. Down-regulation of CAV1 is indicative of negative regulation of apoptosis, while up-regulation of PIR is indicative of involvement of NFκB pathway in apoptosis.

- Cyclin-dependent kinase inhibitor 2B (CDKN2B) and myeloid leukaemia factor 1 (MLF1), the two genes that are involved in cell cycle arrest, was down- and up-regulated, respectively. The former (CDKN2B) was cell growth regulator that inhibits cell cycle G1 progression, while the later functions in induction of cell cycle arrest. The down-regulation of CDKN2B gene promotes cell proliferation. The up-regulation of MLF1 gene that is involved in cell cycle arrest was reflective of cell death event.

- Four genes that are involved in DNA replication and cell cycle: betacellulin (BTC), dual specificity phosphatase 5 (DUSP5) and RET proto-oncogene (RET) were down-regulated. Betacellulin and RET proto-oncogene promote cell proliferation and act as positive regulation of cell cycle, whereas DUSP5 is negative regulation of cell proliferation. On the other hand, KLF10 (kruppel-like

factor 10) that acts as transcriptional repressor and inhibits growth of cancer cell was up-regulated.

- Nine genes that are involved in proteolysis (see Table 5.4). The five genes that are involved in proteolysis were all up-regulated, whereas the other four genes that are coded for protease inhibitor or negative regulation of proteolysis were all down-regulated. Together, these suggest that there was an overall increase in proteolysis, which is reflective of cell death event.

- Four genes that are involved in oxidative stress, including cytochrome P450, family 1, subfamily A, polypeptide 1 (CYP1A1), cytochrome P450, family 1, subfamily B, polypeptide 1 (CYP1B1), glutathione peroxidase 2 (GPX2), and microsomal glutathione S-transferase 1 (MGSTI). All these genes were up-regulated. In particular, CYP1A1 and CYP1B1 both were very substantially up-regulated (33.9- and 6.1-folds, respectively). While the up-regulation of both GPX2 and MGSTI, the two genes involved in responses to oxidative stress are expected, the very substantial up-regulation of the two cytochrome P450 enzyme genes are interesting as they will presumably further enhance the LAAO-induced oxidative stress by producing more ROS.

- Sequestosome 1 (SQSTM1) gene, which is involved in autophagy, is known to be up-regulated by oxidative stress. The up-regulation of this gene contributes to apoptosis and cell death induced by OH-LAAO.

It is interesting to note that none of the caspase related genes (CASP3, CASP7, CASP8 and CASP9) were found to be differentially expressed, even though enzymatic assays did demonstrate clearly the increase in these activities (Chapter 4, Section 4.9.1 & 4.11.1). Presumably, the relevant gene expression alterations may be too low to be

detected in the present study design. The other possibility is by the time the RNAs were collected for microarray assay (72 h after OH-LAAO treatment), expression of caspase might have dropped to the normal values.

It is also interesting to note that the expressions of cytochrome P450 genes (CYP1A1 and CYP1B1) were increased very substantially following OH-LAAO treatment. In particular, expression of CYP1A1 gene increased 33.9-fold. These results of microarray analysis were also validated by RT-PCR, whereby expression of CYP1A1 gene was increased by 29-fold, and also by increase in CYP1A1 and CYP1B1 enzyme activities in MCF-7 cells, though only by 2.3-fold. This difference is expected as microarray and RT-PCR measured changes at transcription levels, whereas enzymatic activities measured changes at translation levels.

Cytochrome P450s are known to induce oxidative stress by producing excessive ROS (Dostalek *et al*., 2008), which can results in an imbalance of the redox homeostasis within the cells (Ramadass *et al*., 2003). Thus, the substantial activation of the ROS generating cytochrome P450 may contributes to the potent cytotoxic action of OH-LAAO, further enhancing the oxidative stress.

Measurement of intracellular ROS concentrations demonstrated that indeed there was a significant increased in the ROS in LAAO-treated MCF-7 cells. Similar observations have been reported by Sun *et al*. (2003).

What then are the causes of the extensive alterations of gene expression, in particular those related to apoptotic events and cell death? The alterations of gene expression may be due directly to the modulation effects of H_2O_2 or other ROS generated during the enzymatic reaction, as these are known to serve as second messengers for various physiological stimuli (Kannan and Jain, 2000; Verzola *et al*., 2004). However, it is unlikely that the ROS could serve as second messengers for so many processes or

pathways that led to alterations of expression of hundreds of genes. Rather, it is more likely that the alterations of gene expression observed were largely caused by oxidative modifications of signalling proteins, such as transcriptional factors (Trachootham *et al*., 2008). These modifications further modulate the activity of the signalling proteins in redox-sensitive signal transduction pathways as well as in transcriptional regulatory networks. This probably explains why**,** while most pro-apoptotic genes were up-regulated, some others were down-regulated. Nevertheless, the overall results of the gene expression alterations appear to favour apoptotic cell death, with involvement of proteolysis, autophagy and regulation of cell cycle.

In conclusion, the direct cytotoxic effect of H_2O_2 liberated by enzymatic action of the OH-LAAO, as well as the oxidative modifications of signalling molecules may be the primary events leading eventually to apoptosis and cell death. The very substantial up-regulation of the expression of the cytochrome P450 genes, which may lead to further excessive ROS production, certainly plays a key role in apoptosis activation, even though the molecular events that lead to the up-regulation of the genes remain to be elucidated.

CHAPTER 6

ALTERATIONS OF PROTEOME OF MCF-7 CELLS INDUCED BY KING COBRA (*Ophiophagus hannah*) VENOM L-AMINO ACID OXIDASE TREATMENT

INTRODUCTION

Proteomics is a study of structure, function and expression of proteins in a complex biological sample. In combination with high resolution protein separation (2D electrophoresis) and mass spectrometry (MS) analyses, proteomics has become a popular approach for the study of proteome profiling, comparative protein expression analysis, localization and identification of protein post-translational modifications, and protein-protein interactions (Chandramouli and Qian, 2009). Protein expression analysis could provide useful information on cellular processes in response to the external stimuli (treatment conditions). It should be noted that much of the regulation of physiological processes occurs post-transcriptionally. Thus, measurement of mRNA levels (gene expression) alone is insufficient to give a complete picture of cellular activity in response to the external stimuli and therefore some other approaches such as proteomic study may be necessary in coupling with gene expression analysis. This chapter describes the investigation of the alterations of protein expression profile of MCF-7 cells as a result of OH-LAAO treatment, using 2D electrophoresis proteomic approach. The differentially expressed proteins were then classified into few different groups based on their biological functions.

METHODS

6.1 Preparation of protein samples

6.1.1 Preparation of cell lysate

Protein samples for two-dimensional polyacrylamide gel electrophoresis (2D-PAGE) and western blot analysis were prepared as follows: MCF-7 cells were seeded onto cell culture flask and incubated overnight in 37 °C humidified incubator for the cells to attach. Cells were treated with 0.04 µg/mL (IC_{50} value) of OH-LAAO for 72 h. After treatment, cells were harvested by trypsin-EDTA and washed twice with PBS. Cell pellet was re-suspended in lysis buffer [containing urea (7 M), thiourea (2 M), CHAPS (4% w/v), IPG buffer (2% v/v), DTT (40 mM), and protease inhibitor mix]. The mixture was allowed to stand on ice for 30 min and vortexed rigorously every 10 min. After centrifugation at 10,000 x g for 30 min at 4 °C, the supernatant was recovered and stored at -80 °C.

6.1.2 Protein precipitation and solubilization

Proteins were precipitated using 2-D clean-up kit according to the manufacturer's guideline (GE Healthcare, Sweden). In brief, 100 µL of the protein sample was mixed with 300 µL of the precipitant and the mixture was incubated on ice for 15 min. Co-precipitant (300 µL) was then added into the mixture, mixed and centrifuged at 12,000 × g for 5 min. Supernatant was discarded. Forty microlitres of the co-precipitant was layered on top of the pellet and kept on ice for 5 min. After centrifugation for another 5 min, the supernatant was discarded. Milli-Q® water (25 µL) was then pipetted on top of the pellet and vortexed. Subsequently, pre-chilled wash buffer (1 mL) and additive (5 µL) were added and vortexed until the pellet is fully dispersed. The mixture was incubated at -20 °C for 30 min and vortexed rigorously every 10 min. After spin down

at 12,000 × g for 5 min, supernatant was discarded. Protein pellet was air-dried for 5 min and solubilised in 30 µL of thiourea rehydration buffer [containing urea (7 M), thiourea (2 M), CHAPS (2% w/v), IPG buffer (0.5% v/v), 0.002% v/v of 1% orange G stock solution, and DTT (18 mM)].

6.1.3 Protein concentration determination

Protein concentration was determined using 2-D quant kit according to the manufacturer's protocol (GE Healthcare, Sweden) with slight modifications as described in general methods (Chapter 2, Section 2.9.2).

6.2 Two dimensional polyacrylamide gel electrophoresis (2D-PAGE)

6.2.1 Sample loading and rehydration of immobilized pH gradient (IPG) strip

For isoelectric focusing (IEF), 150 µg of the protein samples were dissolved in the thiourea rehydration buffer to a final volume of 250 µL. Total volume of the mixture (250 µL) was pipetted onto the slot of the re-swelling tray. Subsequently, the dried gel side of the IPG strip (13 cm, linear pH 3 - 10 gradient) was placed onto the slot that contained the protein sample. To prevent evaporation and urea crystallization, 2 mL of the cover fluid was overlaid on top of the strip. Strip rehydration was performed at room temperature for 16 - 18 h.

6.2.2 First dimensional isoelectric focusing

Rehydrated strips were transferred onto the channels of the manifold with gel side faced up. Pre-wetted paper wicks were placed at the acidic and basic ends of each strip. Subsequently, the electrode was placed on top of the paper wicks and the cams were swivelled into closed position. All the channels of the manifold were flooded with the

cover fluid. The Ettan IPGphor3 Isoelectric Focusing System (GE Healthcare, Amersham Biosciences, Sweden) was programmed with the parameters as follows:

Step	Ramping mode	Voltage (V)	Time (h:min)	kVh
Step 1	Step and hold	500	1:30	0.5
Step 2	Gradient	1000	1:00	0.8
Step 3	Gradient	8000	2:30	11.3
Step 4	Step and Hold	8000	1:15	4.4

6.2.3 Preparation of 12.5% resolving gel

Resolving gel (12.5%) was prepared according to the method of Laemmli (1970). Compositions of resolving gel are listed below:

Milli-Q® water	31.8 mL
Acrylamide/Bis-acrylamide (30% stock)	41.7 mL
10% (w/v) SDS	1.0 mL
1.5 M Tris-HCl, pH 8.8	25.0 mL
10% (w/v) ammonium persulfate	0.5 mL
TEMED	33.0 µL

Solutions or reagents were mixed and poured into the gel cassette to a level which is sufficient for the rehydrated IPG strip to be inserted later. The gel was overlaid with water and gel cassette was allowed to stand at room temperature for 30 min for it to polymerize.

6.2.4 Equilibration of immobilized pH gradient (IPG) strip

After IEF, IPG strip was equilibrated with 5 mL of the SDS equilibration buffer I [6 M urea, 50 mM Tris-HCl (pH 8.8), 30% (v/v) glycerol, 2% (w/v) SDS, 0.002% (w/v)

orange G, and 50 mg (w/v) DTT] for 15 min at room temperature with agitation. Subsequently, SDS equilibration buffer I was replaced with 5 mL of the SDS equilibration buffer II [6 M urea, 50 mM Tris-HCl (pH 8.8), 30% (v/v) glycerol, 2% (w/v) SDS, 0.002% (w/v) orange G, and 125 mg (w/v) IAA] and the IPG strip was equilibrated for another 15 min at room temperature with shaking. The IPG strip was rinsed with 1X SDS electrophoresis running buffer [25 mM Tris-HCl (pH 8.3), 192 mM glycine, and 0.1% (w/v) SDS].

6.2.5 Second dimensional sodium dodecyl sulphate polyacrylamide gel electrophoresis (SDS-PAGE)

Second dimensional SDS-PAGE was performed using SE 600 Ruby electrophoresis tank (GE Healthcare, Amersham Biosciences, Sweden). The IPG strip was transferred onto the surface of the 12.5% resolving gel. Two millilitres of the sealing solution [contained 0.5% (w/v) agarose and 0.002% (w/v) Orange G] was poured into the gel cassette to seal the IPG strip with the resolving gel. Upper chamber of the tank was filled with 2X SDS electrophoresis running buffer while the lower chamber was filled with 1X SDS electrophoresis running buffer. The running parameter was programmed as follows:

Step	Current (mA/gel)	Voltage (V)	Duration (h:min)
1	15	80	0:20
2	40	200	6:00

Electrophoresis was stopped when the front dye reached half centimetre to the bottom of the gel.

6.2.6 Protein staining

Silver staining was performed using Pierce® silver stain for mass spectrometry kit according to the manufacturer's protocol (Thermo Scientific Pierce, USA). Briefly, gel was washed twice with milli-Q® water for 5 min each and fixed overnight in the fixing solution (60% water, 30% ethanol, and 10% acetic acid) at room temperature with agitation. After overnight fixation, gel was washed with 10% ethanol, followed by milli-Q® water for 5 min each wash. Gel was then incubated in the sensitizer working solution for 1 min, and washed with two changes of milli-Q® water for 1 min each wash. Subsequently, gel was incubated in the silver stain [containing 1% (v/v) silver stain enhancer] for 5 min and washed with two changes of milli-Q® water for 20 sec each wash. Developer working solution was then added onto the gel and the spot intensity was monitored for about 7 min. Once the desired intensity is reached, the developer working solution was replaced with the stop solution (5% acetic acid in milli-Q® water) and incubated for another 10 min with agitation.

6.2.7 Image acquisition and analysis

Image acquisition was performed using ImageScanner™ III (LabScan6.0, Swiss Institute of Bioinformatics). Differences in the protein expression were identified by ImageMaster™ 2D Platinum 7.0 software (GE Healthcare, Amersham Biosciences, Sweden). The images of the samples of the control and LAAO-treated groups were analysed by creating a match sets followed by classes. Gel image from each group with high resolution was assigned as the image master. Three landmark points were defined on the gel images and the spots matching procedure was performed manually to correct the mismatching spots generated by the software. Protein spots that displaying at least 1.5-fold difference in expression (ANOVA P-value < 0.05) were excised manually from

the gels and subjected to in-gel trypsin digestion and subsequent MALDI-TOF/TOF identification.

6.3 Protein identification

6.3.1 In-gel trypsin digestion

Differentially regulated protein spots were excised manually from the 2-D gels, and destained with 50 mM sodium thiosulphate containing 15 mM potassium ferricyanide. After destaining, gel plugs were washed 3 times with 500 µL of 50% acetonitrile containing 100 mM NH_4HCO_3 for 20 min each wash, and subsequently dehydrated by incubating in 50 µL of 100% acetonitrile for 15 min with shaking and dried completely using speed vacuum for 15 min. Trypsin digestion was performed by overnight incubation with 25 µL of 50 mM NH_4HCO_3 containing 150 ng of trypsin at 37 °C. After trypsin digestion, 50 µL of 50% acetonitrile was added into the sample and incubated for a further 15 min at room temperature with shaking. The supernatant was collected. Peptides remaining in the gel plugs were extracted again by adding 50 µL of 100% acetonitrile and followed by incubation at room temperature for 15 min. The supernatant was collected and pooled into the previous tube. Finally, peptides were dried completely using speed vacuum and stored at -20 °C for further analysis.

6.3.2 Samples cleaned-up

Peptides were reconstituted with 10 µL of 0.1% (v/v) formic acid prior to desalting. The C18ZipTip® was rinsed with 10 µL of the wetting solution [50% (v/v) acetonitrile in H_2O] and equilibrated with 0.1% (v/v) formic acid. Ten microlitres of the reconstituted peptide proteins were aspirated into the pre-equilibrated C18ZipTip® and dispensed. This step was repeated for 10 times. C18ZipTip® was washed three times with the

washing solution [0.1% (v/v) formic acid]. Subsequently, peptides were eluted with 4 µL of the 50% acetonitrile containing 0.1% (v/v) formic acid.

6.3.3 MALDI-TOF/TOF mass spectrometry analysis

The peptide proteins were mixed with an equal volume of α-cyano-4-hydroxycinnamic acid matrix [(10 mg/mL in 50% (v/v) acetonitrile containing 0.1% (v/v) trifluoroacetic acid]. Two microlitres of the peptide mixtures were spotted on Opti-TOF™ LC/MALDI INSERT (123 x 81 mm) (Applied Biosystems Inc., CA, USA). The MALDI-TOF/TOF was performed using MDS SCIEX 4800 Plus MALDI TOF/TOF™ analyser (Applied Biosystems Inc., CA, USA). Each sample was first analysed with MALDI-TOF mass spectrometry to generate the peptide mass fingerprinting (PMF) data [Scanning range: 900 - 4000 mass-to-charge ratio (m/z)]. The five most abundant peptides that exceeded the set threshold were then selected for further fragmentation (MALDI-TOF/TOF) analysis to generate the full scan mass spectrum.

6.3.4 Database searching

All acquired spectra from samples were processed using Data Explorer™ 4.0 software (Applied Biosystems Inc., CA, USA). The data was searched against SwissProt database (Date of database searched: December 2012) using MASCOT searching engine version 2.2 (Matrix Science Inc., MA, USA). Protein score obtained by MASCOT was based on the MOWSE scoring algorithm. The MASCOT search analysis settings were as follows:

Taxonomy: *Homo sapiens*

Protease for digestion: trypsin

Fixed modification: carbamidomethyl

Variable modification: oxidation

MS/MS fragment tolerance: ± 0.2 Da

Precursor tolerance: 75 ppm

Peptide charge: + 1; monoisotopic

6.4 Western blot analysis

6.4.1 Cell lysate proteins preparation and quantitation

Cell lysate proteins for western blot analysis were prepared as described previously in this chapter (Section 6.1.1). Protein concentration was determined using 2-D quant kit according to the manufacturer's protocol as described in general methods (Chapter 2, Section 2.9.2).

6.4.2 Sodium dodecyl sulphate polyacrylamide gel electrophoresis

Sodium dodecyl sulphate polyacrylamide gel electrophoresis was performed as described in general methods (Chapter 2, Section 2.10). Briefly, cell lysate containing 20 µg of the proteins were mixed with the sample incubation buffer at an equal ratio and heated at 70 - 80 °C for 5 - 10 min. The samples were then separated on 12.5% SDS-PAGE at 90 V for about 2 h.

6.4.3 Western blotting

Following SDS-PAGE, proteins were transferred onto iBlot™ Polyvinylidene fluoride (PVDF) membrane using iBlot™ dry blotting system, iBlot™ gel transfer device (Invitrogen™, Grand Island, USA) at 20 V for 8 min. Gel sandwich was arranged in the following order from the bottom iBlot™ copper anode to the top copper cathode:

PVDF membrane ⟶ SDS-PAGE gel ⟶ pre-wet filter paper

The PVDF membrane was removed from the blotting device and blocked with blocking solution (5% BSA in TBS-T) for 1 h with agitation at room temperature, followed by overnight hybridization at 4 °C with primary antibody in 2% BSA blocking solution. After 3 times washing with TBS-T, membrane was further incubated at room temperature for 1 h in 2% BSA blocking solution containing HRP-anti mouse secondary antibody. The membrane was washed with TBS-T and the reactive bands were developed using 1-step 3,3',5,5'-tetramethylbenzidine (TMB)-blotting solution for 3 - 5 min. Summary of antibody dilutions are listed in Table 6.1.

Table 6.1: Antibodies for western blotting analysis

Antibody	**Source**	**Supplier**	**Dilution**
Monoclonal anti-Hsc 70	Mouse	Abcam®	1:10,000
Monoclonal anti-Grp 75	Mouse	Abcam®	1:1,000
Monoclonal anti-beta actin	Mouse	Abcam®	1:2,000
Anti-mouse IgG- HRP conjugate	Goat	Thermo Scientific Pierce	1:1,000

6.4.4 Stripping of PVDF membrane

For repeated hybridization with antibody against beta-actin as a loading control, membrane was stripped in the stripping buffer [0.4 M Glycine, 2% (v/v) Tween-20, and 0.2% (w/v) SDS, pH 2.2] at room temperature for 10 - 20 min. After stripping, membrane was washed twice with TBS-T and blocked with 5% BSA blocking solution for 1 h before re-hybridize with the loading control.

6.5 Statistical analysis

Differences in the protein expression were analysed by ImageMaster™ 2D Platinum 7.0 software and ANOVA *P*-values were applied (GE Healthcare, Sweden). Changes of 1.5-fold or greater in protein expression ($P < 0.05$) were considered as significant.

6.6 Proteomic analysis of MCF-7 cells treated with L-amino acid oxidase

The MCF-7 cells were treated with 0.04 µg/mL of OH-LAAO or vehicle for 72 h. Total cell lysate proteins of 150 µg were separated by 2D-PAGE. First dimensional isoelectric focusing (IEF) was performed on a linear IPG (pH 3 - 10) strips. The second dimensional SDS-PAGE was performed on 12.5% polyacrylamide resolving gels. Gels were visualized by silver staining. The 2D gel images (n = 3) were analysed by ImageMaster™ 2D Platinum 7.0 software. The representative gel images are shown in Figure 6.1. A total of 823 well-defined protein spots were detected but of these, only 21 protein spots were (as indicated by numbered circles) excised for protein identification by mass spectrometry. These protein spots appeared in all replicates and exhibiting 1.5-fold or greater ($P < 0.05$) change in expression.

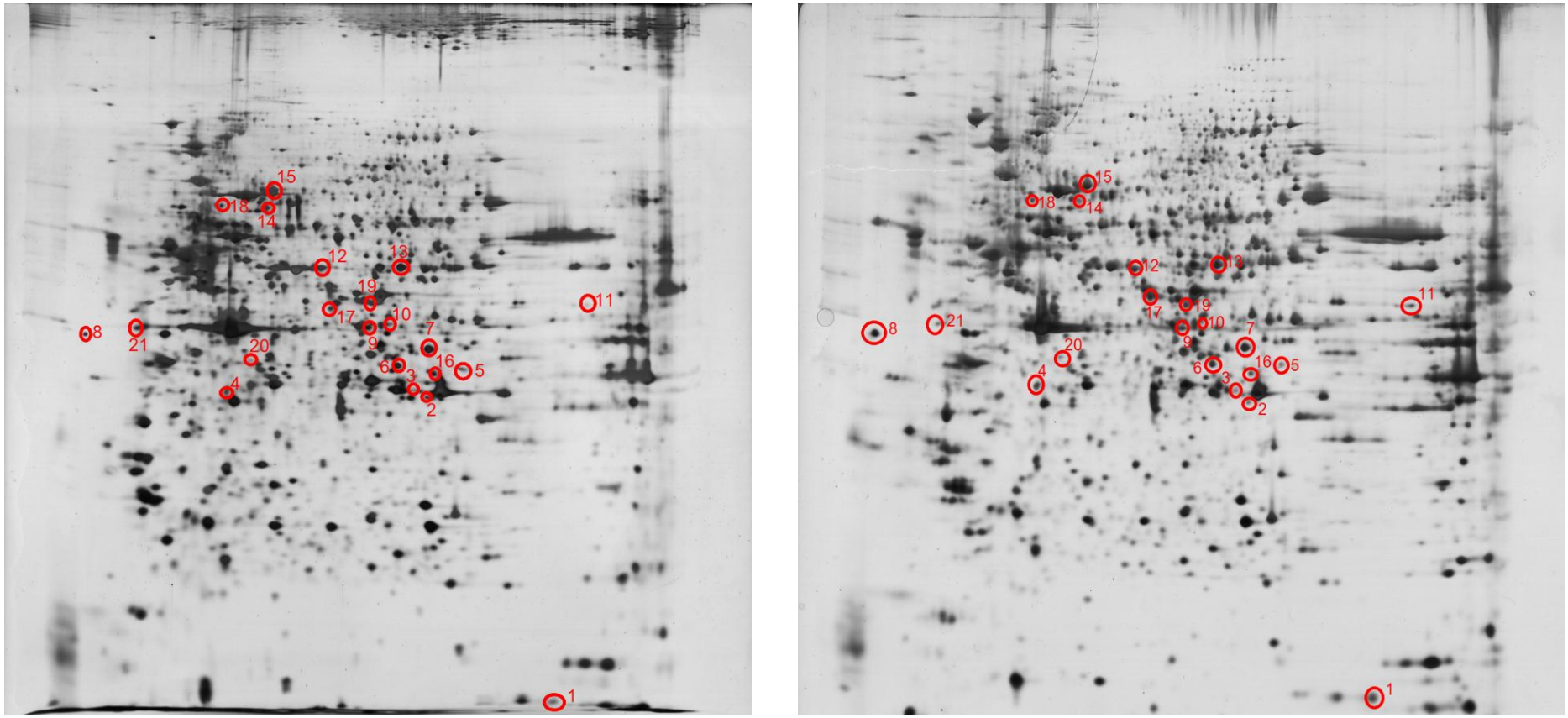

Figure 6.1: 2D gel images of MCF-7 cell lysate proteins with and without OH-LAAO treatment. Representative 2D gel images stained with silver stain. MCF-7 cells were treated with PBS (vehicle, left) or OH-LAAO (0.04 µg/mL, right) for 72 h. The 21 differentially expressed protein spots excised for mass spectrometry analyses are indicated by circles with numeral.

6.7 Identification of the differentially expressed proteins by MALDI-TOF/TOF

The 21 differentially expressed proteins in the 2D gels stained by silver stain were identified by MALDI-TOF/TOF, as shown in Table 6.2. Of the 21 proteins, 10 (47.6%) were up-regulated and 11 (52.4%) were down-regulated. The identified proteins were further classified according to their biological functions according to SwissProt and Gene Ontology Databases (Table 6.2).

6.7.1 Regulation of proteins involved in metabolism

Only two proteins that are involved in metabolism were differentially expressed: cytosolic 10-formyltetrahydrofolate dehydrogenase (up-regulated), and UDP-glucose 4-epimerase (down-regulated). .

6.7.2 Regulation of proteins involved in mRNA processing and translation

Four proteins were found to be differentially expressed in the LAAO-treated MCF-7 cells. Of these, 3 proteins were down-regulated (neuroguidin, poly(rC)-binding protein 1, and heterogeneous nuclear ribonucleoprotein H). The up-regulated protein was 40S ribosomal protein SA.

6.7.3 Regulation of proteins involved in nucleotide and amino acid biosynthesis

Two down-regulated (ribose-phosphate pyrophosphokinase 1, and mitochondrial ornithine aminotransferase) and one up-regulated (nucleoside diphosphate kinase B) proteins were identified in LAAO-treated cells.

6.7.4 Regulation of proteins involved in oxido-reduction

Three proteins involved in oxido-reduction were differentially expressed following LAAO-treatment: NADPH-cytochrome P450 reductase, and mitochondrial monofunctional C1-tetrahydrofolate synthase were up-regulated; while D-3-phosphoglycerate dehydrogenase was down-regulated.

6.7.5 Regulation of proteins involved in protein ubiquitination and proteolysis

A protein that is involved in ubiquitination was up-regulated (E3 ubiquitin-protein ligase UBR5), whereas another protein that acts as protease inhibitor or negative regulator of proteolysis was down-regulated (alpha-1-antichymotrypsin). Indicating that, OH-LAAO treatment promotes proteolysis.

6.7.6 Regulation of stress-related proteins

Heat shock cognate 71 kDa protein, and stress-70 protein were all found to be up-regulated in the treated cells

6.7.7 Regulation of proteins involved in structural integrity

Three proteins involved in structural integrity were found to be differentially expressed in the LAAO-treated cells. The up-regulated proteins were lamin-B1, and keratin type II cytoskeletal 8. The down-regulated protein was actin cytoplasmic 1.

6.7.8 Regulation of proteins involved in other functions

The differentially expressed proteins that were grouped under this category are solute carrier family 25 member 52, and growth/differentiation factor 8. Both were down-regulated.

Table 6.2: Differentially expressed proteins identified by MALDI-TOF/TOF mass spectrometry

Spot no	UniProtKB/Swiss-Prot (Accession number)	Protein description	Fold-change	Protein scores	Sequence coverage (%)
Metabolism					
4	O75891	Cytosolic 10-formyltetrahydrofolate dehydrogenase	3.3	49	9
16	Q14376	UDP-glucose 4-epimerase	-1.8	64	13
mRNA processing and translation					
6	Q8NEJ9	Neuroguidin	-1.8	35	9
7	Q15365	Poly(rC)-binding protein 1	-1.5	137	22
12	P31943	Heterogeneous nuclear ribonucleoprotein H	-1.6	313	20
21	P08865	40S ribosomal protein SA	2.0	195	19
Nucleotide and amino acid biosynthesis					
1	P22392	Nucleoside diphosphate kinase B	1.6	70	15
2	P60891	Ribose-phosphate pyrophosphokinase 1	-1.6	108	18
17	P04181	Ornithine aminotransferase, mitochondrial	-1.7	84	18
Protein ubiquitination and proteolysis					
8	O95071	E3 ubiquitin-protein ligase UBR5	3.2	42	10
19	P01011	Alpha-1-antichymotrypsin (SERPINA3)	-2.6	70	15

Table 6.2, Continued

Spot no	UniProtKB/Swiss-Prot (Accession number)	Protein description	Fold-change	Protein scores	Sequence coverage (%)
Oxido-reduction					
5	P16435	NADPH-cytochrome P450 reductase	1.5	64	12
11	Q6UB35	monofunctional C1-tetrahydrofolate synthase, mitochondrial	2.3	58	10
13	O43175	D-3-phosphoglycerate dehydrogenase	-1.5	104	17
Stress-related protein					
14	P11142	Heat shock cognate 71 kDa (Hsc70)	1.9	100	21
15	P38646	Stress-70 protein, mitochondrial (Grp75)	6.6	508	35
Structural integrity					
9	P60709	Actin, cytoplasmic 1	-1.5	79	18
18	P20700	Lamin-B1	1.6	95	17
20	P05787	Keratin, type II cytoskeletal 8	2.0	76	16
Others					
3	Q3SY17	Solute carrier family 25 member 52	-2.2	52	9
10	O14793	Growth/differentiation factor 8	-2.6	43	9

A positive fold-change indicates up-regulated, while a negative fold-change indicates down-regulated in protein expression in relative to the control cells. Protein scores > 55 are significant ($P < 0.05$). Data was obtained from triplicate analyses (n = 3) (Date of database searched: December 2012).

6.8 Validation of differential expression of proteins by western blot analysis

Western blot analyses were performed to validate the observed alterations in protein expression by 2D gel proteomic analysis. The heat shock cognate 71 kDa (Hsc70) and stress-70 proteins (Grp75) were selected for western blot validation, using beta-actin as a loading control. Equal amounts (20 µg) of cell lysate proteins extracted from MCF-7 cells treated with 0.04 µg/mL of OH-LAAO or PBS (vehicle) were used in the western blot analysis. As shown in Figure 6.2, both proteins examined were up-regulated in the LAAO-treated cells compared with the vehicle-treated cells. The results were consistent with the observations in the 2D gel proteomic analysis.

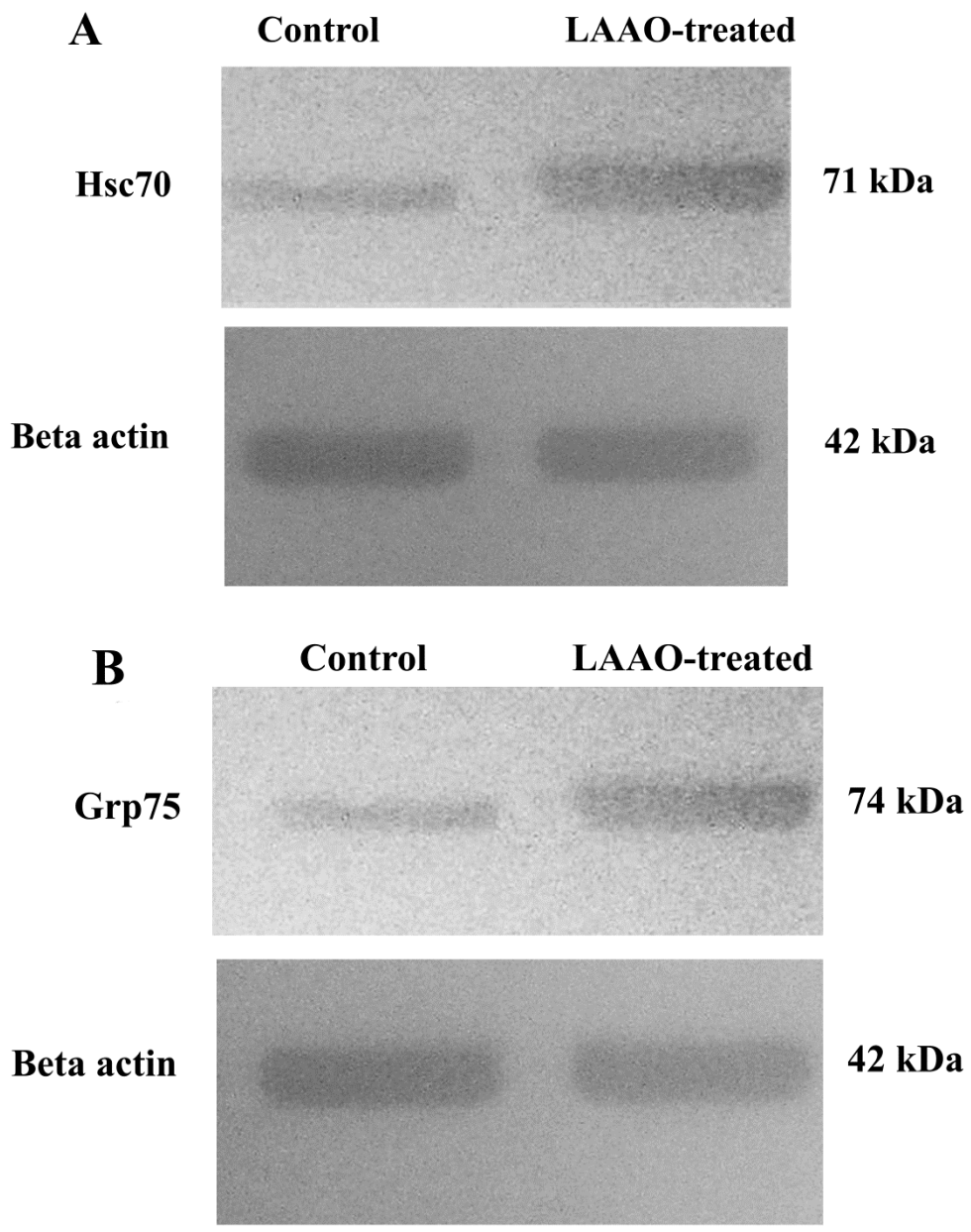

Figure 6.2: Western blot analysis of Hsc70 and Grp75 in LAAO-treated MCF-7 cells. The expression level of (A) Hsc70 and (B) Grp75 in the LAAO-treated cells was compared to the control. Beta-actin was used as an equal loading control. Molecular weights are indicated on the right. The images are representative of three independent experiments.

DISCUSSION

The present study investigated the alterations of protein expression profile of MCF-7 cells as a result of OH-LAAO treatment, using 2D electrophoresis proteomic approach. The results show that a total of 21 proteins were expressed differentially as a result of the treatment. Based on their biological functions, the differentially expressed proteins can be divided into different groups (Table 6.2). As the main purpose of the study is to investigate the molecular events that occur during the OH-LAAO treatment of the cancer cells, only those proteins that are related to cell death were considered in greater detail:

6.9 Modulation of proteins involved in stress response

King cobra venom LAAO (OH-LAAO) has been shown to induce intracellular oxidative stress through the production of H_2O_2 during the enzymatic reaction (Chapter 5). Synthesis of stress proteins is a ubiquitous characteristic for cells in response to various environment insults including oxidative stress (Gomer *et al*., 1991). Increased expressions of stress proteins confer cellular resistance against oxidative stress condition.

The increased in the expression of heat shock cognate 71 kDa (Hsc70) and mitochondria stress-70 protein (Grp75) further confirm the role of oxidative stress in LAAO-mediated cell death. The increased in the expression of these two proteins were also validated by Western blot analysis.

The Hsc70, and Grp75 function to regulate cell survival and confer cytoprotection from oxidative stress (Wang *et al*., 2013) through the modulation of the activity of ROS scavenger such as glutathione peroxidase (Guo *et al*., 2007; Williamson *et al*., 2008). It

is interesting to note that microarray analysis also demonstrates an increased in expression of glutathione peroxidase 2 (GPX2) (Chapter 5).

The observed increased expression of the stress-related proteins that functions to counteract cellular stress is in agreement with the suggestion that the primary event leading to cell death as a result of the OH-LAAO treatment is due to oxidative stress induced by H_2O_2. However, since the amount of enzyme used in the study (0.04 µg/mL) is so low, the net amount of H_2O_2 released by the enzymatic action must be rather limited, yet the enzyme exhibits extremely potent cytotoxic activity. We have earlier (Chapter 4) suggested that the potent cytotoxic effect induced by OH-LAAO may be due to its ability to bind to cancer cells, and thereby releasing high local levels of H_2O_2 in the cancer cells. Nevertheless, there is also the possibility of involvement of other molecular mechanisms that can trigger excessive production of cellular ROS. Such mechanism may involve cellular oxido-reductases that regulate the balance between cellular oxidant and reductant levels, as discussed below.

6.10 Modulation of proteins involved in oxido-reduction

The differentially expressed proteins that are involved in oxido-reduction (NADPH-cytochrome P450 reductase, monofunctional C1-tetrahydrofolate synthase, and D-3-phosphoglycerate dehydrogenase) are the enzymatic components of ROS production system during endoplasmic reticulum stress response (Bhandary *et al*., 2012). The observed increased expression of cytochrome P450 reductase (CPR) is particularly interesting, as this will facilitate the transfer of electrons from NADPH to cytochrome P450 isoenzymes (Döhr *et al*., 2001), and as a result increases the production of ROS during the reaction cycle and hence, contribute further to cellular oxidative stress (Fleming, 2001). It is interesting to note that microarray and RT-PCR analysis also demonstrated very substantial up-regulation of expression of the two cytochrome P450

genes (CYP1A1 and CYP1B1), and that the enzyme activities of CYP1A1 and CYP1B1 were both significantly increased in the LAAO-treated MCF-7 cells (Chapter 5).

6.11 Modulation of proteins involved in ubiquitination and proteolysis

The E3 ubiquitin-protein ligase confers specificity to the ubiquitination process and directs the conjugation of ubiquitin (a polypeptide co-factor) to specific target proteins. The ubiquitinated proteins lead to the recognition by the 26S proteasome that degrades ubiquitinated proteins into small peptides (Lecker *et al*., 2006). Numerous studies have demonstrated that the ubiquitination-mediated degradation plays an important role in controlling the levels of various cellular proteins including many molecules that regulate cell death machinery, such as p53, caspases, and Bcl-2 family members. Ubiquitination-degradation of ring finger-containing members of the IAP (inhibitor of apoptosis) family proteins is required for apoptosis to occur, indicating that apoptosis proceeds through death pathways as well as ubiquitin-proteasome pathway (Yang and Yu, 2003).

Thus, the up-regulation of E3 ubiquitin-protein ligase UBR5 and down-regulation of alpha-1-antichymotrypsin (SERPINA3), a serine-protease inhibitor, suggest that there was likely to be an overall increase in ubiquitination-mediated degradation and proteolysis, which contributed to cell death. It is noteworthy that the down-regulation of expression of SERPINA3 is in agreement with the results of alteration of SERPNA3 gene in microarray analysis (Chapter 5).

6.12 Modulation of proteins involved in cell proliferation and apoptosis

The three proteins; keratin type II cytoskeletal 8 (grouped under structural integrity), cytosolic 10-formyltetrahydrofolate dehydrogenase (group under metabolism), and 40S ribosomal protein SA (grouped under mRNA processing and translation) are all

involved in the regulation of apoptosis. Studies have suggested that keratin type II cytoskeletal 8 (K8) was involved in modulating of cellular responses to pro-apoptotic stimuli by desensitising the cells to pro-apoptotic signalling mediated by tumour necrosis factor-α (TNF-α) or by Fas ligand, by binding to their receptors (Owens and Lane, 2003). Cytosolic 10-formyltetrahydrofolate dehydrogenase has been shown to induce G1 cell cycle arrest and p53-dependent apoptosis (Hoeferlin *et al*., 2011). The 40S ribosomal protein SA (67-kDa laminin receptor), functions as a cancer-specific death receptor induced apoptosis via cGMP-mediated pathway (Kumazoe *et al*., 2013). The up-regulation of these proteins all confirmed that OH-LAAO induces apoptosis, as was discussed in the earlier chapters (Chapter 4 and 5).

6.13 Conclusions: what can we learn about mechanism of LAAO-induced apoptosis from proteomic studies?

In Chapter 5, the present study reports the investigation of the alterations of gene expression that occurred as a result of OH-LAAO treatment, using microarray analysis. The results showed that the oxidative stress induced by H_2O_2 liberated during the enzymatic reaction of OH-LAAO resulted in the alterations of expression of 178 genes, out of which at least 27 genes are involved in apoptosis and cell death. Of particular interest was the substantial up-regulation of the ROS generating cytochrome P450 genes which may further contribute to the cytotoxic action of the H_2O_2 generated by the enzymatic actions of OH-LAAO.

In the present proteomic studies, 21 proteins were found to be differentially expressed as a result of OH-LAAO treatment. However, only a few of the altered proteins are related to the genes that were found to be expressed differentially in microarray analysis, including alpha-1-antichymotrypsin (SERPINA3, gene expression down-regulated 1.9-fold, protein expression down-regulated 2.6-fold) and cytochrome P450 reductase.

Apart from that, an increased in the expression of Hsc70 and Grp75 proteins were also partly associated with the up-regulation of glutathione peroxidase 2 (GPX2) gene. The lack of congruence between the results of gene expression studies (microarray studies) and protein expression studies (proteomic studies), however, are expected. While the former investigated the alterations at transcriptional level, the proteomic studies investigated the alterations at translational level. Also, even though samplings of lysate proteins (for proteomic studies) and RNA (for microarray studies) were both done after 72 h OH-LAAO treatment, the proteome was more a reflection of the transcriptome of the cells existed sometime earlier before the harvest of the cellular RNA. It is reasonable to expect the cell's transcriptome to change as time progress, as the H_2O_2 and ROS generated as a result of OH-LAAO treatment continue to cause oxidative damages to the cellular proteins. Another complicating factor is the dose of OH-LAAO used in the two studies differs.

What then can we learn about the mechanism of LAAO-induced apoptosis from proteomic studies? From the results of gene expression (microarray) studies, it is postulated that the alterations of gene expression observed were largely caused by non-specific oxidative modifications of signalling proteins, such as transcriptional factors, which further modulate the activity of the signalling proteins in redox-sensitive signal transduction pathways as well as in transcriptional regulatory networks. Results from the proteomic studies support this postulate: A total of 21 proteins involved in different/unrelated pathway and cellular functions were differently expressed, indicating that it is likely due to the result of non-specific oxidative modifications of signalling proteins caused by the cellular ROS generated.

CHAPTER 7

CONCLUSION AND FUTURE STUDIES

CONCLUSION

- King cobra venom LAAO (OH-LAAO) is a very potent antibacterial agent. It was effective in inhibiting the two Gram-positive bacteria (*S. aureus* and *S. epidermidis*) and was moderately effective against the Gram-negative bacteria (*P. aeruginosa, K. pneumonia,* and *E. coli*) tested. On a molar basis, the antibacterial activity of OH-LAAO against all bacteria tested was far more potent than most of the commonly used antibiotics examined. Bacterial binding affinity of the enzyme plays an important role in its antibacterial activity.

- King cobra venom LAAO is an extremely potent and selective cytotoxic agent against tumorigenic cells. Its cytotoxicity was far more potent than that of doxorubicin, a commonly used anti-cancer chemotherapeutic agent. The cytotoxic action of the enzyme is exerted through induction of apoptosis, and is associated with the increase in caspase-3/7 activities, positive staining of annexin V to cell membrane and formation of DNA fragmentation in the LAAO-treated cells. Its apoptosis induction activity is via both intrinsic and extrinsic pathways as indicated by increase in caspase-9 and -8 activities as well as increased cytochrome *c* levels in both cytosolic and mitochondria fractions in the LAAO-treated cells.

- Gene expression and proteomic profiling of the LAAO-treated MCF cells suggested that the primary events leading eventually to apoptosis and cell death were largely caused by non-specific oxidative modifications of signalling proteins, such as transcriptional factors, which further modulate the activity of the signalling proteins in redox-sensitive signal transduction pathways as well as in transcriptional regulatory networks. In addition, the very substantial up-regulation of the expression of the cytochrome P450 genes, which may lead to

further excessive ROS production, certainly plays a key role in the apoptosis activation.

- The effectiveness of the enzyme in suppressing the growth of solid tumours *in vivo* without causing much significant toxic effects supports its potential as an anti-cancer agent.

FUTURE STUDIES

- Therapeutic application of the enzyme as an antibacterial agent will always have its limitations due to its relatively high production cost (either purified from venom or via cloning). The design of new antibacterial drugs or new therapeutic approaches which mimic the mode of antibacterial action of OH-LAAO could be a promising alternative.

- The high molecular weight of the OH-LAAO (130 kDa) may hinder its penetration into the solid tumour; thereby limiting its effectiveness as anti-cancer agent. Further development in delivery system is required. In addition, the enzyme is probably more effective against cancer cell suspensions such as leukaemia and ascites, than in solid tumours. Alternatively, the enzyme could be cloned and transfected to tumour cells to induce cell death *in situ*.

REFERENCES

REFERENCES

Aebersold, R., & Goodlett, D. R. (2001). Mass spectrometry in proteomics. *Chemical Reviews,* 101(2), 269-295.

Ahn, M. Y., Lee, B. M., & Kim, Y. S. (1997). Characterization and cytotoxicity of L-amino acid oxidase from the venom of king cobra (*Ophiophagus hannah*). *The International Journal of Biochemistry & Cell Biology,* 29(6), 911-919.

Ali Syed Abid, Stoeva Stanka, Abbasi Atiya, Alam Junaid M., Kayed Rakez, Faigle Marion, *et al*. (2000). Isolation, structural, and functional characterization of an apoptosis-inducing L-amino acid oxidase from leaf-nosed viper (*Eristocophis macmahoni*) snake venom. *Archives of Biochemistry and Biophysics,* 384(2), 216-226.

Alves, R. M., Antonucci, G. A., Paiva, H. H., Cintra, A. C. O., Franco, J. J., Mendonça-Franqueiro, E. P., *et al*. (2008). Evidence of caspase-mediated apoptosis induced by L-amino acid oxidase isolated from *Bothrops atrox* snake venom. *Comparative Biochemistry and Physiology Part A: Molecular & Integrative Physiology,* 151(4), 542-550.

Alves, R. M., de Freitas Figueiredo, R., Antonucci, G. A., Paiva, H. H., de Lourdes Pires Bianchi, M., Rodrigues, K. C., *et al*. (2011). Cell cycle arrest evidence, parasiticidal and bactericidal properties induced by L-amino acid oxidase from *Bothrops atrox* snake venom. *Biochimie,* 93(5), 941-947.

Ande, S. R., Kommoju, P. R., Draxl, S., Murkovic, M., Macheroux, P., Ghisla, S., & Ferrando-May, E. (2006). Mechanisms of cell death induction by L-amino acid oxidase, a major component of ophidian venom. *Apoptosis,* 11(8), 1439-1451.

Arias, C.A., & Murray, B.E. (2009). Antibiotic-resistant bugs in the 21st century - A clinical super-challenge. *New England Journal of Medicine,* 360(5), 439-443.

Arya, M., Shergill, I. S., Williamson, M., Gommersall, L., Arya, N., & Patel, H. R. (2005). Basic principles of real-time quantitative PCR. *Expert Review of Molecular Diagnostics,* 5(2), 209-219.

Arya, R., Mallik, M., & Lakhotia, S. C. (2007). Heat shock genes - integrating cell survival and death. *Journal of Biosciences,* 32(3), 595-610.

Beere, H. M. (2005). Death versus survival: functional interaction between the apoptotic and stress-inducible heat shock protein pathways. *Journal of Clinical Investigation,* 115(10), 2633-2639.

Belizário, J. E. (2009). Immunodeficient mouse models: an overview. *The Open Immunology Journal,* 2, 79-85.

Bergmeyer, H.U. (1983). *L-amino acid oxidase: methods in enzymatic analysis*. Weinheim, Germany: Verlag Chimie, GmbH.

Bhandary, B., Marahatta, A., Kim, H. R., & Chae, H. J. (2012). An involvement of oxidative stress in endoplasmic reticulum stress and its associated diseases. *International Journal of Molecular Sciences,* 14(1), 434-456.

Bjelakovic, G., Nagorni, A., Bjelakovic, M., Stamenkovic, I., Arsic, R., & Katic, V. (2005). APOPTOSIS: programmed cell death and its clinical implications. *Medicine and Biology,* 12 (1), 6-11.

Blankenberg, F. G. (2008). *In vivo* detection of apoptosis. *Journal of Nuclear Medicine,* 49(Suppl 2), 81S-95S.

Bolha, L., Dusanic, D., Narat, M., & Oven, I. (2012). Comparison of methods for relative quantification of gene expression using real-time PCR. *Acta Agriculturae Slovenica,* 100(2), 97-106.

Borner, C. (2003). The Bcl-2 protein family: sensors and checkpoints for life-or-death decisions. *Molecular Immunology,* 39(11), 615-647.

Bortner, C. D., Oldenburg, N. B. E., & Cidlowski, J. A. (1995). The role of DNA fragmentation in apoptosis. *Trends in Cell Biology*, 5(1), 21-26.

Bradford, M. M. (1976). A rapid and sensitive method for the quantitation of microgram quantities of protein utilizing the principle of protein-dye binding. *Analytical Biochemistry, 72*(1–2), 248-254.

Braga, M. D. M., Martins, A. M. C., Amora, D. N., de Menezes, D. B., Toyama, M. H., Toyama, D. O., *et al*. (2008). Purification and biological effects of L-amino acid oxidase isolated from *Bothrops insularis* venom. *Toxicon,* 51(2), 199-207.

Braxton, S., & Bedilion, T. (1998). The integration of microarray information in the drug development process. *Current Opinion in Biotechnology*, 9(6), 643-649.

Bregge-Silva, C., Nonato, M, C., de Albuquerque, S., Ho, P, L., Junqueira de Azevedo, I, L. M., Vasconcelos Diniz, M, R., *et al*. (2012). Isolation and biochemical, functional and structural characterization of a novel L-amino acid oxidase from *Lachesis muta* snake venom. *Toxicon*, 60(7), 1263-1276.

Bustin, S. A. (2000). Absolute quantification of mRNA using real-time reverse transcription polymerase chain reaction assays. *Journal of Molecular Endocrinology*, 25(2), 169-193.

Bustin, S. A., Benes, V., Nolan, T., & Pfaffl, M. W. (2005). Quantitative real-time RT-PCR - a perspective. *Journal of Molecular Endocrinology,* 34(3), 597-601.

Chandramouli, K., & Qian, P. Y. (2009). Proteomics: challenges, techniques and possibilities to overcome biological sample complexity. *Human Genomics & Proteomics*. doi: 10.4061/2009/239204

Chapman, M. E., Hu, L., Plato, C. F., & Kohan, D. E. (2010). Bioimpedance spectroscopy for the estimation of body fluid volumes in mice. *American Journal of Physiology*: *Renal Physiology*, 299(1), F280-283.

Chen, S. T., Pan, T. L., Tsai, Y. C., & Huang, C. M. (2002). Proteomics reveals protein profile changes in doxorubicin-treated MCF-7 human breast cancer cells. *Cancer Letters,* 181(1), 95-107.

Chomczynski, P. (1993). A reagent for the single-step simultaneous isolation of RNA, DNA and proteins from cell and tissue samples. *Biotechniques,* 15(3), 532-537.

Chomczynski, P., & Sacchi, N. (1987). Single-step method of RNA isolation by acid guanidinium thiocyanate-phenol-chloroform extraction. *Analytical Biochemistry*, 162(1), 156-159.

Chuthapisith, S., Layfield, R., Kerr, I. D., Hughes, C., & Eremin, O. (2007). Proteomic profiling of MCF-7 breast cancer cells with chemoresistance to different types of anti-cancer drugs. *International Journal of Oncology,* 30(6), 1545-1551.

Ciscotto, P., Machado de Avila, R. A., Coelho, E. A. F., Oliveira, J., Diniz, C. G., Farías, L. M., *et al*. (2009). Antigenic, microbicidal and antiparasitic properties of an l-amino acid oxidase isolated from *Bothrops jararaca* snake venom. *Toxicon,* 53(3), 330-341.

Coles, C. J., Edmondson, D. E., & Singer, T. P. (1977). Reversible inactivation of L-amino acid oxidase. Properties of the three conformational forms. *Journal of Biological Chemistry*, 252(22), 8035-8039.

Collins, J. A., Schandi, C. A., Young, K. K., Vesely, J., & Willingham, M. C. (1997). Major DNA fragmentation is a late event in apoptosis. *Journal of Histochemistry and Cytochemistry,* 45(7), 923-934.

Collins, S. J., Gallo, R. C., & Gallagher, R. E. (1977). Continuous growth and differentiation of human myeloid leukaemic cells in suspension culture. *Nature,* 270(5635), 347-349.

Cooper, C. (2001). Applications of microarray technology in breast cancer research. *Breast Cancer Research,* 3(3), 158-175.

Crow, M. T., Mani, K., Nam, Y. J., & Kitsis, R. N. (2004). The mitochondrial death pathway and cardiac myocyte apoptosis. *Circulation Research,* 95(10), 957-970.

Curti, B., Massey, V., & Zmudka, M. (1968). Inactivation of snake venom L-amino acid oxidase by freezing. *Journal of Biological Chemistry,* 243(9), 2306-2314.

Danial, N. N., & Korsmeyer, S. J. (2004). Cell death: critical control points. *Cell,* 116(2), 205-219.

Das, I. (2006). *A Photographic Guide to Snakes and Other Reptiles of Borneo*. London: New Holland Publishers (UK) Ltd.

deKok, A., & Rawitch, A. B. (1969). Studies on L-amino acid oxidase. II. Dissociation and characterization of its subunits. *Biochemistry,* 8(4), 1405-1411.

Denizot, F., & Lang, R. (1986). Rapid colorimetric assay for cell growth and survival. Modifications to the tetrazolium dye procedure giving improved sensitivity and reliability. *Journal of Immunological Methods,* 89(2), 271-277.

Döhr, O., Paine, M. J., Friedberg, T., Roberts, G. C., & Wolf, C. R. (2001). Engineering of a functional human NADH-dependent cytochrome P450 system. *Proceedings of the National Academy of Sciences of the United States of America,* 98(1), 81-86.

Dostalek, M., Hardy, K. D., Milne, G. L., Morrow, J. D., Chen, C., Gonzalez, F. J., *et al*. (2008). Development of oxidative stress by cytochrome P450 induction in rodents is selective for barbiturates and related to loss of pyridine nucleotide-dependent protective systems. *The Journal of Biological Chemistry,* 283(25), 17147-17157.

Drobyshev, A., Mologina, N., Shik, V., Pobedimskaya, D., Yershov, G., & Mirzabekov, A. (1997). Sequence analysis by hybridization with oligonucleotide microchip: identification of beta-thalassemia mutations. *Gene,* 188(1), 45-52.

Edinger, A. L., & Thompson, C. B. (2004). Death by design: apoptosis, necrosis and autophagy. *Current Opinion in Cell Biology,* 16(6), 663-669.

Ehara, T, Kitajima, S., Kanzawa, N., Tamiya, T., & Tsuchiya, T. (2002). Antimicrobial action of achacin is mediated by L-amino acid oxidase activity. *FEBS Letters,* 531(3), 509-512.

Elmore, S. (2007). Apoptosis: a review of programmed cell death. *Toxicology Pathology,* 35(4), 495-516.

Enari, M., Sakahira, H., Yokoyama, H., Okawa, K., Iwamatsu, A., & Nagata, S. (1998). A caspase-activated DNase that degrades DNA during apoptosis, and its inhibitor ICAD. *Nature,* 391(6662), 43-50.

Flanagan, S. P. (1966). 'Nude', a new hairless gene with pleiotropic effects in the mouse. *Genetics Research,* 8(3), 295-309.

Fleming, I. (2001). Cytochrome p450 and vascular homeostasis. *Circulation Research,* 89(9), 753-762.

Fotakis, G., & Timbrell, J. A. (2006). *In vitro* cytotoxicity assays: Comparison of LDH, neutral red, MTT and protein assay in hepatoma cell lines following exposure to cadmium chloride. *Toxicology Letters,* 160(2), 171-177.

Gallagher, R., Collins, S., Trujillo, J., McCredie, K., Ahearn, M., Tsai, S., *et al*. (1979). Characterization of the continuous, differentiating myeloid cell line (HL-60) from a patient with acute promyelocytic leukemia. *Blood,* 54(3), 713-733.

Gavrieli, Y., Sherman, Y., & Ben-Sasson, S. A. (1992). Identification of programmed cell death *in situ* via specific labeling of nuclear DNA fragmentation. *Journal of Cell Biology,* 119(3), 493-501.

Geyer, A., Fitzpatrick, T. B., Pawelek, P. D., Kitzing, K., Vrielink, A., Ghisla, S., & Macheroux, P. (2001). Structure and characterization of the glycan moiety of L-amino-acid oxidase from the Malayan pit viper *Calloselasma rhodostoma*. *European Journal of Biochemistry,* 268(14), 4044-4053.

Giard, D. J., Aaronson, S. A., Todaro, G. J., Arnstein, P., Kersey, J. H., Dosik, H., & Parks, W. P. (1973). *In vitro* cultivation of human tumors: establishment of cell lines derived from a series of solid tumors. *Journal of the National Cancer Institute,* 51(5), 1417-1423.

Ginzinger, D. G. (2002). Gene quantification using real-time quantitative PCR: An emerging technology hits the mainstream. *Experimental hematology,* 30(6), 503-512.

Gomer, C. J., Ferrario, A., Rucker, N., Wong, S., & Lee, A. S. (1991). Glucose regulated protein induction and cellular resistance to oxidative stress mediated by porphyrin photosensitization. *Cancer Research,* 51(24), 6574-6579.

Gorg, A., Weiss, W., & Dunn, M. J. (2004). Current two-dimensional electrophoresis technology for proteomics. *Proteomics,* 4(12), 3665-3685.

Grant, G. M., Fortney, A., Gorreta, F., Estep, M., Del Giacco, L., Van Meter, A., *et al*. (2004). Microarrays in cancer research. *Anticancer Research,* 24(2A), 441-448.

Guo, C. M., Liu, S. Q., Yao, Y. W., Zhang, Q. Q., & Sun, M. Z. (2012). Past decade study of snake venom L-amino acid oxidase. *Toxicon,* 60(3), 302-311.

Guo, S., Wharton, W., Moseley, P., & Shi, H. (2007). Heat shock protein 70 regulates cellular redox status by modulating glutathione-related enzyme activities. *Cell Stress Chaperones,* 12(3), 245-254.

Hansen, M. B., Nielsen, S. E., & Berg, K. (1989). Re-examination and further development of a precise and rapid dye method for measuring cell growth/cell kill. *Journal of Immunological Methods,* 119(2), 203-210.

Harrington, C. A., Rosenow, C., & Retief, J. (2000). Monitoring gene expression using DNA microarrays. *Current Opinion in Microbiology,* 3(3), 285-291.

Hathout, Y., Riordan, K., Gehrmann, M., & Fenselau, C. (2002). Differential protein expression in the cytosol fraction of an MCF-7 breast cancer cell line selected for resistance toward melphalan. *Journal of Proteome Research,* 1(5), 435-442.

Hayes, M. B., & Wellner, D. (1969). Microheterogeneity of L-amino acid oxidase. Separation of multiple components by polyacrylamide gel electrofucusing. *Journal of Biological Chemistry,* 244(24), 6636-6644.

Hegde, P., Qi, R., Abernathy, K., Gay, C., Dharap, S., Gaspard, R., *et al*. (2000). A concise guide to cDNA microarray analysis. *BioTechniques,* 29(3), 548-562.

Heller, R. A., Schena, M., Chai, A., Shalon, D., Bedilion, T., Gilmore, J., *et al*. (1997). Discovery and analysis of inflammatory disease-related genes using cDNA microarrays. *Proceedings of the National Academy of Sciences of the United States of America,* 94(6), 2150-2155.

Henriksen, P. A., & Kotelevtsev, Y. (2002). Application of gene expression profiling to cardiovascular disease. *Cardiovascular Research,* 54(1), 16-24.

Hingorani, R., Deng, J., Elia, J., McIntyre, C., & Mittar, D. (2011). *Detection of apoptosis using the BD Annexin V FITC assay on the BD FACSVerse™ system*, USA: BD Biosciences.

Hoeferlin, L. A., Oleinik, N. V., Krupenko, N. I., & Krupenko, S. A. (2011). Activation of p21-dependent G1/G2 arrest in the absence of DNA damage as an antiapoptotic response to metabolic stress. *Genes Cancer,* 2(9), 889-899.

Holland, P. M., Abramson, R. D., Watson, R., & Gelfand, D. H. (1991). Detection of specific polymerase chain reaction product by utilizing the 5'-3' exonuclease activity of Thermus aquaticus DNA polymerase. *Proceedings of the National Academy of Sciences of the United States of America*, 88(16), 7276-7280.

Hoogland, C., Sanchez, J. C., Walther, D., Baujard, V., Baujard, O., Tonella, L., *et al*. (1999). Two-dimensional electrophoresis resources available from ExPASy. *Electrophoresis,* 20(18), 3568-3571.

Hotchkiss, R. S., & Nicholson, D. W. (2006). Apoptosis and caspases regulate death and inflammation in sepsis. *Nature Reviews Immunology,* 6(11), 813-822.

Howard-Jones, N. (1985). A CIOMS ethical code for animal experimentation. *WHO Chronicle,* 39(2), 51-56.

Hsu, H., Xiong, J., & Goeddel, D. V. (1995). The TNF receptor 1-associated protein TRADD signals cell death and NF-kappa B activation. *Cell,* 81(4), 495-504.

Hughes, A. J. F., Ariffin, N., Huat, T. L., Molok Habibah Abdul R. N., Salbiah Hashim, Sarijo, J. R. N., *et al*. (2005). Prevalence of nosocomial infection and antibiotic use at a University Medical Center in Malaysia. *Infection Control and Hospital Epidemiology,* 26(1), 100-104.

Iskandar, D. T., & Colijn, E. (2001). *A Checklist of Southeast Asian and New Guinean Reptiles. Part I: Serpentes.* Jakarta: Kodokijo-Binamitra.

Izidoro, L. F. M., Ribeiro, M. C., Souza, G. R. L., Sant'Ana, C. D., Hamaguchi, A., Homsi-Brandeburgo, M. I., *et al*. (2006). Biochemical and functional characterization of an L-amino acid oxidase isolated from *Bothrops pirajai* snake venom. *Bioorganic & Medicinal Chemistry,* 14(20), 7034-7043.

Janicke, R. U. (2009). MCF-7 breast carcinoma cells do not express caspase-3. *Breast Cancer Research and Treatment,* 117(1), 219-221.

Jin, Y., Lee, W. H, Zeng, L., & Zhang, Y. (2007). Molecular characterization of L-amino acid oxidase from king cobra venom. *Toxicon,* 50(4), 479-489.

Joza, N., Susin, S. A., Daugas, E., Stanford, W. L., Cho, S. K., Li, C. Y., *et al*. (2001). Essential role of the mitochondrial apoptosis-inducing factor in programmed cell death. *Nature*, 410(6828), 549-554.

Jozefczuk, J., & Adjaye, J. (2011). Quantitative real-time PCR-based analysis of gene expression. *Methods in Enzymology*, 500, 99-109.

Kaighn, M. E., Narayan, K. S., Ohnuki, Y., Lechner, J. F., & Jones, L. W. (1979). Establishment and characterization of a human prostatic carcinoma cell line (PC-3). *Investigative Urology*, 17(1), 16-23.

Kannan, K., & Jain, S. K. (2000). Oxidative stress and apoptosis. *Pathophysiology*, 7(3), 153-163.

Karas, M., & Hillenkamp, F. (1988). Laser desorption ionization of proteins with molecular masses exceeding 10,000 daltons. *Analytical Chemistry*, 60(20), 2299-2301.

Khosravi, F. R., & Esposti, M. D. (2004). Death receptor signals to mitochondria. *Cancer Biology & Therapy*, 3(11), 1051-1057.

Kicman, A. T., Parkin, M. C., & Iles, R. K. (2007). An introduction to mass spectrometry based proteomics-detection and characterization of gonadotropins and related molecules. *Molecular and Cellular Endocrinol*, 260-262, 212-227.

Kischkel, F. C., Hellbardt, S., Behrmann, I., Germer, M., Pawlita, M., Krammer, P. H., & Peter, M. E. (1995). Cytotoxicity-dependent APO-1 (Fas/CD95)-associated proteins form a death-inducing signaling complex (DISC) with the receptor. *EMBO Journal*, 14(22), 5579-5588.

Kitani, Y, Kikuchi, N, Zhang, G. H., Ishizaki, S., Shimakura, K., Shiomi, K., & Nagashima, Y. (2008). Antibacterial action of L-amino acid oxidase from the skin mucus of rockfish *Sebastes schlegelii*. *Comparative Biochemistry and Physiology Part B: Biochemistry and Molecular Biology*, 149(2), 394-400.

Kumar, R., Sharma, A., & Tiwari, R. K. (2012). Application of microarray in breast cancer: An overview. *Journal of Pharmacy & Bioallied Sciences*, 4(1), 21-26.

Kumazoe, M., Sugihara, K., Tsukamoto, S., Huang, Y., Tsurudome, Y., Suzuki, T., *et al*. (2013). 67-kDa laminin receptor increases cGMP to induce cancer-selective apoptosis. *The Journal of Clinical Investigation*, 123(2), 787-799.

Kurth, J., & Aurich, H. (1976). The effect of pH value and temperature on the stability of L-amino acidoxidase from the venom of the sand viper. *Acta Biologica Et Medica Germanica*, 35(2), 175-182.

Labat-Moleur, F., Guillermet, C., Lorimier, P., Robert, C., Lantuejoul, S., Brambilla, E., & Negoescu, A. (1998). TUNEL apoptotic cell detection in tissue sections: critical evaluation and improvement. *Journal of Histochemistry & Cytochemistry*, 46(3), 327-334.

Laemmli, U. K. (1970). Cleavage of structural proteins during the assembly of the head of bacteriophage T4. *Nature*, 227(5259), 680-685.

LaForge, K. S., Shick, V., Spangler, R., Proudnikov, D., Yuferov, V., Lysov, Y., *et al*. (2000). Detection of single nucleotide polymorphisms of the human mu opioid receptor gene by hybridization or single nucleotide extension on custom oligonucleotide gelpad microchips: potential in studies of addiction. *American Journal of Medical Genetics,* 96(5), 604-615.

Lecker, S. H., Goldberg, A. L., & Mitch, W. E. (2006). Protein degradation by the ubiquitin-proteasome pathway in normal and disease states. *Journal of The American Society of Nephrology*, 17(7), 1807-1819.

Lee, S. H., Jaganath, I. B., Wang, S. M., & Sekaran, S. D. (2011). Antimetastatic effects of *Phyllanthus* on human lung (A549) and breast (MCF-7) cancer cell lines. *PLoS One*, 6(6), e20994. doi: 10.1371/journal.pone.0020994

Levenson, A. S., & Jordan, V. C. (1997). MCF-7: the first hormone-responsive breast cancer cell line. *Cancer Research,* 57(15), 3071-3078.

Li, L. Y., Luo, X., & Wang, X. (2001). Endonuclease G is an apoptotic DNase when released from mitochondria. *Nature,* 412(6842), 95-99.

Lim, K. K. P., Leong, T. M., & Lim, F. L. K. (2011). The king cobra, *Ophiophagus hannah* (cantor) in singapore (Reptilia: Squamata: Elapidae). *Nature In Singapore,* 4, 143-156.

Lin, J., Dong, H. F., Oppenheim, J. J., & Howard, O. M. (2003). Effects of astragali radix on the growth of different cancer cell lines. *World Journal* of *Gastroenterology,* 9(4), 670-673.

Liu, G., Loraine, A. E., Shigeta, R., Cline, M., Cheng, J., Valmeekam, V., *et al*. (2003). NetAffx: Affymetrix probesets and annotations. *Nucleic Acids Research,* 31(1), 82-86.

Livak, K. J., & Schmittgen, T. D. (2001). Analysis of relative gene expression data using real-time quantitative PCR and the $2^{-\Delta\Delta CT}$ Method. *Methods*, 25(4), 402-408.

Lockey, C., Otto, E., & Long, Z. (1998). Real-time fluorescence detection of a single DNA molecule. *Biotechniques,* 24(5), 744-746.

Lockhart, D. J., & Winzeler, E. A. (2000). Genomics, gene expression and DNA arrays. *Nature*, 405(6788), 827-836.

Locksley, R. M., Killeen, N., & Lenardo, M. J. (2001). The TNF and TNF receptor superfamilies: integrating mammalian biology. *Cell*, 104(4), 487-501.

Loo, V. G., Saelens, X., Gurp, V. M., MacFarlane, M., Martin, S. J., & Vandenabeele, P. (2002). The role of mitochondrial factors in apoptosis: a Russian roulette with more than one bullet. *Cell Death & Differentiation*, 9(10), 1031-1042.

Lu, B., Wang, L., Stehlik, C., Medan, D., Huang, C., Hu, S., *et al*. (2006). Phosphatidylinositol 3-kinase/Akt positively regulates Fas (CD95)-mediated apoptosis in epidermal Cl41 cells. *Journal of Immunology,* 176(11), 6785-6793.

Lu, Q. M., Wei, Q., Jin, Y., Wei, J. F., Wang, W. Y., & Xiong, Y. L. (2002). L-amino acid oxidase from *Trimeresurus jerdonii* snake venom: purification, characterization, platelet aggregation-inducing and antibacterial effects. *Journal of Natural Toxins,* 11(4), 345-352.

Lucchini, S., Thompson, A., & Hinton, J. C. (2001). Microarrays for microbiologists. *Microbiology,* 147, 1403-1414.

Macgregor, P. F., & Squire, J. A. (2002). Application of microarrays to the analysis of gene expression in cancer. *Clinical Chemistry,* 48(8), 1170-1177.

Mackay, I. M. (2004). Real-time PCR in the microbiology laboratory. *Clinical Microbiology and Infection,* 10(3), 190-212.

Manduchi, E., Scearce, L. M., Brestelli, J. E., Grant, G. R., Kaestner, K. H., & Stoeckert, C. J. (2002). Comparison of different labeling methods for two-channel high-density microarray experiments. *Physiological Genomics*, 10(3), 169-179.

Mann, M., Hendrickson, R. C., & Pandey, A. (2001). Analysis of proteins and proteomes by mass spectrometry. *Annual Review of Biochemistry,* 70, 437-473.

Marvin, L. F., Roberts, M. A., & Fay, L. B. (2003). Matrix-assisted laser desorption/ionization time-of-flight mass spectrometry in clinical chemistry. *Clinica Chimica Acta,* 337, 11-21.

McDonald, W. H., & Yates, J. R. (2000). Proteomic tools for cell biology. *Traffic,* 1(10), 747-754.

Medzihradszky, K. F., Campbell, J. M., Baldwin, M. A., Falick, A. M., Juhasz, P., Vestal, M. L., & Burlingame, A. L. (2000). The characteristics of peptide collision-induced dissociation using a high-performance MALDI-TOF/TOF tandem mass spectrometer. *Analytical Chemistry,* 72(3), 552-558.

Meltzer, P. S. (2001). Spotting the target: microarrays for disease gene discovery. *Current Opinion in Genetics & Development,* 11(3), 258-263.

Michaud, G., & Snyder, M. (2002). Proteomic approaches for global analysis of proteins. *BioTechniques,* 33, 1308-1318.

Minchinton, A. I., & Tannock, I. F. (2006). Drug penetration in solid tumours. *Nature Review Cancer,* 6(8), 583-592.

Morel, Y., & Barouki, R. (1999). Repression of gene expression by oxidative stress. *Biochemical Journal,* 342, 481-496.

Mosmann, T. (1983). Rapid colorimetric assay for cellular growth and survival: application to proliferation and cytotoxicity assays. *Journal of Immunological Methods,* 65(1-2), 55-63.

Nagata, S., Nagase, H., Kawane, K., Mukae, N., & Fukuyama, H. (2003). Degradation of chromosomal DNA during apoptosis. *Cell Death & Differentiation,* 10(1), 108-116.

National Cancer Registry (NCR). (2007). *Malaysia Cancer Statistics, Data and Figure Peninsular Malaysia 2007*. Retrieved 20 December 2013, from http://www.makna.org.my/PDF/MalaysiaCancerStatistics2007.pdf

National Committee for Clinical Laboratory Standards, NCCLS. (2000). *Methods for dilution and antimicrobial susceptibility tests for bacteria that grow aerobically. Approved Standard M 7 - A5*. Wayne, PA, USA: NCCLS.

Naumann, G. B., Silva, L. F., Silva, L., Faria, G., Richardson, M., Evangelista, K., *et al*. (2011). Cytotoxicity and inhibition of platelet aggregation caused by an L-amino acid oxidase from *Bothrops leucurus* venom. *Biochimica et Biophysica Acta (BBA) - General Subjects*, 1810(7), 683-694.

Nehls, M., Pfeifer, D., Schorpp, M., Hedrich, H., & Boehm, T. (1994). New member of the winged-helix protein family disrupted in mouse and rat nude mutations. *Nature*, 372(6501), 103-107.

Orlando, C., Pinzani, P., & Pazzagli, M. (1998). Developments in quantitative PCR. *Clinical Chemistry and Laboratory Medicine*, 36(5), 255-269.

Ouellet, M., Adams, P. D., Keasling, J. D., & Mukhopadhyay, A. (2009). A rapid and inexpensive labeling method for microarray gene expression analysis. *BMC Biotechnology*, 9(97). doi: 10.1186/1472-6750-9-97.

Owens, D. W., & Lane, E. B. (2003). The quest for the function of simple epithelial keratins. *Bioessays*, 25(8), 748-758.

Pawelek, P. D., Cheah, J., Coulombe, R., Macheroux, P., Ghisla, S., & Vrielink, A. (2000). The structure of L-amino acid oxidase reveals the substrate trajectory into an enantiomerically conserved active site. *EMBO Journal*, 19(16), 4204-4215.

Pfaffl, M. W. (2001). A new mathematical model for relative quantification in real-time RT-PCR. *Nucleic Acids Research,* 29(9), e45. doi: 10.1093/nar/29.9.e45

Ponnudurai, G., Chung, M. C., & Tan, N. H. (1994). Purification and properties of the L-amino acid oxidase from Malayan pit viper (*Calloselasma rhodostoma*) venom. *Archives of Biochemistry and Biophysics,* 313(2), 373-378.

Ramadass, P., Meerarani, P., Toborek, M., Robertson, L. W., & Hennig, B. (2003). Dietary flavonoids modulate PCB-induced oxidative stress, CYP1A1 induction, and AhR-DNA binding activity in vascular endothelial cells. *Toxicological Sciences,* 76(1), 212-219.

Relogio, A., Schwager, C., Richter, A., Ansorge, W., & Valcarcel, J. (2002). Optimization of oligonucleotide-based DNA microarrays. *Nucleic Acids Research,* 30(11), e51. doi: 10.1093/nar/30.11.e51

Rickert, A. M., Lehrach, H., & Sperling, S. (2004). Multiplexed real-time PCR using universal reporters. *Clinical Chemistry,* 50(9), 1680-1683.

Ririe, K. M., Rasmussen, R. P., & Wittwer, C. T. (1997). Product differentiation by analysis of DNA melting curves during the polymerase chain reaction. *Analytical Biochemistry,* 245(2), 154-160.

Rodrigues, R. S., da Silva, J. F., Boldrini Franca, J., Fonseca, F. P. P., Otaviano, A. R., Henrique Silva, F., *et al*. (2009). Structural and functional properties of Bp-LAAO, a new L-amino acid oxidase isolated from *Bothrops pauloensis* snake venom. *Biochimie,* 91(4), 490-501.

Rozaidi, S. W., Sukro, J., & Dan, A. (2001). The incidence of nosocomial infection in the Intensive Care Unit, Hospital Universiti Kebangsaan Malaysia: ICU-acquired nosocomial infection surveillance program 1998-1999. *Medical Journal of Malaysia,* 56(2), 207-222.

Samel, M., Tõnismägi, K., Rönnholm, G., Vija, H., Siigur, J., Kalkkinen, N., & Siigur, E. (2008). L-Amino acid oxidase from *Naja naja oxiana* venom. *Comparative Biochemistry and Physiology Part B: Biochemistry and Molecular Biology,* 149(4), 572-580.

Samel, M., Vija, H., Rönnholm, G., Siigur, J., Kalkkinen, N., & Siigur, E. (2006). Isolation and characterization of an apoptotic and platelet aggregation inhibiting L-amino acid oxidase from *Vipera berus berus* (common viper) venom. *Biochimica et Biophysica Acta (BBA) - Proteins and Proteomics,* 1764(4), 707-714.

Sanchez, J. A., Ault, J. G., Khodjakov, A., & Schneider, E. (2000). Increased mitochondrial cytochrome *c* levels and mitochondrial hyperpolarization precede camptothecin-induced apoptosis in Jurkat cells. *Cell Death & Differentiation,* 7(11), 1090-1100.

Sanchez, J. A., Khodjakov, A., & Schneider, E. (2001). Anticancer drugs induce increased mitochondrial cytochrome *c* expression that precedes cell death. *Cancer Research,* 61(3), 1038-1044.

Sapolsky, R. J., Hsie, L., Berno, A., Ghandour, G., Mittmann, M., & Fan, J. B. (1999). High-throughput polymorphism screening and genotyping with high-density oligonucleotide arrays. *Genetic Analysis,* 14, 187-192.

Schena, M., Heller, R. A., Theriault, T. P., Konrad, K., Lachenmeier, E., & Davis, R. W. (1998). Microarrays: biotechnology's discovery platform for functional genomics. *Trends in Biotechnology,* 16(7), 301-306.

Schena, M., Shalon, D., Davis, R. W., & Brown, P. O. (1995). Quantitative monitoring of gene expression patterns with a complementary DNA microarray. *Science,* 270(5235), 467-470.

Schiller, J. H., & Bittner, G. (1995). Loss of the tumorigenic phenotype with *in vitro*, but not *in vivo*, passaging of a novel series of human bronchial epithelial cell lines: possible role of an alpha 5/beta 1-integrin-fibronectin interaction. *Cancer Research*, 55(24), 6215-6221.

Schimmer, A. D. (2004). Inhibitor of apoptosis proteins: translating basic knowledge into clinical practice. *Cancer Research*, 64(20), 7183-7190.

Schulze, A., & Downward, J. (2000). Analysis of gene expression by microarrays: cell biologist's gold mine or minefield?. *Journal of Cell Science*, 113, 4151-4156.

Schulze, A., & Downward, J. (2001). Navigating gene expression using microarrays - a technology review. *Nature Cell Biology*, 3(8), E190-195.

Selvey, S., Thompson, E. W., Matthaei, K., Lea, R. A., Irving, M. G., & Griffiths, L. R. (2001). Beta-actin - an unsuitable internal control for RT-PCR. *Molecular and Cellular Probes*, 15(5), 307-311.

Shoemaker, D. D., Schadt, E. E., Armour, C. D., He, Y. D., Garrett-Engele, P., McDonagh, P. D., *et al*. (2001). Experimental annotation of the human genome using microarray technology. *Nature*, 409(6822), 922-927.

Skarnes, R. C. (1970). L-amino acid oxidase, a bactericidal system. *Nature*, 225(5237), 1072-1073.

Smart, R. C. (2010). Chemical carcinogenesis and mutagenesis. In E. Hodgson (Ed.), *A textbook of modern toxicology* (pp. 237-264). Hoboken, New Jersey: John Wiley & Sons.

Soule, H. D., Vazguez, J., Long, A., Albert, S., & Brennan, M. (1973). A human cell line from a pleural effusion derived from a breast carcinoma. *Journal of the National Cancer Institute*, 51(5), 1409-1416.

Souza, D. H. F., Eugenio, L. M., Fletcher, J. E., Jiang, M. S., Garratt, R. C., Oliva, G., & Selistre-de-Araujo, H. S. (1999). Isolation and structural characterization of a cytotoxic L-amino acid axidase from *Agkistrodon contortrix laticinctus* snake venom: preliminary crystallographic data. *Archives of Biochemistry and Biophysics*, 368(2), 285-290.

Sprick, M. R., & Walczak, H. (2004). The interplay between the Bcl-2 family and death receptor-mediated apoptosis. *Biochimica et Biophysica Acta*, 1644, 125-132.

Stábeli, R. G., Marcussi, S., Carlos, G. B., Pietro, R. C. L. R., Selistre-de-Araújo, H. S., Giglio, J. R., *at al*. (2004). Platelet aggregation and antibacterial effects of an L-amino acid oxidase purified from *Bothrops alternatus* snake venom. *Bioorganic & Medicinal Chemistry*, 12(11), 2881-2886.

Stábeli, R. G., Sant'Ana, C. D., Ribeiro, P. H., Costa, T. R., Ticli, F. K., Pires, M. G., *et al*. (2007). Cytotoxic L-amino acid oxidase from *Bothrops moojeni*: biochemical and functional characterization. *International Journal of Biological Macromolecules*, 41(2), 132-140.

Stampfer, M. R., & Bartley, J. C. (1985). Induction of transformation and continuous cell lines from normal human mammary epithelial cells after exposure to benzo[α]pyrene. *Proceedings of the National Academy of Sciences of United States of America,* 82(8), 2394-2398.

Stiles, B. G., Sexton, F. W., & Weinstein, S. A. (1991). Antibacterial effects of different snake venoms: purification and characterization of antibacterial proteins from *Pseudechis australis* (Australian king brown or mulga snake) venom. *Toxicon,* 29(9), 1129-1141.

Suhr, S. M., & Kim, D. S. (1996). Identification of the snake venom substance that induces apoptosis. *Biochemical and Biophysical Research Communications,* 224(1), 134-139.

Suhr, S. M., & Kim, D. S. (1999). Comparison of the apoptotic pathways induced by L-amino acid oxidase and hydrogen peroxide. *Journal of Biochemistry,* 125(2), 305-309.

Sun, L. K., Yoshii, Y., Hyodo, A., Tsurushima, H., Saito, A., Harakuni, T., *et al*. (2003). Apoptotic effect in the glioma cells induced by specific protein extracted from Okinawa Habu (*Trimeresurus flavoviridis*) venom in relation to oxidative stress. *Toxicology in Vitro,* 17(2), 169-177.

Sun, M. Z., Guo, C. M., Tian, Y. X., Chen, D., Greenaway, F. T., & Liu, S. Q. (2010). Biochemical, functional and structural characterization of Akbu-LAAO: A novel snake venom L-amino acid oxidase from *Agkistrodon blomhoffii ussurensis*. *Biochimie,* 92(4), 343-349.

Takatsuka, H., Sakurai, Y., Yoshioka, A., Kokubo, T., Usami, Y., Suzuki, M., *et al*. (2001). Molecular characterization of L-amino acid oxidase from *Agkistrodon halys blomhoffii* with special reference to platelet aggregation. *Biochimica et Biophysica Acta (BBA) - Protein Structure and Molecular Enzymology,* 1544, 267-277.

Tan, N. H. (1998). L-amino acid oxidases and lactate dehydrogenases. In G.S. Bailey (ed.), *Enzymes from snake venom* (pp. 579-598). Fort Collins: Alaken Inc.

Tan, N. H., & Fung, S. Y. (2009). Snake venom L-amino acid oxidase. In S. Mackessy (Ed.), *Handbook of venoms and toxins of reptiles* (pp. 219-232). New York: CRC Press.

Tan, N. H., & Ponnudurai, G. (1992). Biochemical characterization of snake venoms. In P. Gopalakrishnakone & C. K. (Eds), *Recent advances in toxinology research* (pp. 210-58). Singapore: National University of Singapore.

Tan, N. H., & Saifuddin, M. N. (1989). Isolation and characterization of an unusual form of L-amino acid oxidase from King cobra (*Ophiophagus hannah*) venom. *Biochemistry International,* 19(4), 937-944.

Tan, N. H., & Saifuddin, M. N. (1991). Substrate specificity of king cobra (*Ophiophagus hannah*) venom L-amino acid oxidase. *International Journal of Biochemistry,* 23(3), 323-327.

Tarca, A. L., Romero, R., & Draghici, S. (2006). Analysis of microarray experiments of gene expression profiling. *American Journal of Obstetrics & Gynecology*, 195(2), 373-388.

Tõnismägi, K., Samel, M., Trummal, K., Rönnholm, G., Siigur, J., Kalkkinen, N., & Siigur, E. (2006). L-amino acid oxidase from *Vipera lebetina* venom: isolation, characterization, effects on platelets and bacteria. *Toxicon,* 48(2), 227-237.

Torii, S., Naito, M., & Tsuruo, T. (1997). Apoxin I, a novel apoptosis-inducing factor with L-amino acid oxidase activity purified from Western diamondback rattlesnake venom. *The Journal of Biological Chemistry*, 272(14), 9539-9542.

Torres, A. F, C., Dantas, R, T., Toyama, M, H., Filho, E, D., Zara, F, J., Rodrigues de Queiroz, M, G., *et al*. (2010). Antibacterial and antiparasitic effects of *Bothrops marajoensis* venom and its fractions: Phospholipase A2 and L-amino acid oxidase. *Toxicon,* 55(4), 795-804.

Torri, A., Beretta, O., Ranghetti, A., Granucci, F., Ricciardi-Castagnoli, P., & Foti, M. (2010). Gene expression profiles identify inflammatory signatures in dendritic cells. *PLoS One*, 5(2), e9404. doi: 10.1371/journal.pone.0009404

Toyama, M. H., Toyama, D. O., Passero, L. F. D., Laurenti, M. D., Corbett, C. E., Tomokane, T. Y., *et al*. (2006). Isolation of a new l-amino acid oxidase from Crotalus durissus cascavella venom. *Toxicon*, 47(1), 47-57.

Trachootham, D., Lu, W., Ogasawara, M. A., Nilsa, R. D., & Huang, P. (2008). Redox regulation of cell survival. *Antioxidants & Redox Signaling*, 10(8), 1343-1374.

Tsai, Y. L., Wang, H. T., Chang, H. F., Tsai, C. F., Lin, C. K., Teng, P. H., *et al*. (2012). Development of TaqMan probe-based insulated isothermal PCR (iiPCR) for sensitive and specific on-site pathogen detection. *PLoS One,* 7(9), e45278. doi: 10.1371/journal.pone.0045278

Tweedie, M. W. F. (1983). *The Snakes of Malaya* (3rd Ed.). Singapore: Singapore National Printers (Pte) Ltd.

Van Engeland, M., Ramaekers, F. C., Schutte, B., & Reutelingsperger, C. P. (1996). A novel assay to measure loss of plasma membrane asymmetry during apoptosis of adherent cells in culture. *Cytometry*, 24(2), 131-139.

Vande V, C., Cizeau, J., Dubik, D., Alimonti, J., Brown, T., Israels, S., *et al*. (2000). BNIP3 and genetic control of necrosis-like cell death through the mitochondrial permeability transition pore. *Molecular and Cellular Biology*, 20(15), 5454-5468.

Vargas, L. J., Quintana, J. C., Pereañez, J. A., Núñez, V., Sanz, L., & Calvete, J. (2013). Cloning and characterization of an antibacterial L-amino acid oxidase from *Crotalus durissus cumanensis* venom. *Toxicon,* 64, 1-11.

Vermes, I., Haanen, C., Steffens-Nakken, H., & Reutelingsperger, C. (1995). A novel assay for apoptosis. Flow cytometric detection of phosphatidylserine expression on early apoptotic cells using fluorescein labelled Annexin V. *Journal of Immunological Methods,* 184(1), 39-51.

Verzola, D., Bertolotto, M. B., Villaggio, B., Ottonello, L., Dallegri, F., Salvatore, F., *et al*. (2004). Oxidative stress mediates apoptotic changes induced by hyperglycemia in human tubular kidney cells. *Journal of the American Society Nephrology,* 15, S85-87.

Vidal, I., & Richert, L. (2012). The nude mouse as model for liver deficiency study and treatment and xenotransplantation. *International Journal of Hepatology*, 2012, doi:10.1155/2012/140147

Wang, B. S., Yang, Y., Yang, H., Liu, Y. Z., Hao, J. J., Zhang, Y., *et al*. (2013). PKCiota counteracts oxidative stress by regulating Hsc70 in an esophageal cancer cell line. *Cell Stress Chaperones,* 18(3), 359-366.

Wei, J. F., Wei, Q., Lu, Q. M., Tai, H., Jin, Y., Wang, W. Y., & Xiong, Y. L. (2003). Purification, characterization and biological activity of an L-amino acid oxidase from *Trimeresurus mucrosquamatus* venom. *Acta Biochimica et Biophysica Sinica,* 35(3), 219-224.

Wei, J. F., Yang, H. W., Wei, X. L., Qiao, L. Y., Wang, W. Y., & He, S. H. (2009). Purification, characterization and biological activities of the L-amino acid oxidase from *Bungarus fasciatus* snake venom. *Toxicon,* 54(3), 262-271.

Wei, X. L., Wei, J. F., Li, T., Qiao, L. Y., Liu, Y. L., Huang, T., & He, S. H. (2007). Purification, characterization and potent lung lesion activity of an L-amino acid oxidase from *Agkistrodon blomhoffii ussurensis* snake venom. *Toxicon,* 50(8), 1126-1139.

Weston, C. R., & Davis, R. J. (2002). The JNK signal transduction pathway. *Current Opinion in Genetics & Development*, 12(1), 14-21.

Williamson, C. L., Dabkowski, E. R., Dillmann, W. H., & Hollander, J. M. (2008). Mitochondria protection from hypoxia/reoxygenation injury with mitochondria heat shock protein 70 overexpression. *American Journal of Physiology-Heart and Circulation Physiology,* 294(1), H249-256.

World Health Organization (WHO). (2013). *Cancer Fact Sheet*. Retrieved 20 December 2013, from http://www.who.int/mediacentre/factsheets/fs297/en/index.html

Yang, Y., & Yu, X. (2003). Regulation of apoptosis: the ubiquitous way. *FASEB Journal,* 17(8), 790-799.

Zainol Mohd, Mohd Yusoff Kamaruddin, & Mohd Yusof Mohd. (2013). Antibacterial activity of selected Malaysian honey. *BMC Complementary and Alternative Medicine,* 13, 129. doi: 10.1186/1472-6882-13-129.

Zhang, G., Gurtu, V., Kain, S. R., & Yan, G. (1997). Early detection of apoptosis using a fluorescent conjugate of annexin V. *Biotechniques,* 23(3), 525-531.

Zhang, H., Yang, Q., Sun, M., Teng, M., & Niu, L. (2004). Hydrogen peroxide produced by two amino acid oxidases mediates antibacterial actions. *The Journal of Microbiology*, 42(4), 336-339.

Zhang, L., & Cui, L. (2007). A cytotoxin isolated from *Agkistrodon acutus* snake venom induces apoptosis via Fas pathway in A549 cells. *Toxicology in Vitro,* 21(6), 1095-1103.

Zhang, L., & Wei, L. J. (2007). ACTX-8, a cytotoxic L-amino acid oxidase isolated from *Agkistrodon acutus* snake venom, induces apoptosis in Hela cervical cancer cells. *Life Sciences*, 80(13), 1189-1197.

Zhang, L., & Wu, W. T. (2008). Isolation and characterization of ACTX-6: a cytotoxic L-amino acid oxidase from *Agkistrodon acutus* snake venom. *Natural Product Research*, 22(6), 554-563.

Zhang, Y. J., Wang, J. H., Lee, W. H., Wang, Q., Liu, H., Zheng, Y. T., & Zhang, Y. (2003). Molecular characterization of *Trimeresurus stejnegeri* venom L-amino acid oxidase with potential anti-HIV activity. *Biochemical and Biophysical Research Communications*, 309(3), 598-604.

Zhong, S. R., Jin, Y., Wu, J. B., Jia, Y. H., Xu, G. L., Wang, G. C., *et al*. (2009). Purification and characterization of a new l-amino acid oxidase from *Daboia russellii siamensis* venom. *Toxicon*, 54(6), 763-771.

Appendix I

Ethical clearance for laboratory animal

UNIVERSITY OF MALAYA
KUALA LUMPUR

3rd July 2013

Dr. Fung Shin Yee
Department of Molecular Medicine
Faculty of Medicine

Dear Researcher,

Biomedical and Toxinological Studies on Snake Venom Proteins

This is to inform you that the FOM Institutional Animal Care and Use Committee, University of Malaya (FOM IACUC) has approved your Animal Use Protocol with the above mentioned title for duration of one (1) year until **June 2014**.

Please be advised that should you require changes to be made to the approved protocol, you are responsible to submit an application for amendments. Failure to do so may result in the Approval of your Animal Research Protocol be withdrawn by FOM IACUC.

Your Ethics Reference no. : **2013-06-07/MOL/R/FSY**

Thank you.

Yours sincerely,

Dr. Kiew Lik Voon
Acting Chairperson
Faculty of Medicine Institutional Animal Care and Use Committee (FOM IACUC)

Faculty of Medicine Institutional Animal Care and Use Committee (FOM IACUC)
Deputy Dean (Research), Faculty of Medicine, University of Malaya, 50603, Kuala Lumpur, MALAYSIA
Tel: (603) 7967 7515 • Fax: (603) 7956 8841• E-mail: zura@ummc.edu.my • Website: http://www.resfom.com

Appendix II

Buffer and reagent preparation

A. Preparation of Bradford reagent

Coomassie brilliant blue G-250 (100 mg) was first dissolved in 50 mL of 95% ethanol. One hundred millilitres of 85% phosphoric acid was then added. The reagent mixture was top-up with milli-Q® water to a final volume of 1L and filtered using the filter paper.

B. Preparation of nutrient agar plates

Dehydrated nutrient agar (28 g) was dissolved in 1 L of the autoclaved milli-Q® water and sterilized by autoclaving at 121 °C for 15 minutes. The agar solution was cooled to 50 °C and subsequently poured onto the Petri dish to a level until it completely covered the dish surface. The agar plates were allowed to solidify at room temperature and stored at 4 °C.

C. Preparation of nutrient broth

Dehydrated nutrient broth (13 g) was dissolved in 1 L of the autoclaved milli-Q® water. The broth was autoclaved and stored at 4 °C until used.

D. Preparation of Mueller-Hinton broth

Dehydrated Mueller-Hinton broth (21 g) was dissolved in 1 L of the autoclaved milli-Q® water. After autoclave and overnight chill at 4 °C, The broth was supplemented with the divalent cations of Mg^{2+} (10 mg/L) and Ca^{2+} (20 mg/L) as recommended by National Committee for Clinical Laboratory Standards, (NCCLS) (2000). The cations adjusted Mueller-Hinton broth was stored at 4 °C.

E. Preparation of antibiotics stock solutions

Antibiotics stock solutions were calculated by using the formula below:

$$\text{weight (mg)} = \frac{\text{Volume (mL) x Concentration (µg/mL)}}{\text{Assay potency of antibiotic (µg/mL)}}$$

All the antibiotics were dissolved/diluted in their appropriate solvent/diluents as indicated below:

Antibiotic	Solvent	Diluent
Cefotaxime	Water	Water
Kanamycin	Water	Water
Tetracycline	Ethanol	Water
Vancomycin	Water	Water
Penicillin	Water	Water

Antibiotics solutions were filtered using 0.2 µm membrane filter, aliquoted into the 2 mL vials and stored at -20 °C.

Appendix III

Heat map for differentially expressed genes in MCF-7 cells following L-amino acid oxidase treatment.

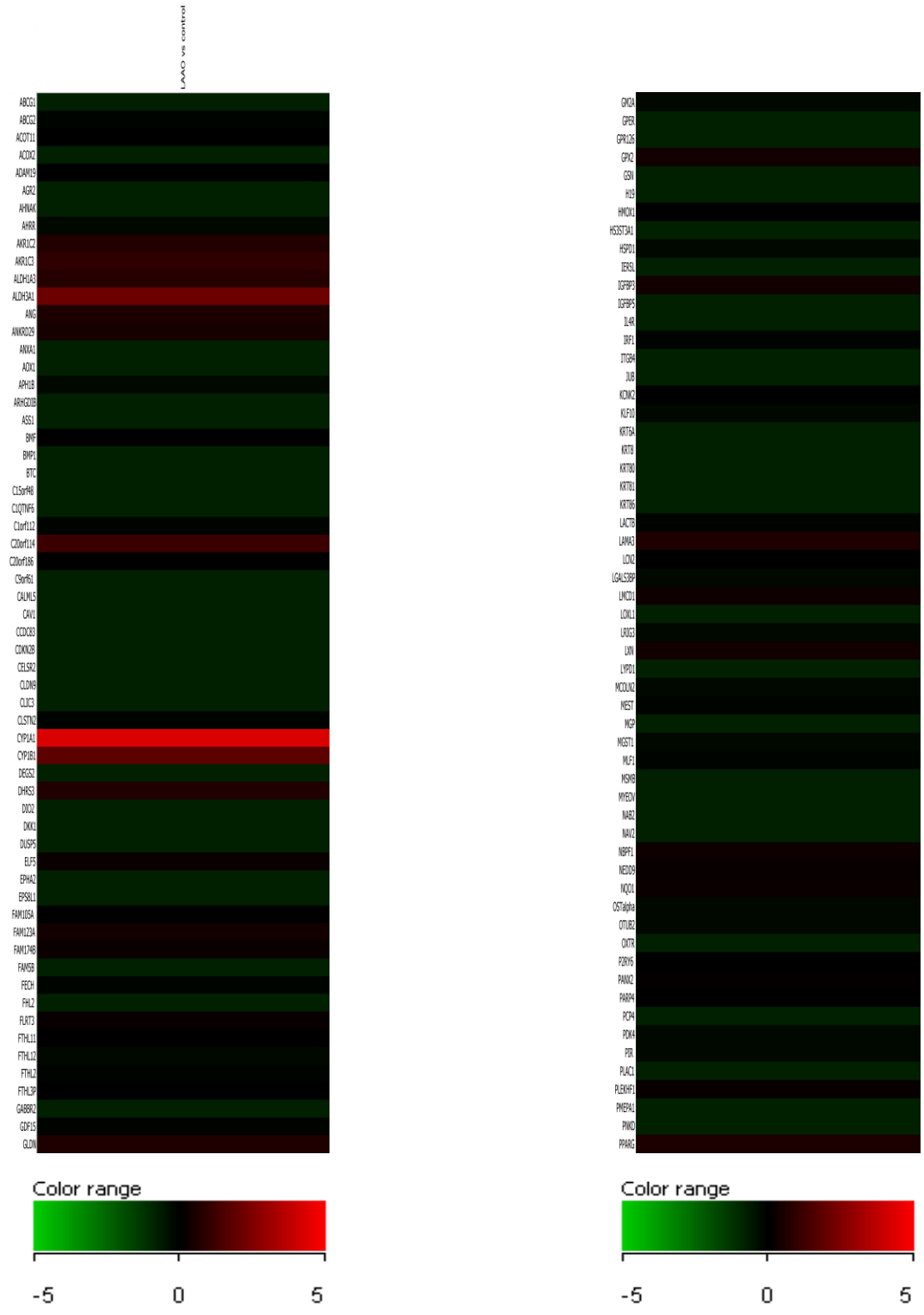

C

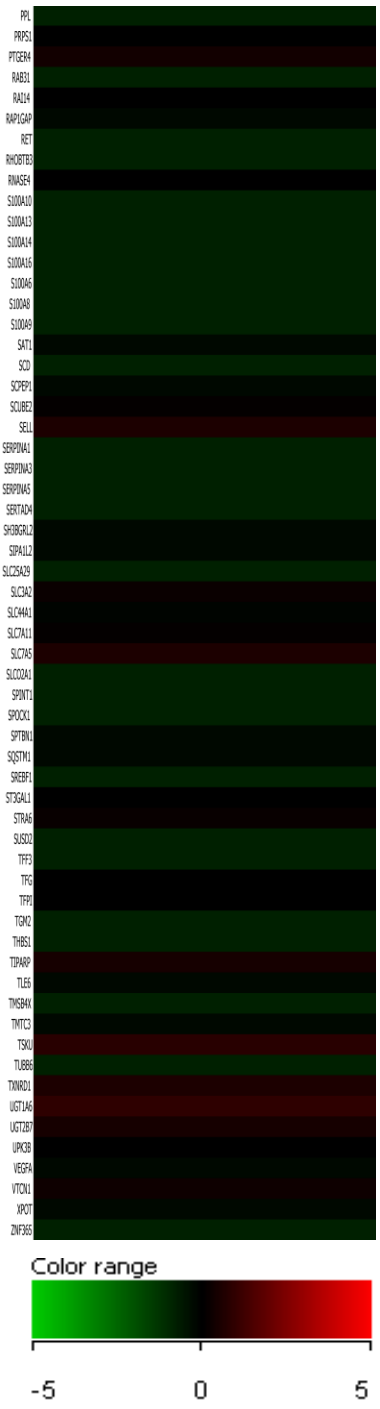

The heat map illustrates the expression level of 178 genes in relative to the corresponding vehicle (PBS) treated cells. Cells were treated with 0.015 µg/mL of LAAO or PBS for 72 h. Microarray analysis was conducted using HumanRef-8 v3.0 Expression BeadChips. The colour scale ranged from saturated green for -5.0-fold and below (decreased expression) to saturated red for 5.0-fold and above (increased expression). Each gene is represented by a single row. (A) Represent genes number 1 to 60. (B) Represent genes number 61 to 120. (3) Represent genes number 121 to 178.

Appendix IV

List of publications in ISI-indexed journals

a) Lee, M. L., Tan, N. H., Fung, S. Y., & Shamala, D. S. (2011). Antibacterial action of a heat-stable form of L-amino acid oxidase isolated from king cobra (*Ophiophagus hannah*) venom. *Comparative Biochemistry and Physiology Part C: Toxicology & Pharmacology*, 153(2), 237-242. (ISI-cited publication).

b) Lee, M. L., Ivy, C., Fung, S. Y., Kanthimathi, M. S., & Tan, N. H. (2013). Anti-proliferative activity of king cobra (*Ophiophagus hannah*) venom L-amino acid oxidase. *Basicic Clinical & Pharmacology Toxicology*. doi: 10.1111/bcpt.12155 (ISI-cited publication).

c) Lee, M. L., Fung, S.Y., Chung, I., Pailoor, J., Cheah, S.H., & Tan, N.H. (2014). King cobra (*Ophiophagus hannah*) venom L-amino acid oxidase induces apoptosis in PC-3 cells and suppresses PC-3 solid tumor growth in a tumor xenograft mouse model. *Int J Med Sci* 11, 593-601. (ISI-cited publication).

Appendix V

List of conference proceedings

a) Cytotoxicity and antibacterial effects of an L-amino acid oxidase isolated from *Ophiophagus hannah* (king cobra) snake venom, 7th - 8th October 2009, 34th Annual Conference of The Malaysian Society For Biochemistry and Molecular Biology, and 3rd Asean Biochemistry Conference, Kuala Lumpur, Malaysia. National.

b) Cytotoxicity of king cobra (*Ophiophagus hannah)* venom L-amino acid oxidase, 26th June - 1st July 2010, 35th FEBS congress, Gothenburg, Sweden. International.

c) Cytotoxic and anti-bacterial effects of L-amino acid oxidase from king cobra (*Ophiophagus hannah)* venom, 20th - 22nd December 2010, 4th International Conference on Natural Toxins, Ismailia, Egypt, International.